

8-2018

Investigating the impact of NRMT1 cancer mutants on catalytic specificity and the DNA damage response.

Kaitlyn Marie Shields
University of Louisville

Follow this and additional works at: <https://ir.library.louisville.edu/etd>

 Part of the [Medicine and Health Sciences Commons](#)

Recommended Citation

Shields, Kaitlyn Marie, "Investigating the impact of NRMT1 cancer mutants on catalytic specificity and the DNA damage response." (2018). *Electronic Theses and Dissertations*. Paper 3034.
<https://doi.org/10.18297/etd/3034>

This Doctoral Dissertation is brought to you for free and open access by ThinkIR: The University of Louisville's Institutional Repository. It has been accepted for inclusion in Electronic Theses and Dissertations by an authorized administrator of ThinkIR: The University of Louisville's Institutional Repository. This title appears here courtesy of the author, who has retained all other copyrights. For more information, please contact thinkir@louisville.edu.

INVESTIGATING THE IMPACT OF NRMT1 CANCER MUTANTS ON
CATALYTIC SPECIFICITY AND THE DNA DAMAGE RESPONSE

By

Kaitlyn Marie Shields

B.S., Missouri Southern State University, 2013

M.S., University of Louisville, 2016

A Dissertation

Submitted to the Faculty of the

School of Medicine of the University of Louisville

In Partial Fulfillment of the Requirements

For the Degree of

Doctor of Philosophy in Biochemistry and Molecular Genetics

Department of Biochemistry and Molecular Genetics

University of Louisville

Louisville, Kentucky

August 2018

INVESTIGATING THE IMPACT OF NRMT1 CANCER MUTANTS ON
CATALYTIC SPECIFICITY AND THE DNA DAMAGE RESPONSE

By

Kaitlyn Marie Shields

B.S., Missouri Southern State University, 2013

M.S., University of Louisville, 2016

A Dissertation Approved on

June 22, 2018

by the following Dissertation Committee:

Alan Cheng, Ph.D.

Christine Schaner Tooley, Ph.D.

Barbara Clark, Ph.D.

Brian Clem, Ph.D.

Nichola Garbett, Ph.D.

DEDICATION

This work is dedicated to my husband, Curtis. Without his loving support, I would not have made it to this point. Thank you for all the sacrifices you have made for me, and for always being my biggest cheerleader. This is also dedicated to my family and friends who have always encouraged me and kept me going.

ACKNOWLEDGEMENTS

I would first like to thank my current advisor, Alan Cheng. Thank you for your mentorship and all you have taught me experimentally, and for giving me the opportunity to finish my dissertation project with you. I am also thankful for my first advisor, Christine Schaner Tooley, for her guidance, especially in my first three years. I would also like to thank the members of my dissertation committee, as well as other faculty of the department, for their teaching and advice. I am also grateful to current and former lab members who have made me laugh and have helped me in many ways. Lastly, I want to acknowledge my undergraduate professors, whose passion inspired me to pursue graduate school. Everyone acknowledged here has helped to scientifically and professionally mold me into who I am now, and I am indebted for that.

ABSTRACT

INVESTIGATING THE IMPACT OF NRMT1 CANCER MUTANTS ON CATALYTIC SPECIFICITY AND THE DNA DAMAGE RESPONSE

Kaitlyn Marie Shields

June 22, 2018

Protein methylation is an established and critical posttranslational modification controlling multiple cellular events. Alterations in protein methylation have been implicated in many diseases, including cancer. My work focused on the N-terminal trimethylase NRMT1 and the N-terminal monomethylase NRMT2. Previous work proposed that NRMT2 assists NRMT1 by priming its substrates for trimethylation. Importantly, NRMT1 mutations have been found in cancers, and loss of NRMT1 has been shown to promote oncogenic phenotypes in cancer cells. Together, this suggests that altered activities of NRMT1/2 may play a role in cancer progression. Although NRMT1/2 are 50% identical, they differ in key aromatic residues in their

active site. Interestingly, mutation of the corresponding aromatic residues in the methyltransferase EZH2 (B-cell lymphoma) changes its activity from a monomethylase to a trimethylase, conferring oncogenicity. Therefore, I hypothesized that the differences in these aromatic residues are responsible for the distinct catalytic activities of NRMT1/2. I also proposed that NRMT1 cancer mutations are responsible for oncogenic phenotypes. My work illustrates that while aromatic residue mutations had no catalytic effect, both NRMT1 cancer mutants N209I (endometrial) and P211S (lung) displayed decreased trimethylase and increased mono-/dimethylase activity. These mutations are located in the peptide-binding channel and suggest there may be a second structural region impacting enzyme specificity. The mutants also required greater time and substrate levels to be comparable to WT NRMT1. Furthermore, in a cellular context lacking endogenous NRMT1, the N209I and P211S mutants were incapable of rescuing trimethylation levels or proliferation. Additional preliminary studies suggested a potential role for NRMT1 in the DNA damage response pathway. However, further studies will be required to shed more light into its cellular function.

TABLE OF CONTENTS

DEDICATION iii

ACKNOWLEDGEMENTS iv

LIST OF FIGURES ix

CHAPTER I: INTRODUCTION 1

 POSTTRANSLATIONAL MODIFICATIONS AND THEIR IMPACT ON
 MOLECULAR INTERACTIONS AND GENE EXPRESSION..... 1

 N-TERMINAL PTMs..... 3

 EFFECTS OF PROTEIN METHYLATION..... 6

 READERS, WRITERS, AND ERASERS..... 8

 BIOLOGICAL IMPACT OF ALTERED METHYLATION LEVELS..... 12

 DNA DAMAGE AND REPAIR..... 14

 SET DOMAINS AND EZH2..... 19

 NRMT AND RCC1..... 21

CHAPTER II: SELECT HUMAN CANCER MUTANTS OF NRMT1 ALTER ITS
CATALYTIC ACTIVITY AND DECREASE N-TERMINAL TRIMETHYLATION
(109) 28

 BACKGROUND..... 28

| | |
|---|-----|
| MATERIALS AND METHODS | 33 |
| RESULTS | 40 |
| DISCUSSION | 82 |
| CHAPTER III: ASSESSING THE CELLULAR EFFECT OF NRMT1 MUTANTS DURING THE DNA DAMAGE RESPONSE | 91 |
| BACKGROUND | 91 |
| MATERIALS AND METHODS | 94 |
| RESULTS | 101 |
| DISCUSSION | 133 |
| CHAPTER IV: FUTURE DIRECTIONS | 138 |
| REFERENCES | 149 |
| APPENDICES: SUPPLEMENTAL DATA | 186 |
| | 192 |
| | 193 |
| | 198 |
| APPENDICES: WORK DISCLAIMER | 200 |
| APPENDICES: COPYRIGHT PERMISSION | 201 |
| CURRICULUM VITAE | 206 |

LIST OF FIGURES

| | |
|---|----|
| Figure 1. Protein sequence alignment of human NRMT1 and NRMT2. | 24 |
| Figure 2. N-terminal methylation patterns of wild type and mutant NRMT1. | 42 |
| Figure 3. N-terminal methylation patterns of wild type and mutant NRMT2. | 44 |
| Figure 4. Y19F and W20Y NRMT1 activity is not altered by changing the RCC1 consensus sequence, but W20Y activity is lost when using peptide substrate. | 48 |
| Figure 5. Mass spectrometry analysis of WT and mutant NRMT1. | 53 |
| Figure 6. ETD MS/MS spectra and sequence coverage of α -N-terminal peptides from recombinant RCC1 methylated by WT NRMT1, N209I, or P211S. | 64 |
| Figure 7. Catalytic studies of WT and mutant NRMT1. | 68 |
| Figure 8. Molecular modeling of NRMT1 mutants. | 73 |
| Figure 9. NRMT1 mutants are not dominant negatives but reduce N-terminal trimethylation when homozygous. | 77 |

| | |
|---|-----|
| Figure 10. NRMT1 genome editing in HCT116 cells. | 80 |
| Figure 11. NRMT1 KO cells transduced with lentivirus. ... | 103 |
| Figure 12. Subcellular localization of WT and mutant NRMT1. | 108 |
| Figure 13. Viability studies of HCT116 cells. | 110 |
| Figure 14. HCT116 toleration of doxorubicin treatment. .. | 114 |
| Figure 15. Viability assay of doxorubicin-treated cont. and NRMT1 KO cells. | 116 |
| Figure 16. Viability assay of doxorubicin-treated cells. | 118 |
| Figure 17. Viability assay of recovered doxorubicin-treated cells. | 121 |
| Figure 18. γ -H2AX foci following 24-hour doxorubicin treatment. | 124 |
| Figure 19. DNA damage signaling of cont. and NRMT1 KO cells. | 127 |
| Figure 20. DNA damage signaling of rescue cell lines. ... | 130 |
| Figure 21. DNA damage signaling quantification. | 132 |
| Figure 22. Model of NRMT1 in the DNA damage response. ... | 146 |
| Figure 23. Mutant NRMT1 SPK methylation pattern. | 187 |
| Figure 24. Viability studies of HCT116 cells. | 191 |
| Figure 25. Viability assay of doxorubicin-treated cont. and NRMT1 KO cells. | 194 |
| Figure 26. Viability assay of doxorubicin-treated cells. | 197 |
| Figure 27. siRNA Studies in HCT116 cells. | 199 |

CHAPTER I: INTRODUCTION

POSTTRANSLATIONAL MODIFICATIONS AND THEIR IMPACT ON MOLECULAR INTERACTIONS AND GENE EXPRESSION

The human genome is predicted to encode approximately 20,000 genes (1-3). However, the human proteome is invariably more complex due to post-transcriptional (namely alternative splicing) and post-translational events. Such events allow a single gene to give rise to multiple protein species, resulting in a proteome that is considerably more immense and diverse than the accompanying genome. One prominent example involves posttranslational modifications (PTMs) that occur on proteins.

PTMs are covalent modifications that can regulate protein function through various means, including activity, enzymatic activation/inactivation, subcellular localization, as well as protein-protein and protein-DNA interactions (4-8). The list of PTMs is extensive, and includes methylation, acetylation, phosphorylation, glycosylation, ubiquitination, sumoylation, hydroxylation,

sulfation, nitrosylation, palmitoylation, as well as a host of infrequent modifications (4,9-12).

As an example, histones are known to be acetylated, phosphorylated, methylated, and ubiquitinated (13-16). These modifications exhibit great clout over transcription, often by directing chromatin remodeling proteins to open or close the conformation of the chromatin (17). One primary effect of this is increased or decreased accessibility of transcription factors – whether enhancers or silencers – to the chromatin, leading to the augmentation or repression of gene expression (18).

Histone acetylation and phosphorylation are mainly associated with transcriptional activation (13,15). Contrastingly, the effect of methylation and ubiquitination of histones is dichotomous. While the ubiquitination of histone H2A is linked with transcriptional repression, the ubiquitination of histone H2B is linked with transcriptional activation (19). Likewise, the methylation of histone H3 lysine 4 and H3 lysine 36 (H3K4, H3K36) is correlated with activation; while others are correlated with repression (i.e. H3K27, H4K20) (20-26). Thus, unlike DNA methylation, not all histone methylation events are repressive.

Besides the modification of histones, PTMs also occur on the side chains of non-histone proteins, as well as on the N- or C-termini of proteins (27-31). This dissertation will focus on those that occur at the N-terminus, while information for a handful of other PTMs can be found in numerous reviews (14,15,21,32-40).

N-TERMINAL PTMs

N-terminal posttranslational modifications can occur on the alpha amino group of the initiating methionine, or on the new alpha amino group if the initiator methionine is first cleaved by a methionine aminopeptidase (7). Although N-terminal methionine excision (NME) is typical for N-terminal PTMs, that is not always the case (41). Currently, the reported N-terminal PTMs include methylation, acetylation, propionylation, ubiquitination, palmitoylation, and myristoylation (6,7,42).

N-terminal myristoylation and palmitoylation result from the addition of a myristic or palmitic acid, by N-terminal myristoyltransferases or palmitoylacyltransferases, respectively (7). This occurs via the donor molecules myristoyl-CoA or palmitoyl-CoA,

leading to the attachment of the fatty acid to an N-terminal Gly residue of their substrates.

Propionylation is a recently identified N-terminal PTM, which is the addition of a molecule derived from propionic acid. Currently, less than 20 proteins have been described to harbor this modification (7). Unexpectedly, the enzyme that catalyzes this reaction is the N-terminal acetyltransferase complex NatA, demonstrating a role for this enzyme outside of N-terminal acetylation (6,7).

N-terminal ubiquitylation adds a ubiquitin protein to the free amine of the first N-terminal residue of the target protein (7). Like internal polyubiquitylation of internal residues, E2 and E3 ubiquitin ligase enzymes are also required. While internal ubiquitination is most recognized for its involvement in proteasomal degradation of target proteins, it also serves in other biological processes, including the DNA damage response and acting as a second messenger molecule in signaling pathways (14). Although N-terminal ubiquitylation has been studied less than its internal counterpart, the N-terminal modification presumably also has roles in the aforementioned processes.

N-terminal acetylation is the transfer of an acetyl moiety from acetyl-CoA to the amine of the N-terminal residue of a protein by an N-terminal acetyltransferase

(NAT) (7,42). NATs recognize the consensus sequence (Q/R)XXGXX(G/A) (7). Interestingly, the six different NAT enzyme subtypes differ in their preference for the initiating methionine, or the N-terminal residue resultant from methionine cleavage, indicating subtle differences in substrate specificity. Four of the subtypes acetylate the initiating methionine residue, while the other two acetylate the N-terminal residue resultant from methionine cleavage (6). The addition of acetyl to the N-terminus changes its positive charge to neutral, which can affect protein-protein interactions (6,43).

Some examples of N-terminal acetylation targets include histone H2A and H4, as well as the H3 variant CENP-A (6,20). This modification occurs in the cytoplasm, and is necessary for functions such as subcellular localization and protein stability (6). To date, an N-terminal deacetylase has not been discovered, so it is considered to be an irreversible PTM (6,7). Contrary to the long-held dogma that a protein could only be N-terminally acetylated or methylated (and never the other in a different cellular context, for example), N-terminal acetylation and N-terminal methylation do not preclude each other. This is evidenced by MYL9, and other proteins, which have been reported to undergo either modification (42,44,45).

Similar to most biological methylation reactions, the methyl added to the N-terminus comes from the methyl donor S-Adenosyl methionine (SAM, or AdoMet). Although N-terminal methylation has been documented for decades, enzymes responsible for this process have only been discovered in the past 10 years (46,47). NRMT (N-terminal RCC1 Methyltransferase, also known as NRMT1) was first discovered in 2010 (47), and subsequently, its homologue NRMT2, was characterized three years later (46). Like N-terminal acetylation, an N-terminal demethylase has also yet to be identified (6). As NRMT is the main thrust of this dissertation, it will be discussed in more detail below.

EFFECTS OF PROTEIN METHYLATION

Although phosphorylation and acetylation have been studied most extensively, protein methylation is also a critical and common PTM that can regulate protein function. Indeed, this PTM plays crucial roles in chromatin stability, DNA repair, and transcriptional regulation (48,49). N-terminal methylation, specifically, has been established as a regulator of the DNA damage response and protein-DNA interactions (6,20,50-52).

Proteins can be mono-, di-, and trimethylated. Each methylation state has a distinct functional readout, dependent upon the lysine or arginine residue methylated, as well as the state of methylation (22,48,53-56). Therefore, methylation of the same residue, yet differing in methylation state, often confers distinctive functions. For instance, mono- and trimethylation of histone H4 lysine 20 (H4K20) are means of transcriptional regulation. Monomethylation of H4K20 promotes transcriptional elongation, while trimethylation of the same residue pauses transcription (RNA Polymerase II pausing) (22). This is a testament to the cooperation of distinct histone modifications and subsequent transcriptional effects, as proposed by Brian Strahl and David Allis in the histone code hypothesis (49).

When H4K20 becomes monomethylated by SETD8 (SET domain containing protein 8), the MSL (male-specific lethal) complex is recruited to gene promoters. Consequently, H4K16 is acetylated by MSL, leading to the phosphorylation of Ser 2 on the C-terminal domain (CTD) of RNA Polymerase II (Pol II), and releasing it from a paused state into active transcriptional elongation (22). On the other hand, trimethylation of H4K20 by Suv420H2 precludes recruitment

of the MSL complex, and thus, prevents the acetylation of H4K16 and the subsequent CTD phosphorylation (22).

A handful of signaling pathways are also regulated by protein methylation, including the RAS-RAF and Wnt signaling pathways. For example, in the Wnt signaling pathway, the methyltransferases PRMT1 and PRMT7 methylate the GTPase-activating protein G3BP2, leading to downstream kinase recruitment and eventual β -catenin activation (21).

The biological impacts or regulation propagated via protein methylation are partly due to the crosstalk between the methylation and other PTMs (i.e. the histone code hypothesis) (21,49). Its effects are also brought about by an induction of a positive charge on the nitrogen of the target residue; whether a positive charge is induced is dependent on the residue methylated, N-terminal or internal side chain methylation, and methylation state. This change in charge can easily disrupt or change the partners with which the methylation target interacts, which can have further downstream effects (32,57).

READERS, WRITERS, AND ERASERS

The terms "Readers," "Writers," and "Erasers" are often used to describe various regulators of the PTM

process. Readers are the proteins that recognize and bind to the protein at its site of modification; writers are the enzymes which perform the modification; and the erasers are the enzymes which remove the PTM. Here, I will only discuss readers, writers, and erasers as they pertain to methylation. Lastly, to clarify, substrate specificity refers to an enzyme's selectivity for an individual substrate over another (i.e. Rb over p53). Catalytic specificity, however, refers to an enzyme's differentiation among different methylation states: whether the enzyme is able to mono-, di-, or trimethylate its substrate (i.e. specificity or differentiation for monomethylation over trimethylation).

As stated previously, writers are the enzymes that add the PTM to the substrate. For N-terminal methylation, the known enzymes are NRMT1 and NRMT2 (46,47). However, for histone and internal side chain methylation, a host of writer enzymes are known (58-62). Some histone methyltransferases are specific to their histone targets, but numerous writers also have non-histone substrates (58-60). Some histone methyltransferases can have the catalytic specificity for only monomethylation, while others may have the specificity for all three methylation

states, or any combination of the three (22,24,25,55,61,63,64).

The most common methyltransferases are lysine methyltransferases and arginine methyltransferases (16,56,58,65-67). While many lysine methyltransferases are known by other names, they are generally referred to as the KMT (lysine methyltransferase) enzymes (68-71). The family members include KMT1-8, with each member having multiple enzyme sub-family members (16). Within the KMT family, catalytic specificities range widely (16). The arginine methyltransferases are known as PRMTs (protein arginine methyltransferases) and consist of PRMT1-9 (72). All PRMTs mono- and dimethylate substrates; there is no arginine trimethylation (72). These are either classified as type I (asymmetric dimethylation) or type II (symmetric dimethylation) (72). Asymmetric dimethylation is asymmetric as both methyl groups are found on the same nitrogen atom, found at the end of the arginine side chain (72). Symmetric dimethylation is symmetric as one methyl group each is placed onto two different nitrogen atoms at the end of the arginine side chain (72).

As previously stated, there is no known eraser for N-terminal methylation, as an N-terminal demethylase has yet to be discovered (7). In contrast, various other lysine

demethylases (KDMs) have been identified. The LSD1 (lysine-specific histone demethylase 1) family members are FAD-dependent enzymes that can remove lysine mono- and dimethylation through oxidation (73,74). The JmjC (Jumonji C)-domain containing demethylases, though, are iron- and 2-oxoglutarate-dependent, and remove all three methylation states via hydroxylation (16,74,75). Thus far, no enzyme has been identified to directly remove arginine methylation. In this case, methylated arginines are converted into citrullines by deimination (66).

PTM functional readouts are generally accomplished by the readers, which contain PTM-specific recognition domains (64,76,77). Several domains are capable of lysine and arginine methylation recognition, including the chromodomain, Tudor, PHD, MBT, and PWWP domains (76,78-81). Reader domains recognize a specific methylation state (or states) on a precise residue, and some domains recognize more than one substrate (64,76-81). The different substrate specificities and/or different methylation state recognition among reader proteins is due to structural differences, specifically, the presence of different residues critical to methyl binding (64,76,77,82).

The methylation recognition leads to recruitment of protein complexes, such as chromatin remodeling complexes,

transcription factors, or DNA repair proteins (22,24,53-55). These complexes usually open up (or close) the chromatin by sliding and repositioning nucleosomes on the DNA (83), which will lead to further recruitment of transcription factors, or other proteins, downstream. One common class of chromatin remodeling complexes is known as Mi2/NURD. This complex has a methylation associating chromodomain, which has a transcriptionally repressive effect (84,85). As such, the reader is ultimately responsible for the functional outcome of the PTM.

BIOLOGICAL IMPACT OF ALTERED METHYLATION LEVELS

The physiological importance of protein methylation has been illustrated by multiple studies involving genetic manipulation of mice (24,63,86-89). For example, the conditional knockout of one or both Suv4-20h histone methyltransferases (responsible for di- and trimethylation of H4K20) in mice results in perinatal lethality. Double knockout animals exhibit a dramatic increase in monomethylation, and a near loss of di- and trimethylation. Furthermore, primary mouse embryonic fibroblasts derived from these double knockout animals exhibit decreased cellular proliferation as well as a heightened sensitivity

to DNA damage (24). This drastic shift in methylation likely impairs the DNA damage response, as the aberrant methylation impacts recruitment of DNA damage proteins, such as 53BP1, to sites of damage with double strand breaks (DSBs) (24).

In yeast, the DNA checkpoint mediator protein Crb2 becomes localized to sites of DNA damage, and associates with H4K20 dimethylation. In cells lacking this dimethylation, the recruitment of Crb2 to DNA damage is abolished, resulting in impaired checkpoint function (53). In another example, SET8 depletion in *Drosophila*, and the subsequent loss of H4K20 monomethylation, has been shown to be detrimental to cell viability, nucleosome dynamics, and nuclear arrangement (61).

Altered methylation patterns have also been demonstrated to play a role in many cancers, including leukemia, lymphoma, lung cancer, and breast cancer, among others (63,87-90). Half of acute myeloid leukemia (AML) patients exhibit abnormal expression of *HOX* genes (86). This dysregulated expression prevents recruitment of the transcription factor AF10, which interacts with the H3K79 histone methyltransferase DOT1L and helps facilitate the methylation of H3K79 (86). The lack of AF10 recruitment inhibits the di- and trimethylation of H3K79, leading to

appropriately low (or no) *HOX* gene expression (86,91). The interaction between AF10 and DOT1L is crucial for leukemic oncogenic transformation, as the deletion or inhibition of either AF10 or DOT1L inhibits the transformation, and increases mouse survival in xenograft assays (86). Importantly, this has been attributed to a reduction in the di- and trimethylation of H3K79 at *HOX* genes (86).

DNA DAMAGE AND REPAIR

The eukaryotic DNA replication machinery is a large complex of proteins that include the DNA polymerases. Despite the high fidelity of polymerases, replication errors sporadically occur (92). When a nucleotide is erroneously incorporated, it is removed by the 3' → 5' exonuclease activity of the polymerase (93).

Despite this proofreading mechanism, these errors are not always repaired, resulting in a mutation – a change in the DNA sequence of the gene. The occurrence of mutations, regardless of the cause or source, are completely random (92). Insertion/deletion (indel) mutations, additional insertions or deletions of base pairs, can also occur, resulting in a frameshift. Because they change the number of bases in the open reading frame, this damage to the DNA

will alter the triplet codons, and therefore the amino acids specified by them, giving rise to potentially deleterious mutations to the protein product of the gene.

However, even if the polymerase error is not detected by the proofreading exonuclease function, the mistake can still be corrected through mismatch repair (MMR). In eukaryotes, MMR involves numerous MutS and MutL proteins, the endonucleolytic removal of the erroneous base pairs, which will be subsequently filled in by DNA polymerases (94).

Besides replication errors that are continually propagated this way (assuming they have gone undetected by all mechanisms of proofreading and correction), or passed down to offspring, DNA damage also occurs by environmental factors or chemical mutagen carcinogens. A chemical mutagen is a carcinogen only if the induced mutation results in a phenotypic alteration.

Two of the most common environmental factors causing DNA damage are cigarette smoke and ultraviolet light (92). This commonly induces the formation of pyrimidine dimers, especially thymine dimers, or other lesions such as bulky DNA adducts (95). These dimers and adducts locally distort the DNA, interfering with replication (92). In prokaryotes and some eukaryotes, damage such as thymine dimers can be

repaired outside of DNA excision and filling in the gap (92). This process is called photoreactivation, which is carried out by DNA photolyases. Humans do not contain DNA photolyase homologues (92). Photoreactivation works by absorption of UV light by the photolyase, and reduction of FADH⁻ and the pyrimidine dimer, effectively severing the dimer lesion (96).

Damaged nucleotides which cannot be fixed by direct repair mechanisms, particularly photoreactivation, can be corrected by base excision repair (BER). BER extracts the damaged base by DNA glycosylases, which split the glycosidic bond between the nitrogenous base and deoxyribose sugar (92). An AP endonuclease then cleaves and removes the remaining deoxyribose sugar along with a few surrounding nucleotides. The final correctional steps are filling in the resulting void by DNA polymerase and sealing the new bases in by DNA ligase (97,98).

After generation of these environmentally propagated bulky DNA lesions, the repair mechanism routinely employed in humans (as we do not have DNA photolyase homologues) is nucleotide excision repair (NER) (92). Xeroderma pigmentosum patients are acutely susceptible to these insults due to mutations in components of the NER system (99). NER entails the recruitment of several factors such

as DDB1 and DDB2 (a NRMT1 target), coordinated by PARP1, nucleolytic excision of the lesion and immediately surrounding DNA, which is filled in by DNA polymerase (100).

Damage by chemical mutagens usually falls under one of two broad categories: point mutations or indel mutations (described above) (92). Point mutations are the replacement of a base with a different base; these mutations are sub-divided into transitions and transversions. A transition mutation is the replacement of a purine (or pyrimidine) base with another purine (or pyrimidine) base (e.g. adenine for guanine, or thymine for cytosine). A transversion mutation, however, is the replacement of a purine (or pyrimidine) base for a pyrimidine (or purine) base (e.g. guanine for cytosine).

DNA intercalating agents can create indel mutations. Ethidium bromide is one such common intercalating agent, and it is frequently used to visualize DNA in gel electrophoresis. The local distortion caused by the incorporation of the intercalating agent often leads to the insertion or deletion of a nucleotide during replication (92,101).

In addition to these point mutation base swaps, reactive oxygen species (ROS) can oxidize bases. Guanine

is commonly oxidized to 8-oxoguanine, which can pair with cytosine or adenine, leading to a point mutation transversion from G • C → T • A (92).

All forms of DNA repair discussed thus far are mechanisms mobilized for single strand mutations and lesions. DNA double-strand breaks (DSBs) are rectified by nonhomologous end-joining (NHEJ) or homologous recombination (92). The homologous proteins Ku70 and Ku80 detect DSBs in eukaryotes (92,102). In NHEJ, the broken DNA strands must be realigned, facilitated by Ku70 and Ku80 (92). After the strands have been realigned, nucleotides must be either removed by nucleases or filled in by DNA polymerase. Finally, the strands will be ligated by DNA ligase. NHEJ is not a perfect solution, as nucleolytic removal causes mutations (92).

Homologous recombination is an important step in meiosis. As a repair mechanism, recombination can repair DSBs through homologous end-joining. In this process, the normal, undamaged sister chromatid serves as the repair template (103). Holliday junctions are formed, which involves the Rad51 protein, and the broken DNA strands intersect each other in these junctions. Following this intersection, DNA polymerase closes the breakage points, which is sealed by DNA ligase (92). Unlike NHEJ,

homologous end-joining is not error-prone and does not result in mutations because it uses the correct and intact sister chromatid as the template for repair (103). Moreover, homologous recombination can also be used to correct an impaired replication fork (92).

SET DOMAINS AND EZH2

As methylation governs such diverse processes, altering methylation levels, or the degree of methylation, can be deleterious. Recent work demonstrated that a subset of B-cell lymphoma patients has mutations in the H3K27 methyltransferase EZH2 – the catalytic component of the polycomb repressive complex 2 (PRC2) (104,105). These mutations occur in aromatic residues in a region surrounding the active site known as the aromatic cage, and many of these residues are conserved in the majority of methyltransferases (105). EZH2 contains the evolutionarily conserved SET domain, which is a catalytic domain of approximately 130 residues found in the majority of methyltransferases (106).

One important feature of the SET domain is the lysine access channel. This connects the sites of cofactor binding as well as substrate binding (106,107). Several

aromatic amino acids comprise this region, and the size of the channel resolves whether the methyltransferase can mono-, di-, or trimethylate substrates, or any combination of the three states (106,107). Noteworthy methyltransferase exceptions which do not contain a SET domain include the H3K79 methyltransferase DOT1L, as well as NRMT1 and NRMT2. NRMT1 and NRMT2 are Class I Rossmann-like fold methyltransferases (108-110).

EZH2 is crucial for proliferation and has been implicated in cancer for years (105,111-114). A handful of mutations of an evolutionarily conserved tyrosine residue within the SET domain of EZH2, Y641, were found in patient samples, including Y641F and Y641N (105). These mutations, as well as Y641C studied by another group (115), result in a shift in the H3K27 methylation pattern, promoting primarily trimethylation over monomethylation (105). As the aromatic cage determines the catalytic specificity of EZH2, the Y641 mutation changes the size of its aromatic cage, and thus its catalytic specificity (105). From that study, mutant EZH2 had the highest *in vitro* enzymatic activity on dimethylated H3K27 peptide substrate (forming trimethylated H3K27 peptide substrate), while for wild type (WT), the enzymatic activity was lowest (105). Besides the resultant shift in methylation state, transcriptional

profiles were found to be altered, with ensuing effects such as increased proliferation and colony formation (anchorage-independent growth) (105,111).

NRMT AND RCC1

My work focuses on the homologous N-terminal methyltransferases NRMT1 (N-terminal regulator of chromatin condensation methyltransferase 1) and NRMT2 (N-terminal regulator of chromatin condensation methyltransferase 2). Following cleavage of the initiator methionine on target proteins, NRMT1 and NRMT2 methylate the α -amine of the subsequent N-terminal residue (46,47). They differ in catalytic specificity in that NRMT2 is only a monomethylase, while NRMT1 is a distributive trimethylase, capable of performing all three states of methylation (46,47). Since NRMT1 is a distributive trimethylase, it binds its substrate and adds one methyl group at a time, dissociating from the substrate after the addition of each methyl group (46). Being a monomethylase, NRMT2 aids in this process by adding the first methyl group to the substrate, resulting in substrates that can be more quickly trimethylated by NRMT1 (46).

NRMT1 (also known as METTL11A, or NTMT1) and NRMT2 (also known as METTL11B) are 25-kD and 32-kD, respectively. They share 50% sequence identity and 75% sequence similarity (44,46) (Fig. 1). In addition, their substrates possess an N-terminal X-P-(K/R) consensus sequence. X can be any amino acid other than tryptophan, isoleucine, leucine, aspartate, or glutamate (46). P is typically any polar or nonpolar amino acid (no charged amino acids), and lysine or arginine is accepted in the third position (44).

Based on the NRMT consensus sequence, it was predicted that these methyltransferases target over 300 substrates (44,50). A handful of these putative substrates have been identified and experimentally verified, including the following: RCC1 (regulator of chromatin condensation 1), Rb, SET, PARP3 [poly(ADP-ribose) polymerase 3], CENP-A (centromere protein A) (116), CENP-B (centromere protein B), DDB2 (damaged DNA-binding protein 2), KLHL31 (kelch-like protein 31), RPL23A (ribosomal protein L23a), and MYL3 (myosin light polypeptide 3) (20,46,47,50,52,117-119).

RCC1 is a 45-kD protein, and the first identified substrate to be N-terminally methylated by NRMT1 (47). It is the only identified guanine-nucleotide exchange factor for the Ran GTPase, and is vital for cytoplasmic-nuclear transport, nuclear envelope development, mitosis and

| | | |
|-------|-----|--|
| NRMT1 | 1 | MTSEVIEDEKQFYSKAKTYWKQIPPTVDGMLGCGYGHISSIDINSSRKFLQRFLRE |
| NRMT2 | 57 | LTSQVINGEMQFYARAKLFYQEVPATEEGMMGNFIELSSPDIQASQKFLRKFV - GGPGRA |
| NRMT1 | 61 | GTSCALDCGAGIGRITKRLLLPLFREVDMVDITEDFLVQAKTYLGEEGKRRVRNYFCCGLQ |
| NRMT2 | 116 | GTDCALDCGSGIGRVSKHVLLPVFNSELVDMMESFLLEAQNYLQVKGDKVESYHCYSLQ |
| NRMT1 | 121 | DFTPEPDSYDVIWIQWVI GHLTDQH LAEFLRRCCKGSLRPNGIIVIKDNMAQEGVILDDVD |
| NRMT2 | 176 | EFTPPFRRYDVIWIQWVSGHLTDKDL LAFLSRCRDGLKENGIIILKDNVAREGCILLDS |
| NRMT1 | 181 | SSVCRDLDVVRRRI CSAGLSLLAEERQENLPDEIYHVYSFALR - - - - |
| NRMT2 | 236 | SSVTRDMDIRSLIRKSGLVVLGQEKQDGFPEQCIPVWMFALHSDRHS |

Figure 1. Protein sequence alignment of human NRMT1 and NRMT2.

Sequence alignment shown for NRMT1 and truncated NRMT2 (NRMT2 shown without the flexible N-terminal domain not found in NRMT1). The amino acid sequences of NRMT1 and NRMT2 are 50% identical and 75% similar. Identical residues are highlighted in black, and similar residues are highlighted in gray.

mitotic spindle assembly, and chromatin association through binding DNA and histones H2A and H2B (120-125).

Nuclear localization of RCC1 is crucial for interphase, and the N-terminal methylation of RCC1 is essential for its association with chromatin, as well as proper mitotic function and mitotic spindle formation (47,120,121). This is evidenced by data showing that the loss of NRMT1 (loss of RCC1 methylation), or the presence of methylation-defective RCC1 mutants, causes reduced chromatin association of RCC1 (decreased DNA binding) during mitosis, giving rise to an abnormal multi-spindle phenotype (as opposed to normal bipolar spindle formation in mitosis) (47,120).

As stated before, unlike EZH2, NRMT1 and NRMT2 do not harbor SET domains (108-110). Importantly though, the aromatic cage residues of NRMT1 and NRMT2 are conserved with respect to EZH2. Given this, I hypothesized that the shape and size of their aromatic cages may similarly dictate the catalytic specificities of NRMT1 and NRMT2. Likewise, I postulated that mutation of these aromatic cage residues in NRMT1 and NRMT2 can therefore alter their catalytic specificities.

It has also been shown that NRMT1 depletion results in oncogenic phenotypes such as increased proliferation, cell

invasion and migration, and an increased sensitivity to DNA damaging agents (50,51). These phenotypes suggest that monomethylation by NRMT2 alone is insufficient to functionally compensate for the loss of trimethylation (50,51).

Importantly, mutations of both NRMT1 and NRMT2 are found in numerous human cancers (COSMIC, Catalogue of Somatic Mutations in Cancer database), and I was interested in determining if any of these mutations result in a shifted degree of N-terminal methylation, similar to the EZH2 mutations. I therefore hypothesized that mutations in or around these aromatic residues in NRMT1 and NRMT2 would shift the degree of N-terminal methylation via altered catalytic specificity. This hypothesis is addressed by aim 1, or Chapter II.

Determining which cancer mutations shift the levels of N-terminal methylation will help to determine their importance to oncogenicity. Biochemical characterization of the mutations is therefore the first step towards that goal. Studying mutations of the conserved aromatic cage residues can also tell us whether these residues, or an alternate structural motif, contribute to the catalytic specificity of NRMT1 and NRMT2.

As previously mentioned, the loss of NRMT1 results in oncogenic phenotypes such as increased proliferation, cell invasion and migration, anchorage-independent growth, as well as an increased sensitivity to DNA damaging agents (50,51). NRMT1 must therefore be crucial for survival, or repair, in response to DNA damage. NRMT1 knockout mice also exhibit premature aging phenotypes, formation of necrotic livers and polycystic ovaries, altered metabolism, and their MEFs (mouse embryonic fibroblasts) manifest an increased sensitivity to oxidative damage (51).

I was thus interested in determining the degree of N-terminal methylation conferred by mutations of NRMT1 and NRMT2, which is detailed in Chapter II. Given the sensitivity of NRMT1-depleted cells to DNA damaging agents, I hypothesized that altered N-terminal methylation patterns would have an impact on cellular proliferation, as well as the DNA damage response. This hypothesis is addressed by aim 2, or Chapter III.

CHAPTER II: SELECT HUMAN CANCER MUTANTS OF NRMT1 ALTER ITS
CATALYTIC ACTIVITY AND DECREASE N-TERMINAL TRIMETHYLATION

(109)

BACKGROUND

Lysine methylation is an important posttranslational modification (PTM) for regulating protein function. This PTM plays crucial roles in chromatin organization, DNA repair, and transcriptional regulation (48,49). The ϵ -amino groups of lysine side chains can be mono-, di-, and trimethylated, and each methylation state has a distinct functional readout, dependent upon the residue methylated (22,48,53-56). These functional readouts are generally accomplished by reader proteins, which contain PTM-specific recognition domains (64,76,77). Readers binding to methyllysine commonly have chromatin organization modifier domains (chromodomains), but can also contain Tudor, MBT, PWWP, PHD finger domains or Ankyrin or WD repeats (126). These methyllysine binding domains are specific for distinct lysine residues and distinct methylation states

(mono-, di-, or tri-) (127). Recognition of methylated lysines by methyllysine readers leads to recruitment of protein complexes, such as chromatin-remodeling complexes, transcriptional machinery, or DNA repair holoenzymes (22,24,53-55).

As methylation governs such diverse processes, altering methylation levels, or the degree of methylation, can be deleterious. Recent work demonstrated that a subset of B-cell lymphoma patients have dominant mutations in the histone H3 lysine 27 (H3K27) methyltransferase EZH2, the catalytic component of the polycomb repressive complex 2 (PRC2) (104,105). These mutations occur in residues that create an aromatic cage in the active site and are conserved in the majority of methyltransferases (105). One of the most commonly mutated residues in EZH2 is tyrosine 641 (Y641) (105). Mutation of this tyrosine to phenylalanine (Y641F) or asparagine (Y641N) shifted the H3K27 methylation pattern, promoting trimethylation over monomethylation (105). The dominant Y641 mutations changed the size of the EZH2 aromatic cage, and thus altered its catalytic specificity (105). As a result of the shift in methylation state, transcriptional profiles were altered, and cellular proliferation rates and colony formation ability increased (105,111).

N-terminal methylation of the free α -amino group is another type of protein methylation, and it has been established as a regulator of protein-DNA interactions (120). Loss of N-terminal methylation of regulator of chromatin condensation 1 (RCC1) results in its mislocalization from chromatin and multi-polar spindle formation, (120) while loss of N-terminal methylation of the DNA repair protein DNA-binding protein 2 (DDB2) impairs its recruitment to damaged DNA, and subsequently, nucleotide excision repair (NER) (52).

My work focuses on the homologous N-terminal methyltransferases NRMT1 (N-terminal RCC1 methyltransferase 1) and NRMT2 (N-terminal RCC1 methyltransferase 2). Following cleavage of the initiating methionine, they methylate the α -amine of the first N-terminal residue of their targets (46,128). They differ in catalytic specificity in that NRMT2 is a monomethylase, and NRMT1 is a trimethylase (46,128). NRMT1 is a distributive trimethylase, as it binds its substrate and adds one methyl group at a time, dissociating from the substrate after the addition of each methyl group (46). NRMT2 primes substrates with the first methyl group, thereby increasing trimethylation rates of NRMT1 (46). NRMT1 and NRMT2 are 50% identical and 75% similar and share an N-terminal X-P-K

consensus sequence (44,46). Based on this consensus sequence, it is predicted that these methyltransferases target over 300 substrates in humans (44).

Y641 of EZH2 aligns with similar tyrosines in the active sites of other methyltransferases, including G9a and SETD7, and confers trimethylase activity to both these methyltransferases when mutated to phenylalanine or alanine (62,107). The corresponding aromatic residues in NRMT1 and NRMT2 are Y19 and F75, respectively (46). Given that mutation of tyrosine to phenylalanine has been shown to change catalytic specificity, (105) I hypothesized these aromatic residues were responsible for the differing catalytic activities of NRMT1 and NRMT2. In addition to Y19 and F75, the active sites of NRMT1 and NRMT2 have differing aromatic residues at positions W20 and Y76, respectively (46). I also tested the effect of these residues on the catalytic specificities of NRMT1 and NRMT2.

Lastly, both NRMT1 and NRMT2 mutations are found in human cancers (Cosmic Catalogue of Somatic Mutations in Cancer; <http://cancer.sanger.ac.uk/cancergenome/projects/cosmic/>). While mutations of Y19 or F75 have yet to be identified, I tested whether other mutations nearby (NRMT1 Q144H - lung cancer) or in the adjacent peptide-binding channel (NRMT1

N209I - endometrial cancer; NRMT1 P211S - lung cancer; and NRMT2 V224L - breast cancer) alter catalytic activity (Cosmic Catalogue of Somatic Mutations in Cancer).

It has been shown that loss of NRMT1 results in oncogenic phenotypes such as increased proliferation, cell invasion and migration, and an increased sensitivity to DNA damaging agents (50,51). These phenotypes suggest that methylation by NRMT2 alone is insufficient to functionally compensate for the loss of trimethylation, (50,51) and indicates a decrease in NRMT1 trimethylase activity will result in similar oncogenic phenotypes. Determining which cancer mutations alter the levels of N-terminal methylation can help to determine their role in promoting tumor progression and also provide a marker for tumors more sensitive to DNA damaging agents. Studying mutations in the conserved aromatic residues of the active site will also tell us whether these residues can universally control catalytic specificity or if alternate structural motifs contribute to the catalytic specificity of NRMT1 and NRMT2.

MATERIALS AND METHODS

Constructs and Antibodies

To make His₆-tagged recombinant protein, the human NRMT1 and NRMT2 ORFs (GE Dharmacon, Marlborough, MA) were amplified to introduce a 5' NdeI restriction site and a 3' XhoI restriction site, and subcloned into pET15b vector (EMD Millipore, Billerica, MA). These were used as templates for constructing all subsequent NRMT1 and NRMT2 mutants using the Quikchange site-directed mutagenesis protocol (Agilent Technologies, Santa Clara, CA). The following forward primers and their reverse complements were used:

Y19F: 5'-CCAAGGCCAAGACCTTCTGGAAACAAATCCCAC-3'

W20Y: 5'-CCAAGGCCAAGACCTACTACAAACAAATCCCACCC-3'

Q144H: 5'-GCCACCTCACCGATCACCACCTGGCCGAGTTC-3'

N209I: 5'-GAGGAGAGGCAGGAGATCCTCCCCGATGAGATC-3'

P211S: 5'-GGCAGGAGAACCTCTCCGATGAGATCTACC-3'

F75Y: 5'-GCCAGAGCTAAACTTTTACTACCAAGAAGTACCAGC-3'

Y76W: 5'-GCCAGAGCTAAACTTTTCTGGCAAGAAGTACCAGCCAC-3'

V224L: 5'-CATATTGAAGGACAATCTGGCCCGGGAGGGCTGTATC-3'

All His₆ proteins were purified as previously described (129).

Primary antibodies used for western blots are as follows: 1:5000 polyclonal rabbit anti-me1/2RCC1 (mono-/dimethylated SPK-RCC1) (120), 1:10,000 polyclonal rabbit anti-me3RCC1 (trimethylated SPK-RCC1) (120), 1:1000 polyclonal goat anti-RCC1 (Santa Cruz Biotechnology, sc-1162, Santa Cruz, CA), 1:2000 polyclonal rabbit anti-NRMT1 (128), 1:3000 polyclonal rabbit anti-GAPDH (Trevigen, Gaithersburg, MD), and 1:1000 monoclonal mouse anti-polyHistidine (Sigma Aldrich, St. Louis, MO). 1:1000 polyclonal rabbit anti-Mettl11a/NRMT1 (Abcam, Cambridge, United Kingdom) was used to detect WT and mutant NRMT1 (Fig. 9) as the NRMT1 antibody created by the lab recognizes an epitope containing N209 and P211. Secondary donkey anti-rabbit, anti-mouse, and anti-goat HRP antibodies were used. For western blots, 10% polyacrylamide gels and tris-glycine separation were used; proteins were transferred to nitrocellulose membranes, which were blocked using 5% nonfat dry milk in TBST (200 mM Tris, 1.37 M NaCl, 0.05% Tween-20; pH 7.5).

***In Vitro* Methylation Assays**

All methylation assays were conducted at 30 °C using 1 µg recombinant enzyme (full-length protein), 0.5 µg

recombinant RCC1 substrate (full-length protein), and 100 μ M AdoMet unless otherwise noted. The reaction volume was adjusted to 50 μ l with methyltransferase buffer (50 mM potassium acetate, 50 mM Tris/HCl, pH 8), and reactions were run for one hour. Methylation assays using varied RCC1 concentration were conducted using 1 μ g recombinant enzyme, 0.1-2 μ g recombinant RCC1 substrate, and 100 μ M AdoMet. The reaction volume and time were unchanged. Methylation assays conducted at varying times used 1 μ g recombinant enzyme, 0.5 μ g recombinant RCC1 substrate, and 100 μ M AdoMet. The reaction volume was unchanged, but reactions were run for 30 minutes to 3 hours. Methylation assays were visualized by western blot analysis, except for mass spectrometry samples. Samples were prepared for MS analysis by performing a methyltransferase assay using 1 μ g recombinant enzyme, 0.5 μ g recombinant RCC1 substrate, and 100 μ M AdoMet. Reaction volume was adjusted to 20 μ l with methyltransferase buffer, and reactions were run for one hour at 30 °C. Reactions were run on an SDS/PAGE gel, and bands visualized by Coomassie Blue stain. The analysis for the presence and extent of RCC1 N-terminal methylation by MS was conducted as previously described (46).

Cell Culture

A549 human lung carcinoma cells (ATCC) were maintained in Dulbecco's Modified Eagle Medium (DMEM) (Life Technologies, Grand Island, NY) with 10% fetal bovine serum (FBS) (Atlanta Biologicals, Atlanta, GA) and 1% penicillin-streptomycin (P/S) (Life Technologies). HCT116 human colorectal carcinoma cells lines (a generous gift from Dr. Ian Macara, Vanderbilt University) were maintained in McCoy's 5a Modified Medium with 10% FBS and 1% P/S. HEK293LT human embryonic kidney cells (also a generous gift from Dr. Ian Macara) were grown in DMEM with 10% FBS and 1% P/S.

Generation of NRMT1 CRISPR/Cas9 Knockout Cell Line

Suitable CRISPR/Cas9 target sites in the human NRMT1 gene were identified using an online CRISPR Design Tool (<http://tools.genome-engineering.org>) (130). A target site in the first exon (Fig. 10) was chosen and the following oligos designed and ordered from Integrated DNA Technologies (IDT, Coralville, IA).

Top: 5'- CACCGACGGTGGACGGCATGCTTGG - 3'

Bottom: 5'- AAACCCAAGCATGCCGTCCACCGTC- 3'

The oligos were annealed, phosphorylated, and subcloned into BbsI-digested pSpCas9(BB)-2A-Puro (Addgene, Cambridge, MA) as previously described (130). Resulting clones were verified by DNA sequencing. 6×10^5 HCT116 cells were transfected with 250 ng either empty pSpCas9(BB)-2A-Puro or the same vector containing the NRMT1 target sequence. 48 hours post-transfections, cells were treated with 2 μ g/ml puromycin for three days. Surviving cells were transferred to individual wells in a 96-well plate. Cells were expanded and passaged. Half were used to make carry plates the other half were used to isolate genomic DNA. For the first six wells, the genomic DNA was PCR amplified with primers flanking the target sequence. The resultant PCR products were sequenced at the University of Louisville Genomics Core. All six clones contained frameshift mutations and were selected for expansion, and analyzed for NRMT1 expression and N-terminal methylation by western blot (Fig. 10). Subclone #6 was used in all subsequent experiments.

Lentivirus Production

Wild type (WT), N209I, or P211S human NRMT1 were amplified from the pet15b vector to introduce a 5' PmeI

restriction site and a 3' PmeI restriction site, and subcloned into pWPI lentiviral expression vector (Addgene). GFP-tagged lentivirus expressing WT NRMT1, N209I NRMT1, or P211S NRMT1 were made by co-transfecting HEK293LT cells with 50 µg pWPI containing the appropriate NRMT1 cDNA, 37.5 µg pSPAX2 packaging vector, and 15 µg pMD2.G envelope plasmid using calcium phosphate transfection. 48 hours post-transfection, viral supernatants were collected, concentrated with 100K ultrafilters (EMD Millipore), and titered in the HEK293LT cells. A549, HCT116, or HCT116 NRMT1 KO cells were infected with virus to a multiplicity of infection (MOI) of 1. Calculations performed to estimate MOI are based on the detection of GFP-positive cells by microscopy, and the dilution of virus necessary to achieve this. Three days post-transduction, cells were counted and used in cell growth assays; remaining cells were used for western blot analysis.

Cell Growth Assays

One thousand control A549, HCT116, HCT116 NRMT1 KO, or HCT116 pSpCas9 cells were plated in triplicate in a 96-well plate in 100 µl of the appropriate cell culture media. Concurrently, A549, HCT116, or HCT116 NRMT1 KO cells

transduced with WT, N209I, or P211S NRMT1-expressing virus were plated in triplicate in 96-well plates. Five sets of triplicates for each condition were made. On the day of plating (day 0), 20 μ l of Aqueous One Solution (Promega, Madison, WI) (CellTiter 96[®] AQueous One Solution Cell Proliferation Assay) was added to the first set of triplicates for each condition and the absorbance at 490 nm was read after two hours. Readings were taken on day 0 and daily for four additional days. Relative fold increase was calculated by dividing average absorbance on each day by average absorbance at day 0.

RESULTS

Aromatic Cage Mutants Do Not Exhibit Altered Methylation Patterns

Y19 is the NRMT1 tyrosine residue that most closely aligns with the position of Y641 in the methyltransferase active site of EZH2. In NRMT2, this residue is replaced by F75. As mutation of EZH2 Y641 to phenylalanine switches its catalytic activity, I hypothesized this amino acid substitution between NRMT1 and NRMT2 might be the cause of their differing catalytic activities. To test this hypothesis, recombinant proteins were made for NRMT1 Y19F and NRMT2 F75Y, and their ability to mono-, di-, or trimethylate full-length recombinant RCC1 over one hour was assayed by western blot. Unexpectedly, neither mutation significantly affected methyltransferase activity (Fig. 2A,B; Fig. 3A,B). Similar to wild type (WT) NRMT1, NRMT1 Y19F exhibited only trimethylase activity (Fig. 2A,B). Similar to WT NRMT2, NRMT2 F75Y exhibited only monomethylase activity (Fig. 3A,B).

In addition to an inability to switch catalytic activities, these mutations also did not significantly alter total methylation levels (Fig. 2C,D; Fig. 3C). This

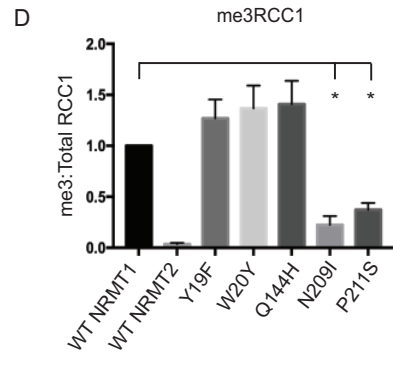
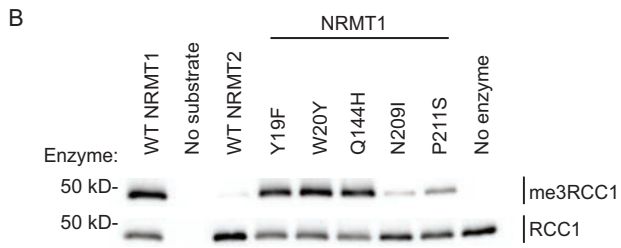
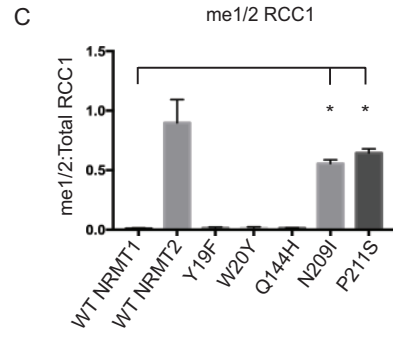
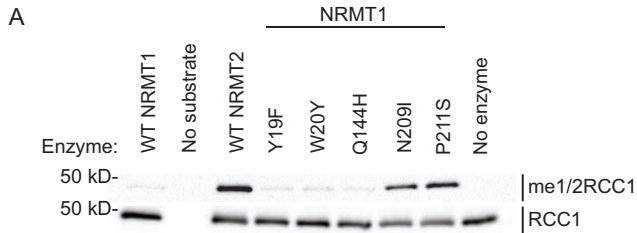


Figure 2. N-terminal methylation patterns of wild type and mutant NRMT1.

The directed mutation of aromatic residues Y19 and W20 in NRMT1 and the Q144H mutation found in human lung cancer showed no effects on (A) monomethylation/dimethylation (me1/2RCC1) or (B) trimethylation (me3RCC1) levels.

However, the NRMT1 mutants N209I (endometrial cancer) and P211S (lung cancer) exhibit (A) increased monomethylation/dimethylation of RCC1 and (B) decreased trimethylation of RCC1 as compared to wild type (WT).

Total RCC1 is shown as loading control. (C) Densitometry analysis of panel A. Ratio of me1/2RCC1:Total RCC1 band intensity. (D) Densitometry analysis of panel B. Ratio of me3RCC1:Total RCC1 band intensity, normalized to WT NRMT1.

Each data point represents the \pm SEM of three independent experiments. * denotes $P < 0.05$, determined by an unpaired two-tailed Student's t -test. Bands were quantified using ImageJ software (NIH).

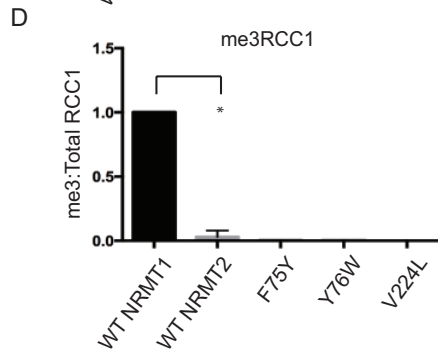
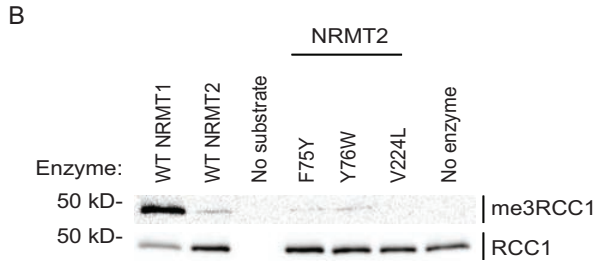
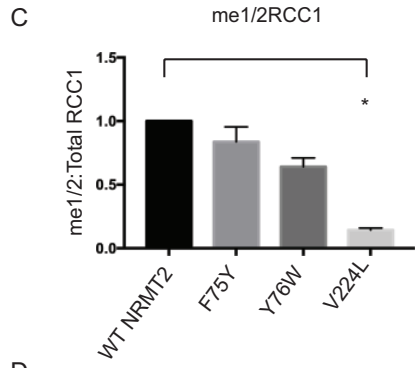
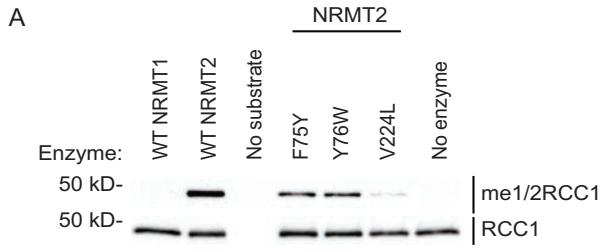


Figure 3. N-terminal methylation patterns of wild type and mutant NRMT2.

The directed mutation of aromatic residues F75 and Y76 in NRMT2 showed no effect on (A) mono-/dimethylase activity (B) but no corresponding increase in trimethylase activity. The breast cancer mutation of V224 in NRMT2 showed a significant decrease in (A) mono-/dimethylase activity (B) but no corresponding increase in trimethylase activity. Total RCC1 is shown as loading control. (C) Densitometry analysis of panel A. Ratio of me1/2RCC1:Total RCC1 band intensity, normalized to WT NRMT2. (D) Densitometry analysis of panel B. Ratio of me3RCC1:Total RCC1 band intensity, normalized to WT NRMT1. As previously shown, trimethylation levels are significantly different between WT NRMT1 and WT NRMT2 (46), but none of the NRMT2 mutants were significantly different from WT NRMT2. Low levels of trimethylation signal seen with WT NRMT2 are not due to trimethylation activity but cross-reactivity of me3RCC1 antibody with lower levels of methylation when no trimethylation is present (46,47). Each data point represents the mean \pm SEM of three independent experiments. * denotes $P < 0.05$, determined by an unpaired two-tailed Student's *t*-test. Bands were quantified using ImageJ software (NIH).

is contrary to published data showing that the NRMT1 Y19F mutation significantly inhibits the ability of WT recombinant NRMT1 to methylate an N-terminal peptide of CENP-A (131). As my assay was done with full-length recombinant RCC1 as substrate, it may be that enzyme/substrate binding is enhanced by interactions with the full protein and the interaction of Y19 with substrate is more imperative for peptide substrates. It may also be consensus sequence dependent. The CENP-A N-terminal sequence is Gly-Pro-Arg (GPR), while the RCC1 N-terminal sequence is Ser-Pro-Lys (SPK). The recently solved crystal structure of human NRMT1 bound to CENP-A N-terminal peptide indicates the Arg residue in the CENP-A consensus sequence forms hydrogen bonds and electrostatic interactions with Y19 (131). These interactions may differ with a lysine residue and make Y19 less crucial for catalytic function.

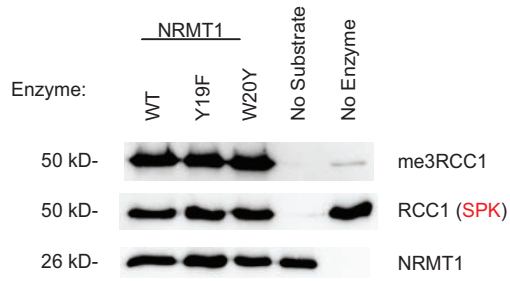
As the mutations in Y19 and F75 did not significantly alter the methyltransferase activities of NRMT1 and NRMT2, I next mutated the other aromatic residue that differs between their active sites. W20 in NRMT1 is replaced with Y76 in NRMT2 (46). Full-length recombinant proteins were made for NRMT1 W20Y and NRMT2 Y76W, and their ability to mono-, di-, or trimethylate full-length recombinant RCC1 was assayed by western blot. Again, neither mutation

significantly affected methyltransferase activity (Fig. 2A,B; Fig. 3A,B). This is also contrary to previous published data showing the W20Y mutation of NRMT1 significantly diminishes its ability to methylate the N-terminal peptide of CENP-A, (131) and further indicates the most important catalytic residues may differ depending on substrate length or consensus sequence.

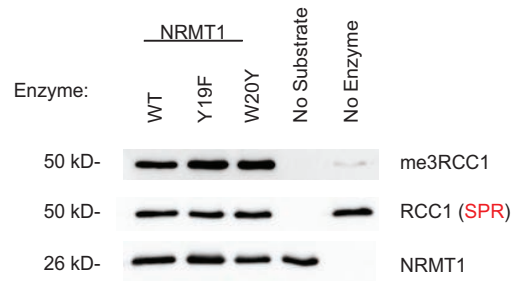
To differentiate between these two possibilities, site directed mutagenesis was performed on the plasmid used to make full-length recombinant RCC1. GPR-RCC1 was made to mimic the CENP-A consensus sequence on a full-length protein, as well as Gly-Pro-Lys (GPK) and Ser-Pro-Arg (SPR)-RCC1 to assess if the first or third amino acid is more important. Wild type SPK-RCC1, as well as all three full-length RCC1 consensus sequence mutants (GPK, SPR, and GPR) could be *in vitro* methylated by WT, Y19F, and W20Y NRMT1 (Fig. 4 A-D), indicating that the impaired Y19F and W20Y activity seen by Wu et al. (110) is not due to a difference in the three amino acid consensus sequence.

To determine if the impaired activity resulted from substrate length, the activity of Y19F and W20Y NRMT1 on a peptide containing the first 15 amino acids of WT RCC1 (SPKRIAKRRSPPADA) was tested by Dr. John Tooley.

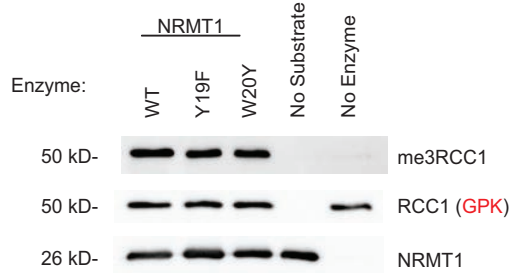
A



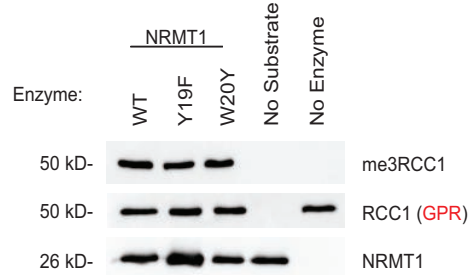
B



C



D



E

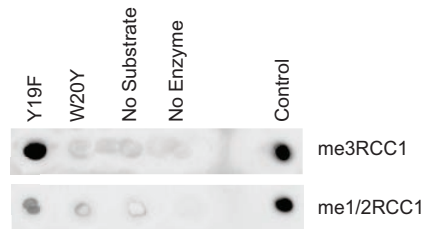


Figure 4. Y19F and W20Y NRMT1 activity is not altered by changing the RCC1 consensus sequence, but W20Y activity is lost when using peptide substrate.

(A) Western blots showing wild type (WT), Y19F, and W20Y NRMT1 all trimethylate WT (SPK) full-length recombinant RCC1 (me3RCC1). Mutation of the RCC1 consensus sequence to (B) SPR, (C) GPK, or (D) GPR does not affect the ability of WT, Y19F, or W20Y to trimethylate the full-length substrate. NRMT1 blots shown to confirm equal loading of enzyme. (E) Dot blot showing W20Y trimethyl (me3RCC1) and mono-/dimethyl (me1/2RCC1) activity is lost when the substrate is switched to a wild type (SPK) RCC1 N-terminal peptide. Tri- or monomethylated RCC1 peptide is shown as a positive control (Control). Blots are representative images of three independent experiments. Work in this figure was performed by John Tooley, State University of New York at Buffalo.

Interestingly, Y19F was still able to trimethylate the peptide, while W20Y was not (Fig. 4E), indicating it is possible for a recombinant enzyme to have different activities towards full-length and peptide substrates with the same consensus sequence.

Mutations Found in Human Cancers Alter NRMT1 and NRMT2 Activities

Human cancer mutations of NRMT1 and NRMT2 were selected from the Cosmic Catalogue of Somatic Mutations in Cancer database based on their proximity to the active site or peptide-binding channel. For NRMT1, I selected Q144H (lung cancer), N209I (endometrial cancer), and P211S (lung cancer). Both the N209I and P211S mutations are in the peptide binding channel of NRMT1, (131) while the Q144H mutation is adjacent to H140, a third aromatic residue in the active site (46). Unlike Y19 and W20, this histidine is conserved between NRMT1 and NRMT2 (46). For NRMT2, I selected V224L (breast cancer). This valine is analogous to M169 in NRMT1, (46) which is directly adjacent to N168, an amino acid that forms both hydrogen bonds and electrostatic interactions with substrate (131,132).

In vitro methylation assays with the full-length recombinant mutants and full-length recombinant RCC1 as a substrate, showed the Q144H lung cancer mutation exhibited similar levels of mono-/dimethylation (Fig. 2A) and trimethylation (Fig. 2B) as WT NRMT1. In contrast, the N209I endometrial and P211S lung cancer mutants displayed significantly increased levels of mono-/dimethylation (Fig. 2A,C) and significantly decreased levels of trimethylation (Fig. 2B,D) compared to WT NRMT1, indicating these mutations in patients could decrease global N-terminal methylation levels in favor of mono-/dimethylation. As seen with WT NRMT2, the NRMT2 V224L breast cancer mutation exhibited no trimethylase activity (Fig. 3B), but it also exhibited significantly decreased monomethylase activity as compared to control (Fig. 3A and C). This indicates patients harboring this mutation would have lower levels of priming activity by NRMT2 and potentially less trimethylation by NRMT1 as a consequence (46).

Mass Spectrometry Verification of N209I and P211S Shifted Methylation Activity

As the N-terminal mono-/dimethyl RCC1 antibody (me1/2RCC1) that was created cannot discriminate between

mono- and dimethylation, mass spectrometry (MS) analysis was used to determine if the N209I and P211S NRMT1 mutants were capable of monomethylation, dimethylation, or both. The results from the MS analysis (Fig. 5, Fig. 6A-J) showed that, of the recombinant RCC1 that underwent successful cleavage of the initiating methionine (a portion of recombinant RCC1 fails to undergo this cleavage and is unable to be methylated *in vitro*), 63% was trimethylated by WT NRMT1 and the remaining 37% remained unmethylated (46). This is consistent with previous results showing WT NRMT1 will almost completely trimethylate RCC1 after one hour *in vitro* (46).

With the N209I mutation, unmethylated RCC1 levels increased to 73%, while RCC1 trimethylation levels dropped to 13%, dimethylation levels increased to 7% and monomethylation levels increased to 6%. With the P211S mutant, unmethylated RCC1 levels also increased to 73%, trimethylation was further decreased to 5%, dimethylation increased to 13%, and monomethylation increased to 9%. The MS analysis is consistent with the western blot results, indicating these mutants exhibit decreased trimethylase activity and increased mono- and dimethylase activity. They also indicate, that unlike the EZH2 mutants which switch catalytic activity from a monomethylase to

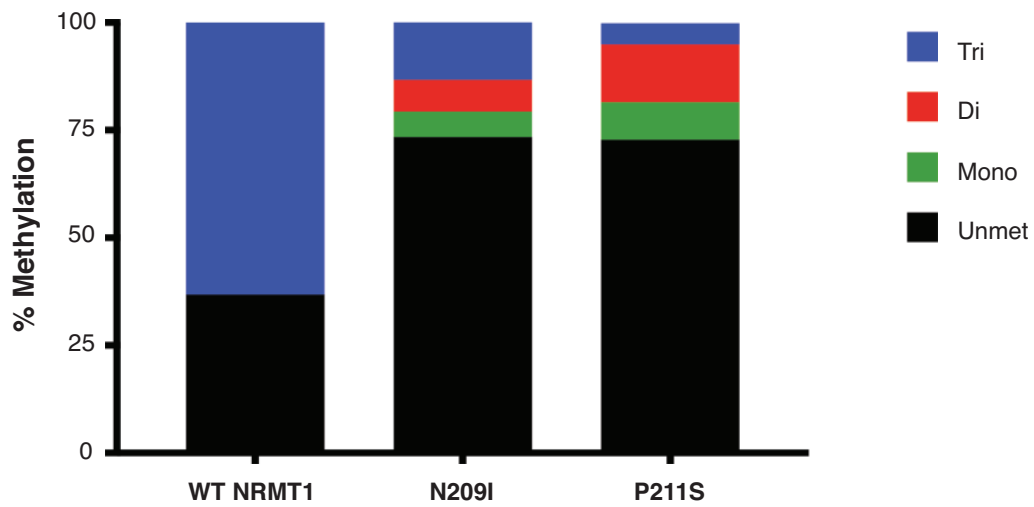
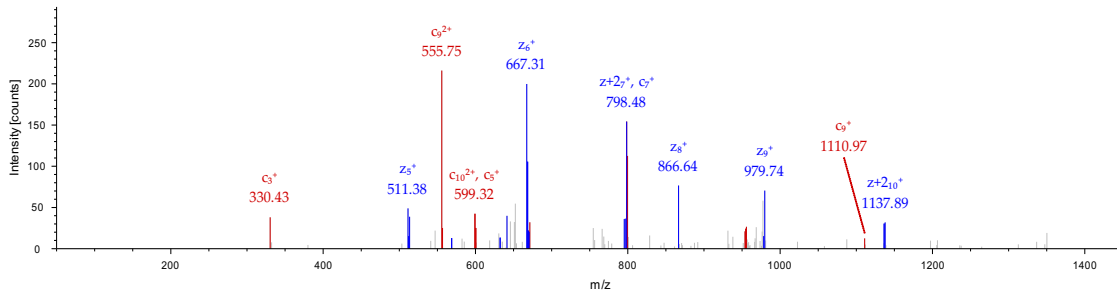


Figure 5. Mass spectrometry analysis of WT and mutant NRMT1.

Of the recombinant RCC1 with cleavage of the initiating methionine, 63% was N-terminally trimethylated by recombinant WT NRMT1. The remaining 37% remained unmethylated. With the N209I mutation, unmethylated RCC1 levels increased to 73%, while RCC1 trimethylation levels dropped to 13%, dimethylation levels increased to 7%, and monomethylation levels increased to 6%. With the P211S mutant, unmethylated RCC1 levels also increased to 73%, trimethylation was further decreased to 5%, dimethylation increased to 13%, and monomethylation increased to 9%. I prepared the graph contained in this figure, but the mass spectrometry analysis was performed by the University of Louisville Mass Spectrometry Core Laboratory and represents one independent experiment.

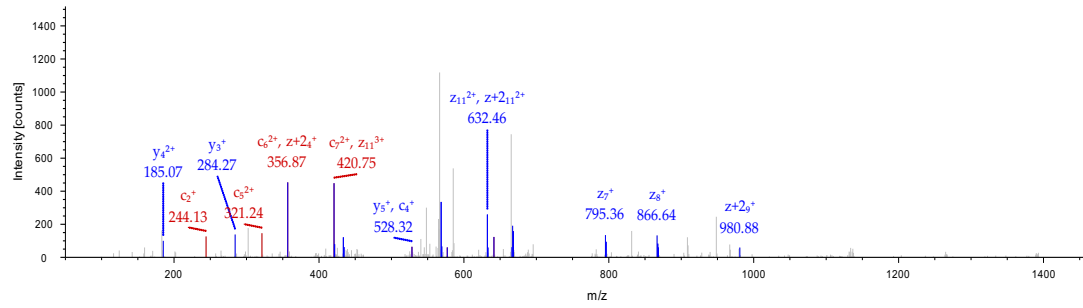
A. Peptide: SPKRIAKRRSPPA



| #1 | c ⁺ | c ²⁺ | Seq. | y ⁺ | y ²⁺ | z ⁺ | z ²⁺ | z ⁺² | z ⁺²⁺ | #2 |
|----|----------------|-----------------|------|----------------|-----------------|----------------|-----------------|-----------------|------------------|----|
| 1 | 105.06586 | 53.03657 | S | | | | | | | 13 |
| 2 | 202.11863 | 101.56295 | P | 1376.85979 | 688.93353 | 1360.84107 | 680.92417 | 1362.85672 | 681.93200 | 12 |
| 3 | 330.21360 | 165.61044 | K | 1279.80702 | 640.40715 | 1263.78830 | 632.39779 | 1265.80395 | 633.40561 | 11 |
| 4 | 486.31472 | 243.66100 | R | 1151.71205 | 576.35966 | 1135.69333 | 568.35030 | 1137.70898 | 569.35813 | 10 |
| 5 | 599.39879 | 300.20303 | I | 995.61093 | 498.30910 | 979.59221 | 490.29974 | 981.60786 | 491.30757 | 9 |
| 6 | 670.43591 | 335.72159 | A | 882.52686 | 441.76707 | 866.50814 | 433.75771 | 868.52379 | 434.76553 | 8 |
| 7 | 798.53088 | 399.76908 | K | 811.48974 | 406.24851 | 795.47102 | 398.23915 | 797.48667 | 399.24697 | 7 |
| 8 | 954.63200 | 477.81964 | R | 683.39477 | 342.20102 | 667.37605 | 334.19166 | 669.39170 | 335.19949 | 6 |
| 9 | 1110.73312 | 555.87020 | R | 527.29365 | 264.15046 | 511.27493 | 256.14110 | 513.29058 | 257.14893 | 5 |
| 10 | 1197.76515 | 599.38621 | S | 371.19253 | 186.09990 | 355.17381 | 178.09054 | 357.18946 | 179.09837 | 4 |
| 11 | 1294.81792 | 647.91260 | P | 284.16050 | 142.58389 | 268.14178 | 134.57453 | 270.15743 | 135.58235 | 3 |
| 12 | 1391.87069 | 696.43898 | P | 187.10773 | 94.05750 | 171.08901 | 86.04814 | 173.10466 | 87.05597 | 2 |
| 13 | | | A | 90.05496 | 45.53112 | 74.03624 | 37.52176 | 76.05189 | 38.52958 | 1 |



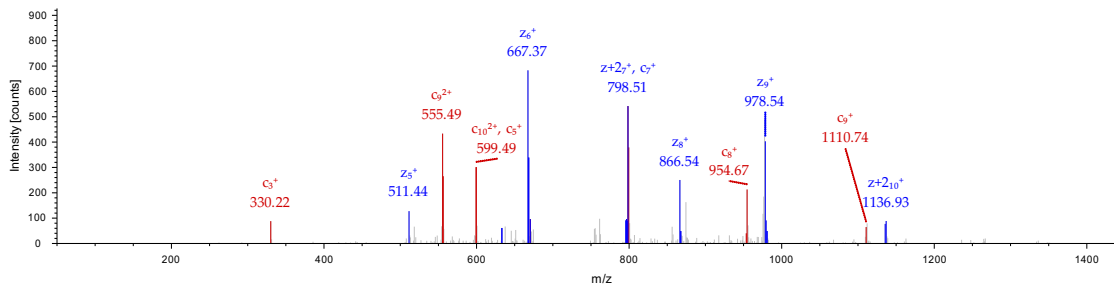
B. Peptide: SPKRIAKRRSPPA, S1-Trimethyl



| #1 | c ⁺ | c ²⁺ | c ³⁺ | Seq. | y ⁺ | y ²⁺ | y ³⁺ | z ⁺ | z ²⁺ | z ³⁺ | z+2 ⁺ | z+2 ²⁺ | z+2 ³⁺ | #2 |
|----|----------------|-----------------|-----------------|-------------|----------------|-----------------|-----------------|----------------|-----------------|-----------------|------------------|-------------------|-------------------|----|
| 1 | 147.11281 | 74.06004 | 49.70912 | S-Trimethyl | | | | | | | | | | 13 |
| 2 | 244.16558 | 122.58643 | 82.06004 | P | 1376.85979 | 688.93353 | 459.62478 | 1360.84107 | 680.92417 | 454.28521 | 1362.85672 | 681.93200 | 454.95709 | 12 |
| 3 | 372.26055 | 186.63391 | 124.75837 | K | 1279.80702 | 640.40715 | 427.27386 | 1263.78830 | 632.39779 | 421.93428 | 1265.80395 | 633.40561 | 422.60617 | 11 |
| 4 | 528.36167 | 264.68447 | 176.79207 | R | 1151.71205 | 576.35966 | 384.57553 | 1135.69333 | 568.35030 | 379.23596 | 1137.70898 | 569.35813 | 379.90784 | 10 |
| 5 | 641.44574 | 321.22651 | 214.48676 | I | 995.61093 | 498.30910 | 332.54183 | 979.59221 | 490.29974 | 327.20225 | 981.60786 | 491.30757 | 327.87414 | 9 |
| 6 | 712.48286 | 356.74507 | 238.16580 | A | 882.52686 | 441.76707 | 294.84714 | 866.50814 | 433.75771 | 289.50756 | 868.52379 | 434.76553 | 290.17945 | 8 |
| 7 | 840.57783 | 420.79255 | 280.86413 | K | 811.48974 | 406.24851 | 271.16810 | 795.47102 | 398.23915 | 265.82852 | 797.48667 | 399.24697 | 266.50041 | 7 |
| 8 | 996.67895 | 498.84311 | 332.89783 | R | 683.39477 | 342.20102 | 228.46977 | 667.37605 | 334.19166 | 223.13020 | 669.39170 | 335.19949 | 223.80208 | 6 |
| 9 | 1152.78007 | 576.89367 | 384.93154 | R | 527.29365 | 264.15046 | 176.43607 | 511.27493 | 256.14110 | 171.09649 | 513.29058 | 257.14893 | 171.76838 | 5 |
| 10 | 1238.81210 | 620.40969 | 413.94222 | S | 371.19253 | 186.09990 | 124.40236 | 355.17381 | 178.09054 | 119.06279 | 357.18946 | 179.09837 | 119.73467 | 4 |
| 11 | 1338.86487 | 668.93607 | 446.29314 | P | 284.16050 | 142.58389 | 95.39168 | 268.14178 | 134.57453 | 90.05211 | 270.15743 | 135.58235 | 90.72399 | 3 |
| 12 | 1433.91764 | 717.46246 | 478.64406 | P | 187.10773 | 94.05750 | 63.04076 | 171.08901 | 86.04814 | 57.70119 | 173.10466 | 87.05597 | 58.37307 | 2 |
| 13 | | | | A | 90.05496 | 45.53112 | 30.68984 | 74.03624 | 37.52176 | 25.35026 | 76.05189 | 38.52958 | 26.02215 | 1 |



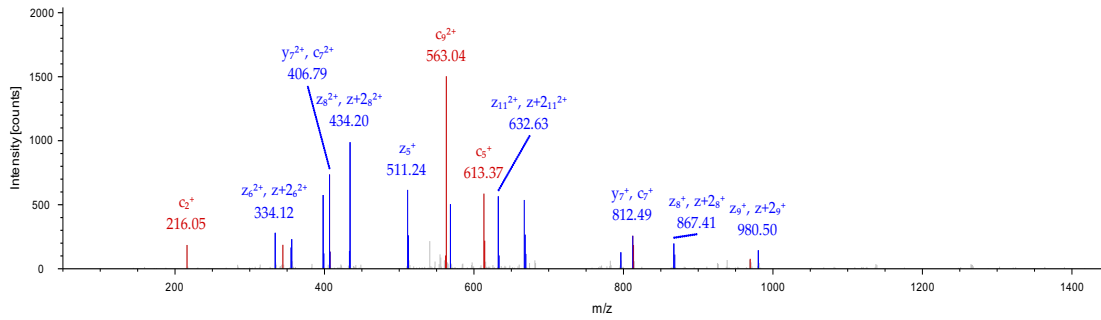
C. Peptide: SPKRIAKRRSPPA



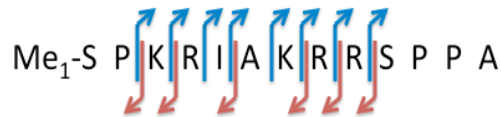
| #1 | c ⁺ | c ²⁺ | Seq. | y ⁺ | y ²⁺ | z ⁺ | z ²⁺ | z+2 ⁺ | z+2 ²⁺ | #2 |
|----|----------------|-----------------|------|----------------|-----------------|----------------|-----------------|------------------|-------------------|----|
| 1 | 105.06586 | 53.03657 | S | | | | | | | 13 |
| 2 | 202.11863 | 101.56295 | P | 1376.85979 | 688.93353 | 1360.84107 | 680.92417 | 1362.85672 | 681.93200 | 12 |
| 3 | 330.21360 | 165.61044 | K | 1279.80702 | 640.40715 | 1263.78830 | 632.39779 | 1265.80395 | 633.40561 | 11 |
| 4 | 486.31472 | 243.66100 | R | 1151.71205 | 576.35966 | 1135.69333 | 568.35030 | 1137.70898 | 569.35813 | 10 |
| 5 | 599.39879 | 300.20303 | I | 995.61093 | 498.30910 | 979.59221 | 490.29974 | 981.60786 | 491.30757 | 9 |
| 6 | 670.43591 | 335.72159 | A | 882.52686 | 441.76707 | 866.50814 | 433.75771 | 868.52379 | 434.76553 | 8 |
| 7 | 798.53088 | 399.76908 | K | 811.48974 | 406.24851 | 795.47102 | 398.23915 | 797.48667 | 399.24697 | 7 |
| 8 | 954.63200 | 477.81964 | R | 683.39477 | 342.20102 | 667.37605 | 334.19166 | 669.39170 | 335.19949 | 6 |
| 9 | 1110.73312 | 555.87020 | R | 527.29365 | 264.15046 | 511.27493 | 256.14110 | 513.29058 | 257.14893 | 5 |
| 10 | 1197.76515 | 599.38621 | S | 371.19253 | 186.09990 | 355.17381 | 178.09054 | 357.18946 | 179.09837 | 4 |
| 11 | 1294.81792 | 647.91260 | P | 284.16050 | 142.58389 | 268.14178 | 134.57453 | 270.15743 | 135.58235 | 3 |
| 12 | 1391.87069 | 696.43898 | P | 187.10773 | 94.05750 | 171.08901 | 86.04814 | 173.10466 | 87.05597 | 2 |
| 13 | | | A | 90.05496 | 45.53112 | 74.03624 | 37.52176 | 76.05189 | 38.52958 | 1 |



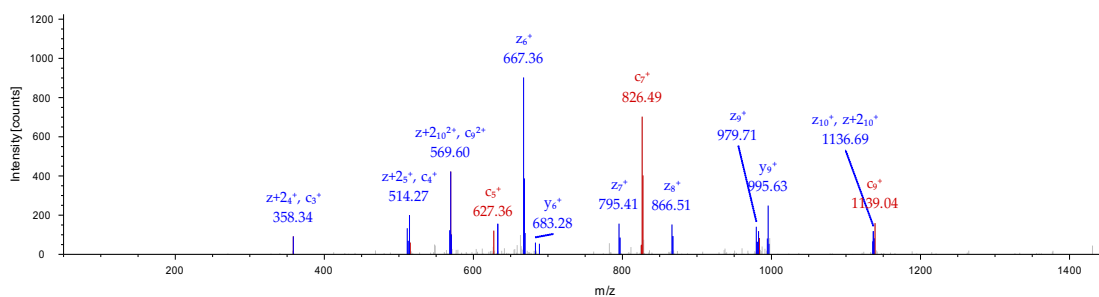
D. Peptide: SPKRIAKRRSPPA, S1-Methyl (14.01564 Da)



| #1 | c' | c ²⁺ | c ³⁺ | Seq. | y' | y ²⁺ | y ³⁺ | z' | z ²⁺ | z ³⁺ | z+2' | z+2 ²⁺ | z+2 ³⁺ | #2 |
|----|------------|-----------------|-----------------|----------|------------|-----------------|-----------------|------------|-----------------|-----------------|------------|-------------------|-------------------|----|
| 1 | 119.08151 | 60.04439 | 40.36535 | S-Methyl | | | | | | | | | | 13 |
| 2 | 216.13428 | 108.57078 | 72.71628 | P | 1376.85979 | 688.93353 | 459.62478 | 1360.84107 | 680.92417 | 454.28521 | 1362.85672 | 681.93200 | 454.95709 | 12 |
| 3 | 344.22925 | 172.61826 | 115.41460 | K | 1279.80702 | 640.40715 | 427.27386 | 1263.78830 | 632.39779 | 421.93428 | 1265.80395 | 633.40561 | 422.60617 | 11 |
| 4 | 500.33037 | 250.66882 | 167.44831 | R | 1151.71205 | 576.35966 | 384.57553 | 1135.69333 | 568.35030 | 379.23596 | 1137.70898 | 569.35813 | 379.90784 | 10 |
| 5 | 613.41444 | 307.21086 | 205.14300 | I | 995.61093 | 498.30910 | 332.54183 | 979.59221 | 490.29974 | 327.20225 | 981.60786 | 491.30757 | 327.87414 | 9 |
| 6 | 684.45156 | 342.72942 | 228.82204 | A | 882.52686 | 441.76707 | 294.84714 | 866.50614 | 433.75771 | 289.50756 | 868.52379 | 434.76553 | 290.17945 | 8 |
| 7 | 812.54653 | 406.77690 | 271.52036 | K | 811.48974 | 406.24851 | 271.16810 | 795.47102 | 398.23915 | 265.82852 | 797.48867 | 399.24697 | 266.50041 | 7 |
| 8 | 968.64765 | 484.82746 | 323.55407 | R | 683.39477 | 342.20102 | 228.46977 | 667.37605 | 334.19166 | 223.13020 | 669.39170 | 335.19949 | 223.80208 | 6 |
| 9 | 1124.74877 | 562.87802 | 375.58777 | R | 527.29365 | 264.15046 | 176.43607 | 511.27493 | 256.14110 | 171.09649 | 513.29058 | 257.14893 | 171.76838 | 5 |
| 10 | 1211.78080 | 606.39404 | 404.59845 | S | 371.19253 | 186.09990 | 124.40236 | 355.17381 | 178.09054 | 119.06279 | 357.18946 | 179.09837 | 119.73467 | 4 |
| 11 | 1308.83357 | 654.92042 | 436.94937 | P | 284.16060 | 142.58389 | 95.39168 | 268.14178 | 134.57453 | 90.05211 | 270.15743 | 135.58235 | 90.72399 | 3 |
| 12 | 1405.88634 | 703.44681 | 469.30030 | P | 187.10773 | 94.05750 | 63.04076 | 171.08901 | 86.04814 | 57.70119 | 173.10466 | 87.05597 | 58.37307 | 2 |
| 13 | | | | A | 90.05496 | 45.53112 | 30.68984 | 74.03624 | 37.52176 | 25.35026 | 76.05189 | 38.52958 | 26.02215 | 1 |



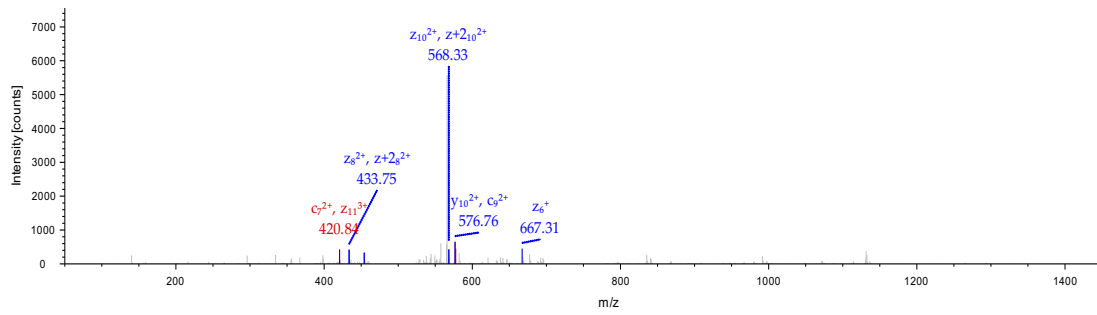
E. Peptide: SPKRIAKRRSPPA, S1-Dimethyl (28.03130 Da)



| #1 | c* | c2* | Seq. | y* | y2* | z* | z2* | z+2* | z+22* | #2 |
|----|------------|-----------|------------|------------|-----------|------------|-----------|------------|-----------|----|
| 1 | 133.09716 | 67.05222 | S-Dimethyl | | | | | | | 13 |
| 2 | 230.14993 | 115.57860 | P | 1376.85979 | 688.93353 | 1360.84107 | 680.92417 | 1362.85672 | 681.93200 | 12 |
| 3 | 358.24490 | 179.62609 | K | 1279.80702 | 640.40715 | 1263.78830 | 632.39779 | 1265.80395 | 633.40561 | 11 |
| 4 | 514.34602 | 257.67665 | R | 1151.71205 | 576.35966 | 1135.69333 | 568.35030 | 1137.70898 | 569.35813 | 10 |
| 5 | 627.43009 | 314.21868 | I | 995.61093 | 498.30910 | 979.59221 | 490.29974 | 981.60786 | 491.30757 | 9 |
| 6 | 698.46721 | 349.73724 | A | 882.52686 | 441.76707 | 866.50814 | 433.75771 | 868.52379 | 434.76553 | 8 |
| 7 | 826.56218 | 413.78473 | K | 811.48974 | 406.24851 | 795.47102 | 398.23915 | 797.48667 | 399.24697 | 7 |
| 8 | 982.66330 | 491.83529 | R | 683.39477 | 342.20102 | 667.37605 | 334.19166 | 669.39170 | 335.19949 | 6 |
| 9 | 1138.76442 | 569.88585 | R | 527.29365 | 264.15046 | 511.27493 | 256.14110 | 513.29058 | 257.14893 | 5 |
| 10 | 1225.79645 | 613.40186 | S | 371.19253 | 186.09990 | 355.17381 | 178.09054 | 357.18946 | 179.09837 | 4 |
| 11 | 1322.84922 | 661.92825 | P | 284.16050 | 142.58389 | 268.14178 | 134.57453 | 270.15743 | 135.58235 | 3 |
| 12 | 1419.90199 | 710.45463 | P | 187.10773 | 94.05750 | 171.08901 | 86.04814 | 173.10466 | 87.05597 | 2 |
| 13 | | | A | 90.05496 | 45.53112 | 74.03624 | 37.52176 | 76.05189 | 38.52958 | 1 |



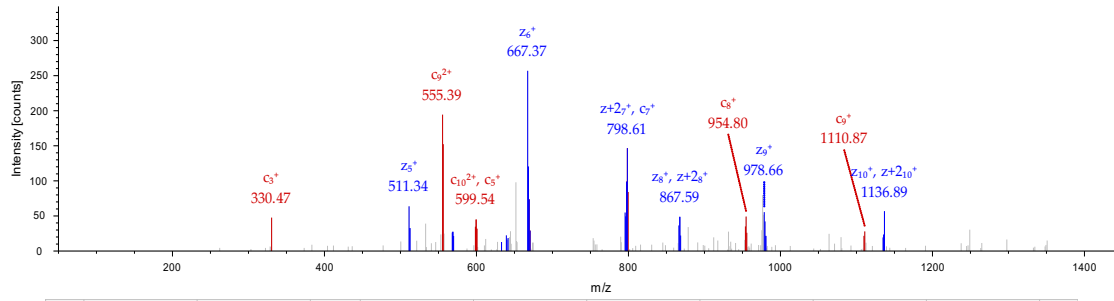
F. Peptide: SPKRIAKRRSPPA, S1-Trimethyl



| #1 | c ⁻ | c ²⁺ | c ³⁺ | Seq. | y ⁻ | y ²⁺ | y ³⁺ | z ⁻ | z ²⁺ | z ³⁺ | z ⁴⁺ | z ⁵⁺ | z ⁶⁺ | #2 |
|----|----------------|-----------------|-----------------|-------------|----------------|-----------------|-----------------|----------------|-----------------|-----------------|-----------------|-----------------|-----------------|----|
| 1 | 147.11281 | 74.06004 | 49.70912 | S-Trimethyl | | | | | | | | | | 13 |
| 2 | 244.16558 | 122.58643 | 82.06004 | P | 1376.85979 | 688.93353 | 459.62478 | 1360.84107 | 680.92417 | 454.28521 | 1362.85672 | 681.93200 | 454.95709 | 12 |
| 3 | 372.26055 | 186.63391 | 124.75837 | K | 1279.80702 | 640.40715 | 427.27386 | 1263.78830 | 632.39779 | 421.93428 | 1265.80395 | 633.40561 | 422.60617 | 11 |
| 4 | 528.36167 | 264.68447 | 176.79207 | R | 1151.71205 | 576.35966 | 384.57553 | 1135.69333 | 568.35030 | 379.23596 | 1137.70898 | 569.35813 | 379.90784 | 10 |
| 5 | 641.44574 | 321.22651 | 214.48676 | I | 995.61093 | 498.30910 | 332.54183 | 979.59221 | 490.29974 | 327.20225 | 981.60786 | 491.30757 | 327.87414 | 9 |
| 6 | 712.48286 | 356.74507 | 238.16580 | A | 882.52686 | 441.76707 | 294.84714 | 866.50814 | 433.75771 | 289.50756 | 868.52379 | 434.76553 | 290.17945 | 8 |
| 7 | 840.57783 | 420.79255 | 280.86413 | K | 811.48974 | 406.24851 | 271.16810 | 795.47102 | 398.23915 | 265.82852 | 797.48667 | 399.24697 | 266.50041 | 7 |
| 8 | 996.67895 | 498.84311 | 332.89783 | R | 683.39477 | 342.20102 | 228.46977 | 667.37605 | 334.19166 | 223.13020 | 669.39170 | 335.19949 | 223.80208 | 6 |
| 9 | 1152.78007 | 576.89367 | 384.93154 | R | 527.29365 | 264.15046 | 176.43607 | 511.27493 | 256.14110 | 171.09649 | 513.29058 | 257.14893 | 171.76838 | 5 |
| 10 | 1239.81210 | 620.40969 | 413.94222 | S | 371.19253 | 186.09990 | 124.40236 | 355.17381 | 178.09054 | 119.06279 | 357.18946 | 179.09837 | 119.73467 | 4 |
| 11 | 1336.86487 | 668.93607 | 446.29314 | P | 284.16050 | 142.58389 | 95.39168 | 268.14178 | 134.57453 | 90.05211 | 270.15743 | 135.58235 | 90.72399 | 3 |
| 12 | 1433.91764 | 717.46246 | 478.64406 | P | 187.10773 | 94.05750 | 63.04076 | 171.08901 | 86.04814 | 57.70119 | 173.10466 | 87.05597 | 58.37307 | 2 |
| 13 | | | | A | 90.05496 | 45.53112 | 30.68984 | 74.03624 | 37.52176 | 25.35026 | 76.05189 | 38.52958 | 26.02215 | 1 |



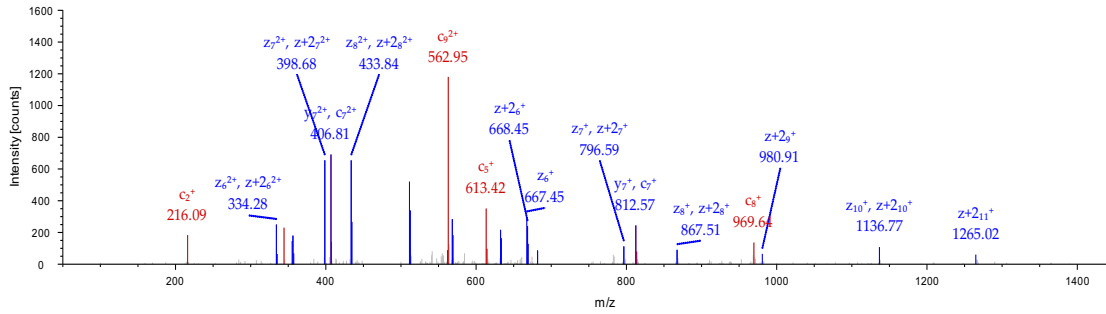
G. Peptide: SPKRIAKRRSPPA



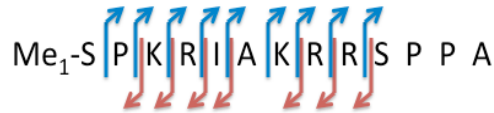
| #1 | c ⁺ | c ²⁺ | Seq. | y ⁺ | y ²⁺ | z ⁺ | z ²⁺ | z+2 ⁺ | z+2 ²⁺ | #2 |
|----|----------------|-----------------|------|----------------|-----------------|----------------|-----------------|------------------|-------------------|----|
| 1 | 105.06586 | 53.03657 | S | | | | | | | 13 |
| 2 | 202.11863 | 101.56295 | P | 1376.85979 | 688.93353 | 1360.84107 | 680.92417 | 1362.85672 | 681.93200 | 12 |
| 3 | 330.21360 | 165.61044 | K | 1279.80702 | 640.40715 | 1263.78830 | 632.39779 | 1265.80395 | 633.40561 | 11 |
| 4 | 486.31472 | 243.66100 | R | 1151.71205 | 576.35966 | 1135.69333 | 568.35030 | 1137.70898 | 569.35813 | 10 |
| 5 | 599.39879 | 300.20303 | I | 995.61093 | 498.30910 | 979.59221 | 490.29974 | 981.60786 | 491.30757 | 9 |
| 6 | 670.43591 | 335.72159 | A | 882.52686 | 441.76707 | 866.50814 | 433.75771 | 868.52379 | 434.76553 | 8 |
| 7 | 798.53088 | 399.76908 | K | 811.48974 | 406.24851 | 795.47102 | 398.23915 | 797.48667 | 399.24697 | 7 |
| 8 | 954.63200 | 477.81964 | R | 683.39477 | 342.20102 | 667.37605 | 334.19166 | 669.39170 | 335.19949 | 6 |
| 9 | 1110.73312 | 555.87020 | R | 527.29365 | 264.15046 | 511.27493 | 256.14110 | 513.29058 | 257.14893 | 5 |
| 10 | 1197.76515 | 599.38621 | S | 371.19253 | 186.09990 | 355.17381 | 178.09054 | 357.18946 | 179.09837 | 4 |
| 11 | 1294.81792 | 647.91260 | P | 284.16050 | 142.58389 | 268.14178 | 134.57453 | 270.15743 | 135.58235 | 3 |
| 12 | 1391.87069 | 696.43898 | P | 187.10773 | 94.05750 | 171.08901 | 86.04814 | 173.10466 | 87.05597 | 2 |
| 13 | | | A | 90.05496 | 45.53112 | 74.03624 | 37.52176 | 76.05189 | 38.52958 | 1 |



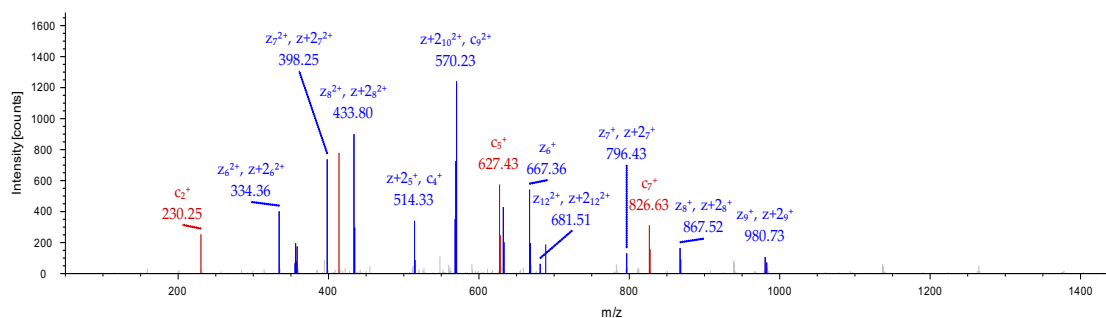
H. Peptide: SPKRIAKRRSPPA, S1-Methyl (14.01564 Da)



| #1 | c ⁻ | c ²⁺ | c ³⁺ | Seq. | y ⁻ | y ²⁺ | y ³⁺ | z ⁻ | z ²⁺ | z ³⁺ | z ²⁺ | z ²⁺ | z ²⁺ | #2 |
|----|----------------|-----------------|-----------------|----------|----------------|-----------------|-----------------|----------------|-----------------|-----------------|-----------------|-----------------|-----------------|----|
| 1 | 119.08151 | 60.04439 | 40.36535 | S-Methyl | | | | | | | | | | 13 |
| 2 | 216.13428 | 108.57078 | 72.71628 | P | 1376.85979 | 688.93353 | 459.62478 | 1360.84107 | 680.92417 | 454.28521 | 1362.85672 | 681.93200 | 454.95709 | 12 |
| 3 | 344.22925 | 172.61826 | 115.41460 | K | 1279.80702 | 640.40715 | 427.27386 | 1263.78830 | 632.39779 | 421.93428 | 1265.80395 | 633.40561 | 422.60617 | 11 |
| 4 | 500.33037 | 250.66882 | 167.44831 | R | 1151.71205 | 576.35966 | 384.57553 | 1135.69333 | 568.35030 | 379.23996 | 1137.70898 | 569.35813 | 379.90784 | 10 |
| 5 | 613.41444 | 307.21086 | 205.14300 | I | 995.61093 | 498.30910 | 332.54183 | 979.59221 | 490.29974 | 327.20225 | 981.60786 | 491.30757 | 327.87414 | 9 |
| 6 | 684.45156 | 342.72942 | 228.82204 | A | 882.52686 | 441.76707 | 294.84714 | 866.50814 | 433.75771 | 289.50756 | 868.52379 | 434.76553 | 290.17945 | 8 |
| 7 | 812.54653 | 406.77690 | 271.52036 | K | 811.48974 | 406.24851 | 271.16810 | 795.47102 | 398.23915 | 265.82852 | 797.48667 | 399.24697 | 266.50041 | 7 |
| 8 | 968.64765 | 484.82746 | 323.55407 | R | 683.39477 | 342.20102 | 228.46977 | 667.37605 | 334.19166 | 223.13020 | 669.39170 | 335.19949 | 223.80208 | 6 |
| 9 | 1124.74877 | 562.87802 | 375.58777 | R | 527.29365 | 264.15046 | 176.43607 | 511.27493 | 256.14110 | 171.09649 | 513.29058 | 257.14893 | 171.76838 | 5 |
| 10 | 1211.78080 | 606.39404 | 404.59845 | S | 371.19253 | 186.09990 | 124.40236 | 355.17381 | 178.09054 | 119.06279 | 357.18946 | 179.09837 | 119.73467 | 4 |
| 11 | 1308.83357 | 654.92042 | 436.94937 | P | 284.16050 | 142.58389 | 95.39168 | 268.14178 | 134.57453 | 90.05211 | 270.15743 | 135.58235 | 90.72399 | 3 |
| 12 | 1405.88634 | 703.44681 | 469.30030 | P | 187.10773 | 94.05750 | 63.04076 | 171.08901 | 86.04814 | 57.70119 | 173.10466 | 87.05597 | 58.37307 | 2 |
| 13 | | | | A | 90.05496 | 45.53112 | 30.68984 | 74.03624 | 37.52176 | 25.35026 | 76.05189 | 38.52958 | 26.02215 | 1 |



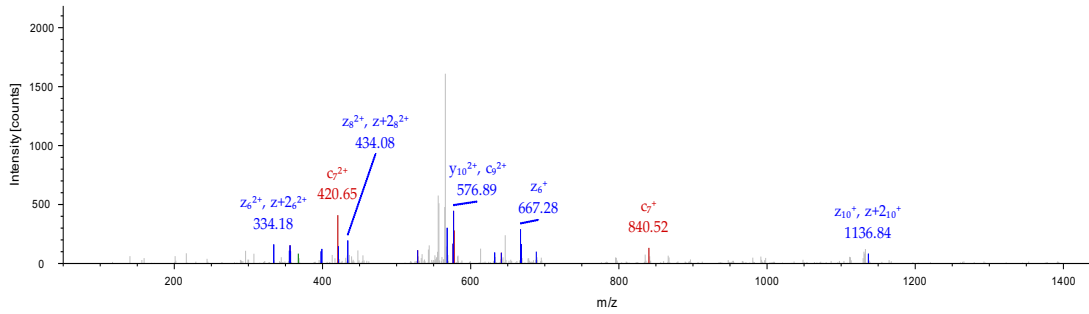
I. Peptide: SPKRIAKRRSPPA, S1-Dimethyl (28.03130 Da)



| #1 | c ⁺ | c ²⁺ | c ³⁺ | Seq. | y ⁺ | y ²⁺ | y ³⁺ | z ⁺ | z ²⁺ | z ³⁺ | z ⁴⁺ | z ⁵⁺ | #2 |
|----|----------------|-----------------|-----------------|------------|----------------|-----------------|-----------------|----------------|-----------------|-----------------|-----------------|-----------------|-----------|
| 1 | 133.09716 | 67.05222 | 45.03724 | S-Dimethyl | | | | | | | | | 13 |
| 2 | 230.14993 | 115.57860 | 77.38816 | P | 1376.85979 | 688.93353 | 459.62478 | 1360.84107 | 680.92417 | 454.28521 | 1362.85672 | 681.93200 | 454.95709 |
| 3 | 358.24490 | 179.62609 | 120.08648 | K | 1279.80702 | 640.40715 | 427.27386 | 1263.78830 | 632.39779 | 421.93428 | 1265.80395 | 633.40561 | 422.60617 |
| 4 | 514.34602 | 257.67665 | 172.12019 | R | 1151.71205 | 576.35966 | 384.57553 | 1135.69333 | 568.35030 | 379.23596 | 1137.70898 | 569.35813 | 379.90784 |
| 5 | 627.43009 | 314.21868 | 209.81488 | I | 995.61093 | 498.30910 | 332.54183 | 979.59221 | 490.29974 | 327.20225 | 981.60786 | 491.30757 | 327.87414 |
| 6 | 698.46721 | 349.73724 | 233.49392 | A | 882.52686 | 441.76707 | 294.84714 | 866.50814 | 433.75771 | 289.50756 | 868.52379 | 434.76553 | 290.17945 |
| 7 | 826.56218 | 413.78473 | 276.19224 | K | 811.48974 | 406.24851 | 271.16810 | 795.47102 | 398.23915 | 265.82852 | 797.48667 | 399.24697 | 266.50041 |
| 8 | 982.66330 | 491.83529 | 328.22595 | R | 683.39477 | 342.20102 | 228.46977 | 667.37605 | 334.19166 | 223.13020 | 669.39170 | 335.19949 | 223.80208 |
| 9 | 1138.76442 | 569.88585 | 380.25966 | R | 527.29365 | 264.15046 | 176.43607 | 511.27493 | 256.14110 | 171.09649 | 513.29058 | 257.14893 | 171.76838 |
| 10 | 1225.79645 | 613.40186 | 409.27033 | S | 371.19253 | 186.09990 | 124.40236 | 355.17381 | 178.09054 | 119.06279 | 357.18946 | 179.09837 | 119.73467 |
| 11 | 1322.84922 | 661.92825 | 441.62126 | P | 284.16050 | 142.58389 | 95.39168 | 268.14178 | 134.57453 | 90.05211 | 270.15743 | 135.58235 | 90.72399 |
| 12 | 1419.90199 | 710.45463 | 473.97218 | P | 187.10773 | 94.05750 | 63.04076 | 171.08901 | 86.04814 | 57.70119 | 173.10466 | 87.05597 | 58.37307 |
| 13 | | | | A | 90.05496 | 45.53112 | 30.68984 | 74.03624 | 37.52176 | 25.35026 | 76.05189 | 38.52958 | 26.02215 |



J. Peptide: SPKRIAKRRSPPA, S1-Trimethyl



| #1 | c ⁺ | c ²⁺ | c ³⁺ | Seq. | y ⁻ | y ²⁺ | y ³⁺ | z ⁻ | z ²⁺ | z ³⁺ | z ⁴⁺ | z ⁵⁺ | z ⁶⁺ | #2 |
|----|----------------|-----------------|-----------------|-------------|----------------|-----------------|-----------------|----------------|-----------------|-----------------|-----------------|-----------------|-----------------|----|
| 1 | 147.11281 | 74.06004 | 49.70912 | S-Trimethyl | | | | | | | | | | 13 |
| 2 | 244.16558 | 122.58643 | 82.06004 | P | 1376.85979 | 688.93353 | 459.62478 | 1360.84107 | 680.92417 | 454.28521 | 1362.85672 | 681.93200 | 454.95709 | 12 |
| 3 | 372.26055 | 186.63391 | 124.75837 | K | 1279.80702 | 640.40715 | 427.27386 | 1263.78830 | 632.39779 | 421.93428 | 1265.80395 | 633.40561 | 422.60617 | 11 |
| 4 | 528.36167 | 264.68447 | 176.79207 | R | 1151.71205 | 576.35966 | 384.57553 | 1135.69333 | 568.35030 | 379.23596 | 1137.70898 | 569.35813 | 379.90784 | 10 |
| 5 | 641.44574 | 321.22651 | 214.48676 | I | 995.61093 | 498.30910 | 332.54183 | 979.59221 | 490.29974 | 327.20225 | 981.60786 | 491.30757 | 327.87414 | 9 |
| 6 | 712.48286 | 356.74507 | 238.16580 | A | 882.52686 | 441.76707 | 294.84714 | 866.50814 | 433.75771 | 289.50756 | 868.52379 | 434.76553 | 290.17945 | 8 |
| 7 | 840.57783 | 420.79255 | 280.86413 | K | 811.48974 | 406.24851 | 271.16810 | 795.47102 | 398.23915 | 265.82852 | 797.48667 | 399.24697 | 266.50041 | 7 |
| 8 | 996.67895 | 498.84311 | 332.89783 | R | 683.39477 | 342.20102 | 228.46977 | 667.37605 | 334.19166 | 223.13020 | 669.39170 | 335.19949 | 223.80208 | 6 |
| 9 | 1152.78007 | 576.89367 | 384.93154 | R | 527.29365 | 264.15046 | 176.43607 | 511.27493 | 256.14110 | 171.09649 | 513.29058 | 257.14893 | 171.76838 | 5 |
| 10 | 1239.81210 | 620.40969 | 413.94222 | S | 371.19253 | 186.09990 | 124.40236 | 355.17381 | 178.09054 | 119.06279 | 357.18946 | 179.09837 | 119.73467 | 4 |
| 11 | 1336.86487 | 668.93607 | 446.29314 | P | 284.16050 | 142.58389 | 95.39168 | 268.14178 | 134.57453 | 90.05211 | 270.15743 | 135.58235 | 90.72399 | 3 |
| 12 | 1433.91764 | 717.46246 | 478.64406 | P | 187.10773 | 94.05750 | 63.04076 | 171.08901 | 86.04814 | 57.70119 | 173.10466 | 87.05597 | 58.37307 | 2 |
| 13 | | | | A | 90.05496 | 45.53112 | 30.68984 | 74.03624 | 37.52176 | 25.35026 | 76.05189 | 38.52958 | 26.02215 | 1 |



Figure 6. ETD MS/MS spectra and sequence coverage of α -N-terminal peptides from recombinant RCC1 methylated by WT NRMT1, N209I, or P211S.

WT NRMT1 produced (A) 37% unmethylated and (B) 63% trimethylated RCC1. N209I produced (C) 73% unmethylated, (D) 6% monomethylated, (E) 7% dimethylated, and (F) 13% trimethylated RCC1. P211S produced (G) 73% unmethylated, (H) 9% monomethylated, (I) 13% dimethylated, and (J) 5% trimethylated RCC1. All spectra were acquired and searched using Mascot (v1.30). **c** ; **y** ; **z** ; **z + 2** fragments were used for searching and the match tolerance was 1.2 Da. Bolded red indicates observed c-ion fragment. Bolded blue indicates observed y- or z-ion fragment. Raw data shown in this figure was generated by the University of Louisville Mass Spectrometry Core Laboratory and represents one independent experiment.

a trimethylase, the NRMT1 mutations are decreasing the overall efficiency of the enzyme and preventing it from both converting unmodified substrate to monomethylated and monomethylated substrate to trimethylated.

NRMT1 Cancer Mutants Remain Distributive Methyltransferases

It was previously shown that NRMT1 works as a distributive enzyme, first monomethylating its substrate, then dissociating and reattaching for each subsequent methylation step (46). Richardson et al. confirmed this distributive nature of NRMT1 and additionally showed it is working through a random sequential bi-bi mechanism (133). It was also shown that for the human RCC1 consensus sequence (Ser-Pro-Lys), affinity of NRMT1 for substrate increases with increasing substrate methylation levels, (46) and it was hypothesized that this helps the enzyme to quickly raise trimethylation levels without the accumulation of mono- or dimethylated substrate. In order to monitor if the N209I and P211S mutants were impaired in the conversion of mono-/dimethylation to trimethylation, I held enzyme and substrate concentrations constant and varied the time of the *in vitro* methylation reactions. Western blot analysis showed that WT NRMT1,

even at just 30 minutes, converted all mono-/dimethylation to trimethylation (Fig. 7A). While low levels of trimethylation can be seen at 30 minutes with both the N209I and P211S mutants, mono-/dimethylation levels are higher and stay steady (N209I) or continue to increase (P211S) up to 2 hours (Fig. 7B,C). Finally, after 2 hours, mono-/dimethylation levels begin to decrease with a corresponding increase in trimethylation, indicating conversion of one to the other (Fig. 7B,C). These data mirror the MS results (Fig. 5) and indicate that while N209I and P211S are still distributive enzymes capable of trimethylation, they are significantly slower at converting mono- and dimethylation into trimethylation.

To assay whether the activity of the mutants could be restored by a significant increase in substrate concentration, I monitored the ability of the mutants to mono-/dimethylate or trimethylate RCC1 at varying substrate concentrations. Western blot analysis of the *in vitro* methylation assays revealed that N209I and P211S require a higher substrate concentration to reach the trimethylation levels seen with WT (Fig. 7D-F). At low substrate levels (0.25 μ g), NRMT1 shows only trimethylated substrate (Fig. 7D), while neither mutation exhibits any methyltransferase activity (Fig. 7E,F). At 0.5 μ g substrate, WT NRMT1

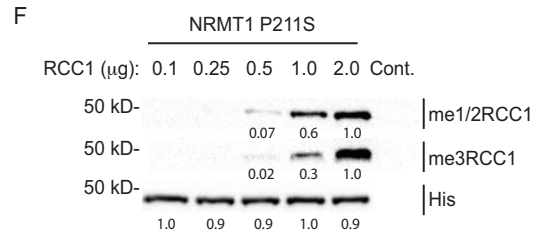
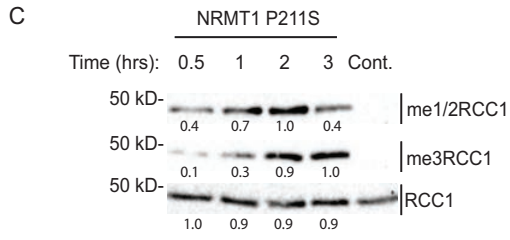
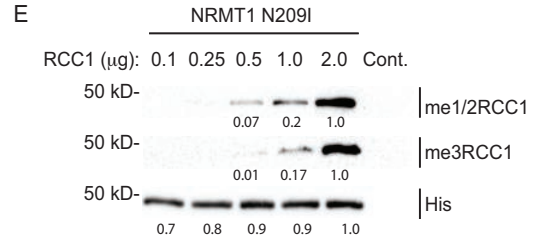
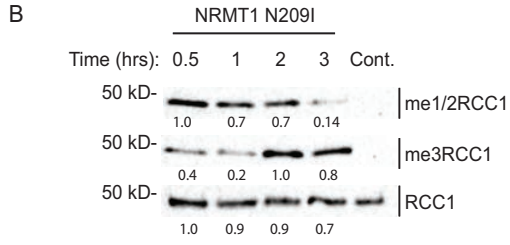
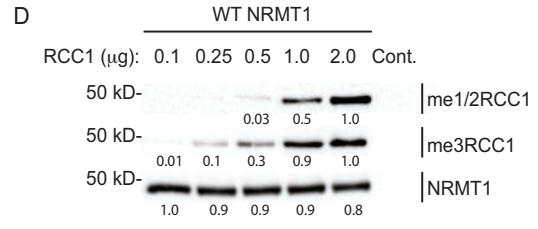
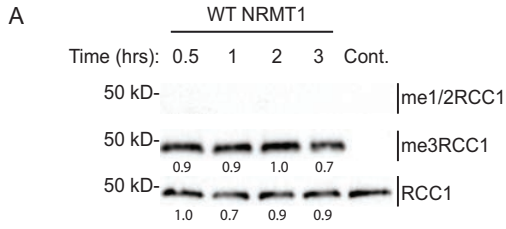


Figure 7. Catalytic studies of WT and mutant NRMT1.

(A) WT NRMT1 fully trimethylates RCC1 (me³RCC1) in less than 30 min, compared to (B) N209I and (C) P211S, which exhibit primarily monomethylation/dimethylation (me^{1/2}RCC1) until 2h, where trimethylation levels begin to rise. The corresponding decrease in monomethylation/dimethylation is evident only after 3h. These data indicate N209I and P211S are still distributive enzymes capable of trimethylation, but they are slower at converting monomethylation to trimethylation. Total RCC1 is shown as a loading control. Control (Cont.) reactions done without enzyme. (D) At low substrate levels, WT NRMT1 proceeds almost completely to trimethylation. As substrate concentration increases, the levels of monomethylation/dimethylation by NRMT1 increase because the ratio of unmodified substrate to previously methylated substrate is higher. (E-F) At low substrate levels, the NRMT1 N209I and P211S mutants show no methyltransferase activity. As substrate concentration increases, trimethylation begins to appear but does not reach WT levels until a 1:1 molar ratio of enzyme to substrate, indicating a higher substrate concentration is needed for optimum trimethylase activity. Anti-NRMT1 is shown as a loading control for WT. Anti-His is shown as a loading control for mutant NRMT1, as this NRMT1 antibody

recognizes an epitope containing N209 and P211 (47). Blots are representative images of three independent experiments. Bands were quantified using ImageJ software (NIH) and internally normalized to brightest band of each set, which was set at 1.0.

predominantly shows trimethylation (Fig. 7D), while both mutants are just beginning to exhibit mono-/dimethylase activity (Fig. 7E,F). At 1.0 μg substrate, WT NRMT1 still favors trimethylated product, while both N209I and P211S still favor mono-/dimethylation (Fig. 7D-F). It is not until the molar amount of mutant enzyme equals the molar amount of substrate (1 μg of NRMT = 40 pmol; 2 μg of RCC1 = 40 pmol) that the mutants have mono-/di- and trimethylation levels comparable to WT NRMT1 (Fig 7D-F). This indicates the mutants require a higher substrate concentration to reach maximal activity.

Molecular Modeling of N209I and P211S

The examination of the NRMT1 crystal structure (128) showed N209I and P211S to be in the peptide-binding channel near the aromatic residues (Y19, W20, H140) of the active site (132). NRMT1 is a class I methyltransferase consisting of a seven-stranded β sheet surrounded by five α -helices (128). In addition, there are three helices in the N-terminus segment, a pair of β hairpins, and a series of loops connecting the structural elements (131). It has been determined that the helices in the N-terminal segment cluster with loop 4 (L4) and loop 67 (L67) to create the

peptide-binding domain, which is integrated by residues L31, Y34, I37, W136, L210, P211, I214, V217, Y215, and E213 (131). While both N209 and P211 are in L67 (Fig. 8A), neither was previously predicted to directly interact with substrate (131).

To determine how the N209I and P211S mutations might otherwise affect the peptide-binding channel, molecular modeling was performed (134). The modeling revealed that P211 is oriented toward the peptide-binding channel, and its mutation to serine could alter the shape of the cavity itself (Fig. 8B). Alternatively, prolines confer distinct shapes to unstructured regions, so its mutation to serine could change the configuration of L₆₇ in an unpredictable manner. Mutation of N209 to isoleucine does not make any visually obvious changes to the structure of the peptide-binding channel (Fig. 8B). However, asparagine to isoleucine mutations have previously been shown to affect protein characteristics (135). The amide group of asparagine can hydrogen bond, while the isoleucine side chain is hydrophobic and does not. While these hydrogen bonds might not be directly formed with substrate, they may be necessary for proper orientation of L₆₇. Taken together, I hypothesize that residues in the peptide-binding channel that do not directly interact with the substrate can still

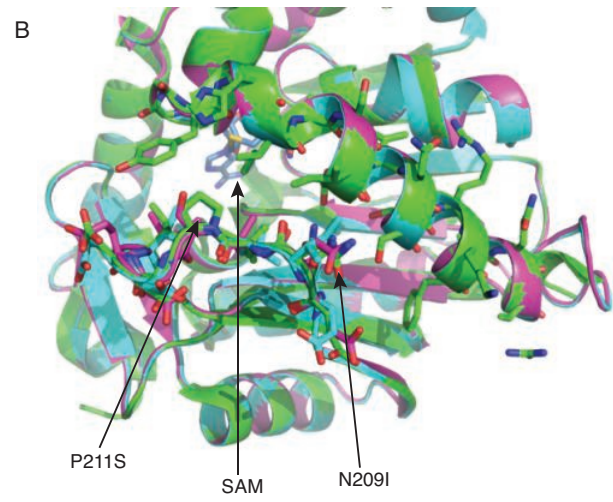
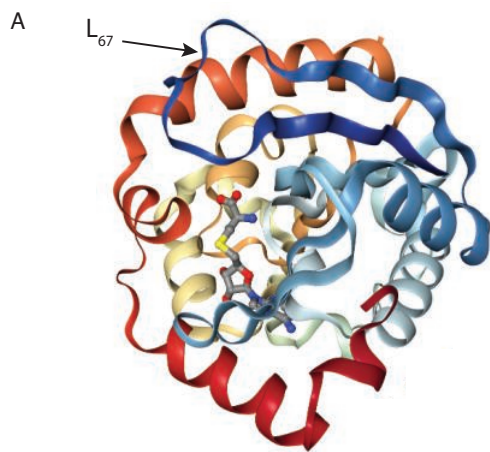


Figure 8. Molecular modeling of NRMT1 mutants.

(A) Full crystal structure of NRMT1. Arrow denotes loop₆₇ (L₆₇, navy blue) where N209 and P211 are located. The methyltransferase co-factor S-adenosyl-methionine (SAM) bound to the active site is indicated in gray. (B) Model comparing wild type NRMT1 (green, PDB code 2EX4) to mutated NRMT1 (pink), as calculated by the Robetta server (136). The schematic shows a zoomed in area of the active site. Molecular modeling was performed by Janusz Petkowski, Massachusetts Institute of Technology.

regulate substrate binding by altering the overall orientation of L₆₇.

NRMT1 Mutations Do Not Act as Dominant Negatives in Cancer Cells

It was determined that the EZH2 Y641 mutation acted in a dominant manner by exogenously expressing both WT EZH2 and Y641F EZH2 in HEK293T cells, which already harbor WT EZH2 activity, and monitoring H3K27me3 levels (105). While expression of WT EZH2 produced a barely detectable increase in H3K27me3, expression of Y641F EZH2 resulted in a significant increase in H3K27me3, (105) indicating even with WT EZH2 present, the Y641F can change H3K27 methylation levels. HEK293T cells expressing Y641F EZH2 were also more resistant to a small-molecule inhibitor of single-carbon transfer methyltransferases (105).

To monitor if the P211S and N209I NRMT1 mutations worked in a similar dominant fashion, both were exogenously expressed using lentivirus at an MOI of 1 in A549 human lung carcinoma cells (as P211S was originally found in a lung cancer sample) (137). Though expression levels of WT, N209I, and P211S NRMT1 were similar, only WT NRMT1 showed a

slight increase in N-terminal trimethylation levels (Fig. 9A). Neither N209I nor P211S significantly changed either mono-/di- or trimethylation levels of endogenous RCC1 (Fig. 9A), indicating they are not acting in a dominant negative manner. Expression of the mutants also did not significantly affect cellular proliferation (Fig. 9B). The role of NRMT1 in lung cancer remains unclear, though it has been found to have slightly decreased expression in non-small cell lung carcinoma (138). NRMT1 is most commonly found under-expressed in breast cancer, glioblastoma, and leukemia (139-142). It has been correspondingly shown that in breast cancer NRMT1 is acting as a tumor suppressor, and its loss promotes oncogenic growth (50). Conversely, NRMT1 has shown to be robustly overexpressed in a variety of colon cancer samples, (143-145) where I predict NRMT1 may be acting as an oncogene.

To monitor if the P211S and N209I mutations have a differential effect in a cancer type that typically overexpresses NRMT1, the same overexpression experiments were performed in HCT116 human colorectal carcinoma cells. As in A549 cells, neither expression of P211S nor N209I were able to change mono-/di- or trimethylation levels of endogenous RCC1 (Fig. 9C) or alter cellular proliferation levels (Fig. 9D).

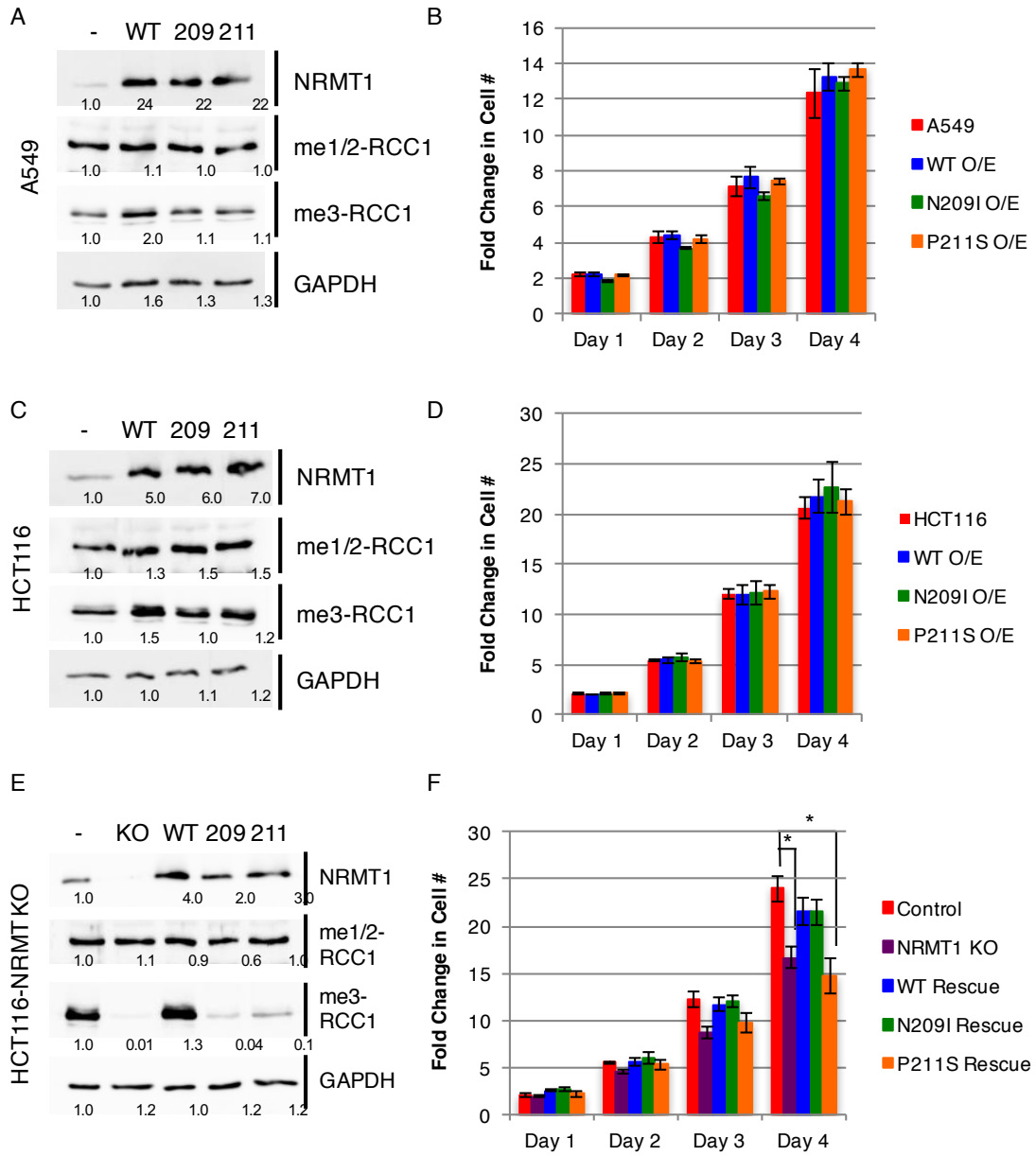


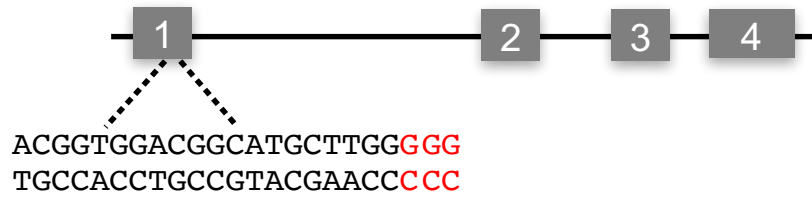
Figure 9. NRMT1 mutants are not dominant negatives but reduce N-terminal trimethylation when homozygous.

(A-D) When overexpressed in (A) A549 or (C) HCT116, neither the N209I nor the P211S NRMT1 mutants (A,C) alter the level of RCC1 N-terminal monomethylation/dimethylation (me_{1/2}RCC1) or trimethylation (me₃RCC1) or (B,D) cellular growth rates as compared to control cells expressing empty vector (-) or cells overexpressing wild type (WT) NRMT1. When expressed in HCT116 cells where NRMT1 expression has been knocked out (KO) through CRISPR/Cas9 genome editing, (E) neither the N209I nor P211S mutant can restore N-terminal trimethylation levels, and (F) P211S is also unable to rescue the growth defect seen with NRMT1 knockout. Each data point represents the mean \pm SEM of three independent experiments. * denotes $P < 0.05$, determined by a paired two-tailed Student's *t*-test. GAPDH is shown as a loading control. Anti-Mettl11a/NRMT1 (Abcam) used to determine WT and mutant NRMT1 expression levels. Blots are representative images of three independent experiments. Bands were quantified using ImageJ software (NIH) and internally normalized to wild type untransfected bands, which were set at 1.0. Work in this figure was performed by John Tooley, State University of New York at Buffalo.

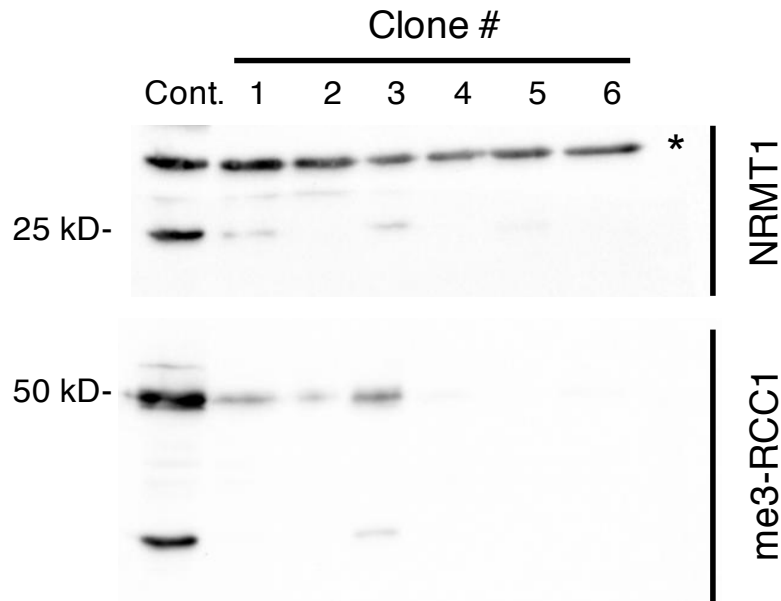
A CRISPR/Cas9 HCT116 NRMT1 knockout strain was recently made, which completely lacks NRMT1 expression and N-terminal trimethylation, while maintaining wild type mono-/dimethylation levels (Fig. 10 and Fig. 9E). To test if the P211S and N209I mutations could alter cellular phenotypes as homozygous mutations, the NRMT1 knockout cell lines were transduced with both mutations at an MOI of 1. As opposed to rescue with WT NRMT1, neither mutation could rescue N-terminal trimethylation levels, though they were expressed at similar levels for over 72 hours (Fig. 9E).

These data confirm the impaired biochemical activities of these mutants cannot be overcome in cells with endogenous substrate levels, even after prolonged exposure. As loss of NRMT1 function has been shown to alter cellular growth rates, the ability of N209I and P211S to rescue cellular proliferation rates in the HCT116 NRMT1 knockout line was also performed. As compared to control pSpCas9 transfected cells, the NRMT1 knockout strain grows significantly slower (Fig. 9F). This would be expected if NRMT1 acts as an oncogene in this cell type. Rescue with transduction of WT NRMT1 restores proliferation rates (Fig. 9F). Surprisingly, expression of the N209I mutant also restores proliferation rates, though the P211S mutation does not (Fig. 9F). Why one mutation can restore

A



B



C

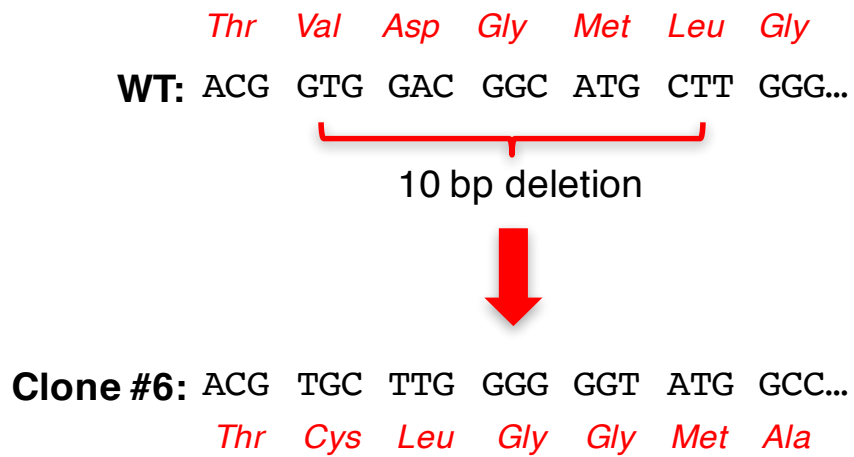


Figure 10. NRMT1 genome editing in HCT116 cells.

(A) NRMT1 target site selected for sgRNA design.

Protospacer adjacent motif (PAM) highlighted in red. (B)

Western blot analysis of first six expanded clones. All

clones had reduced NRMT1 (25 kD band) and N-terminal

trimethylation (me³-RCC1) levels as compared to control

(Cont.) cells transfected with empty pSpCas9(BB)-2A-Puro.

*denotes non-specific band recognized by NRMT1 antibody.

(C) DNA frameshift mutation found in clone #6, which was

subsequently used in all experiments. Cell line was

generated by John Tooley, State University of New York at

Buffalo.

proliferation and the other cannot, though neither restores N-terminal trimethylation levels, now remains to be determined. These data indicate the NRMT1 mutations are loss-of-function mutations and not neomorphic gain-of-function alleles, like the EZH2 mutations, and will need to become homozygous or combined with other NRMT1 loss-of-function mutations before effects on proliferation and other oncogenic phenotypes will be seen.

DISCUSSION

My work contributed to the findings that describe a biochemical alteration in NRMT1 and NRMT2 methyltransferase activities resulting from mutations identified in human cancer samples. In addition, I also showed that NRMT1 mutations in the conserved aromatic residues of the active site did not result in switched catalytic specificities or altered levels of substrate methylation.

This is contrary to what is seen in the SET domain histone methyltransferase EZH2, where mutation of its Y641 residue to either a phenylalanine or asparagine changes its catalytic specificity from a monomethylase to a trimethylase (105). There are a few possible explanations for this divergence. First, while EZH2 is a SET domain methyltransferase, NRMT1 and NRMT2 are seven- β -strand methyltransferases (46). Though both types of methyltransferases contain a series of aromatic residues in their active site that are reminiscent of the aromatic cages found in methyllysine-binding proteins and likely contribute to substrate specificity, they are structurally distinct methyltransferases which may have different modes of substrate recognition (46,105).

Alternatively, in addition to the aromatic residue composition, there is a second structural feature of NRMT1 and NRMT2 that could dictate catalytic specificity. Despite the high sequence conservation between NRMT1 and NRMT2, NRMT2 possesses an extra 60 amino acid N-terminal domain "tail" which is not found in NRMT1 (46). Given the apparent flexibility of this tail, it is possible it could partially fold over the active site and limit substrate entrance. This would then take precedence over the aromatic residues in substrate selection and binding.

A similar regulatory mechanism is seen in the human arginine methyltransferase PRMT1 (146). PRMT1 has seven alternative splice variants that differ in their N-terminal composition, and these unique sequences influence both catalytic activity and substrate specificity (146). To address this possibility for NRMT1 and NRMT2, I attempted to make NRMT2 with the tail domain deleted and NRMT1 with the tail domain added. Future experiments will be needed to fully address this issue.

Although the NRMT1 aromatic cage mutants showed no alteration in catalytic specificity, the cancer mutations N209I and P211S (endometrial and lung, respectively) showed a significant decrease in trimethylase activity and a significant increase in mono-/dimethylase activity. The

NRMT2 breast cancer mutation V224L also showed a significant decrease in monomethylase activity but lacked a reciprocal gain in trimethylation activity. The recently solved crystal structures of NRMT1 complexed with substrate peptides illustrates that N209I and P211S are in the peptide binding channel, (131) and V224 is adjacent to an asparagine that forms both hydrogen bonds and electrostatic interactions with substrate, (131) indicating the mutations do not directly change catalytic specificity but alter substrate preference. This is validated by my western blots showing N209I and P211S are still distributive enzymes capable of trimethylation. However, they are less efficient at methylating unmodified substrate and converting mono-/dimethylated substrate into trimethylated.

Whether these mutations can act as drivers of oncogenesis or promote further oncogenic transformation remains to be elucidated. My data indicate it may depend on the type of cancer it is found in. As seen in the HCT116 NRMT1 knockout line, cancers that typically overexpress NRMT1 may find mutants with decreased trimethylase activity detrimental to their growth. In addition, loss of N-terminal trimethylation has been shown to impair DNA repair, (50,52) so it may also make these tumors more sensitive to DNA damaging chemotherapeutics or

γ -irradiation. Cancers, such as breast, that become more oncogenic with loss of NRMT1 (50) may find these mutations as helpful drivers of oncogenesis, though the potential for increased sensitivity to DNA damaging agents would remain.

In the case of NRMT1, I propose its ability to work both as an oncogene and a tumor suppressor is likely dependent on which pathways are driving oncogenesis in specific tissues. For example, one well-studied NRMT1 target is the tumor suppressor retinoblastoma protein (Rb). It was previously shown that NRMT1 is acting as a tumor suppressor in estrogen receptor (ER) positive MCF-7 breast cancer cells, as its loss promotes DNA damage accumulation, and increased proliferation, migration, and xenograft tumor formation (50). Patients with ER+ tumors have poorer disease outcomes if they have an Rb mutation (147). If methylation of Rb by NRMT1 activates Rb-dependent transcription, loss of NRMT1 could mimic an Rb mutation and increase oncogenicity.

In contrast, NRMT1 is found overexpressed in colon cancers, (143-145) indicating it may be acting as an oncogene in this tissue. One difference between breast cancers and colon cancers is that colon cancer cells harboring activating K-Ras mutations require wild type Rb for oncogenic transformation and prevention of apoptosis

(148,149). Thus, in this particular tumor type, overexpression of NRMT1 could be beneficial.

Little is known about NRMT1 expression levels in human lung cancer samples, though one study found a 1.5-fold decrease in NRMT1 expression in non-small cell lung carcinomas (NSCLC) (138). Unlike small cell lung carcinomas (SCLC), which frequently harbor Rb mutations, NSCLC tumors favor mutation in CDKN2A (150). As an inhibitor of MDM2 activity, CDKN2A indirectly controls both p53 and Rb protein levels, so NSCLC cancer harboring both a CDKN2A and NRMT1 mutation would have reduced levels of Rb with potentially reduced activity.

In fact, the NRMT1 P211S mutation was found in a cell line derived from a metastatic lymph node of a patient with NSCLC (137), and Functional Analysis through Hidden Markov Models (FATHMM), which predicts the functional consequences of single nucleotide variants, rates it as strongly pathogenic (Cosmic Catalogue of Somatic Mutations in Cancer). The NRMT1 N209I mutation was identified as a somatic mutation in an endometrial tumor sample and also has a strongly pathogenic FATHMM prediction (Cosmic Catalogue of Somatic Mutations in Cancer). Of the 48 currently reported NRMT1 cancer mutations, eight are missense mutations in the L₄ and L₆₇ loop regions that help

create the peptide-binding channel, and seven of these eight mutations have strongly pathogenic FATHMM predictions (Cosmic Catalogue of Somatic Mutations in Cancer).

My supposition that NRMT1 can act as an oncogene or a tumor suppressor, dependent on the type of cancer, is based on the under- or overexpression of NRMT1 seen in different cancer types. This dual type of behavior is not uncommon. There are proteins which have been documented to act as an oncogene or a tumor suppressor in different cancers, or even in the same cancer type. E-cadherin is commonly considered a tumor suppressor, and its loss occurs in many epithelial cancers, including colon and liver cancers (151,152). On the other hand, the overexpression of E-cadherin has also been observed in advanced glioblastoma tumors, and its knockdown in SF767 glioma cells inhibited proliferation (153).

Another example is RAD9, which participates in DNA repair and cell cycle regulation. It can act as an oncogene in breast cancer, and its overexpression has also been correlated with prostate and thyroid cancers. It has been additionally reported that deletion of RAD9 in mouse keratinocytes leads to the development of skin cancer, suggesting its role as a tumor suppressor in such a context (154). Lastly, RASSF1 seems to function as a tumor

suppressor in most neuroendocrine lung tumors, but as an oncogene in neuroendocrine lung tumors that are high grade (155).

Why loss of N-terminal trimethylation by NRMT1 would result in phenotypes despite the continued presence of monomethylation by NRMT2 (or NRMT1 mutants) also remains to be elucidated. As with lysine methylation, I predict the different levels of N-terminal methylation promote different functional outcomes. For example, in the case of histone H4 lysine 20 (H4K20) methylation, monomethylation promotes transcriptional elongation by recruiting the MSL complex, increasing local histone H4 lysine 16 acetylation, and releasing RNA polymerase II (Pol II) into active elongation (22). In contrast, H4K20 trimethylation promotes Pol II pausing by inhibiting MSL recruitment (22). These distinct functional outcomes are driven by the specificity of the MSL chromodomain for H4K20 mono- and dimethylation and its inability to bind trimethylation (77). Whether the different levels of N-terminal methylation also have readers with distinct structural domains or whether monomethylation simply is unable to promote strong DNA-protein interactions are currently under investigation.

The discovery of the Y641 EZH2 mutations as drivers of B cell lymphoma has led to the development of many new EZH2 inhibitors. Two of these inhibitors, GSK126 and EPZ-6438, both highly selective S-adenosyl-methionine-competitive small molecule inhibitors, have been respectively shown to inhibit the proliferation of EZH2 diffuse large B-cell lymphoma cell lines and mouse xenografts expressing the Y641 mutation (156-158). However, unlike the EZH2 Y641 mutations, the identified NRMT1 mutations are not gain-of-function, and therapeutic use of NRMT1 inhibitors would have to be context specific.

In tumors such as colorectal, that significantly overexpress NRMT1, NRMT1 inhibitors could be a viable therapeutic option (143-145). In breast cancers, however, use of NRMT1 inhibitors alone could be detrimental, but beneficial in combination with DNA-damaging chemotherapeutics or γ -irradiation. As it has been shown that neither the N209I or P211S NRMT1 mutations can restore N-terminal trimethylation after loss of NRMT1, homozygosity for these mutations may also be a useful marker for tumors especially susceptible to chemo and irradiation therapies. Novel bisubstrate analogues and potent inhibitors of NRMT1 have recently been designed and continue to be optimized, (159,160) and it will be interesting to see if any of the

derivatives affect cancer cell proliferation and/or sensitivity to chemo and radiation therapy in a tissue-specific manner.

CHAPTER III: ASSESSING THE CELLULAR EFFECT OF NRMT1 MUTANTS
DURING THE DNA DAMAGE RESPONSE

BACKGROUND

From the data in Chapter II, I demonstrated that the NRMT1 cancer mutants (N209I, endometrial cancer; P211S, lung cancer) impair catalytic activity *in vitro* (Figs. 2, 5-7) (109). However, the significance of this in a cellular context is unclear and is the focus of the work presented in this chapter.

In the MCF-7 and LCC9 breast cancer cell lines, the loss of NRMT1 resulted in an increased sensitivity to DNA damage (50,51). Additionally, NRMT1 knockout MEFs display an increased sensitivity to oxidative damage (51). Together, these data suggest that NRMT1 may be crucial for cell survival in response to cellular insults. Given that the N209I and P211S mutants are also incapable of rescuing N-terminal trimethylation activity in cells (Fig. 9) (109), I hypothesize that they will be unable to promote cell

survival of NRMT1 knockout cells in response to DNA damaging agents.

DNA damaging agents are often employed as chemotherapeutic agents in the treatment of cancer. Two examples include etoposide (brand name Etopos) and doxorubicin (brand name Adriamycin). Etoposide intercalates with DNA, causing DNA DSBs, and is also a topoisomerase II inhibitor. It is capable of inducing caspase-mediated apoptosis at high concentrations (161-163). Doxorubicin belongs to the anthracycline class of drugs (161), and it also intercalates with DNA, causing DNA DSBs. Additionally, it can also cause oxidative stress (161,164-166), leading to the mitochondrial route of apoptosis (167-169). While NRMT1-depleted cells have a heightened sensitivity to etoposide (50), their response to doxorubicin remains untested.

To begin to address this question, I utilized NRMT1-deficient HCT116 cells that had already been generated using CRISPR technology (Fig. 10; hereby referred to as KO cells). An additional advantage of using these cells is based on their similarity to MCF-7 cells, in regards to having wild-type p53 status (170). Thus, to investigate whether the N209I or P211S mutations in NRMT1 would have any functional consequence in the context of cellular

proliferation or DNA damage, I expressed these mutants, as well as wild-type NRMT1, into the KO cell line, and assessed their sensitivity towards doxorubicin.

The cellular response towards DNA damaging agents (specifically, doxorubicin) has been extensively characterized (171). In the absence of p53, or its downstream target p21, cells exhibit an increase in doxorubicin-induced cell death (172). Thus, as an additional measure, I monitored p53 and p21 expression in my cell lines.

MATERIALS AND METHODS

Constructs and Antibodies

To generate C-terminal GFP-tagged NRMT1 constructs, human NRMT1 (GE Dharmacon, Marlborough, MA), which had been subcloned into the pKGFP2 vector, was used as the template for site-directed mutagenesis to produce N209I and P211S NRMT1 using the Quikchange site-directed mutagenesis protocol (Agilent Technologies, Santa Clara, CA). The following forward primers and their reverse complements were used:

N209I: 5'-GAGGAGAGGCAGGAGATCCTCCCCGATGAGATC-3'

P211S: 5'-GGCAGGAGAACCTCTCCGATGAGATCTACC-3'

Both mutants were confirmed by DNA sequencing.

Primary antibodies used for western blots are as follows: 1:5000 polyclonal rabbit anti-me1/2RCC1 (mono-/dimethylated SPK-RCC1) (120), 1:10,000 polyclonal rabbit anti-me3RCC1 (trimethylated SPK-RCC1) (120), 1:1000 polyclonal goat anti-RCC1 (Santa Cruz Biotechnology, sc-1162, Santa Cruz, CA), 1:2000 polyclonal rabbit anti-NRMT1 (128), 1:500 monoclonal rabbit γ -H2AX (Abcam, 20E3, Cambridge, United Kingdom), 1:1000 monoclonal rabbit HSP90 (Cell Signaling Technology, C45G5, Danvers, MA), 1:1000

monoclonal mouse α -tubulin (Sigma Aldrich, St. Louis, MO), 1:1000 monoclonal mouse p53 (Santa Cruz Biotechnology, sc-098), 1:1000 polyclonal rabbit p21 (Santa Cruz Biotechnology, sc-397), 1:1000 monoclonal mouse Rb, and 1:1000 monoclonal mouse DDB2 (Abcam, ab51017). 1:1000 polyclonal rabbit anti-Mettl11a/NRMT1 (Abcam, ab102664) was used to detect KO+WT, and KO+N209I and KO+P211S NRMT1. Secondary antibodies used were as follows: goat anti-rabbit IRDye[®] 680 RD (Li-Cor, 926-68071, Lincoln, NE), goat anti-mouse IRDye[®] 800 CW (Li-Cor, 926-32210), and donkey anti-goat IRDye[®] 800 CW (Li-Cor, 925-32214). All antibodies were diluted in 2% BSA (in TBST).

SDS polyacrylamide gel electrophoresis (SDS PAGE) was performed using tris-glycine separation with running buffer (25 mM Tris, 192 mM glycine, 0.1% SDS, pH 8.3). Gels were run at 125V until the bromophenol blue tracker dye reached the end of the gel (approximately 90 minutes). Proteins were transferred to nitrocellulose membranes for 90 minutes at a constant current of 400mA in transfer buffer (25 mM Tris, 192 mM glycine, pH 8.3), which were then blocked using 2% BSA in TBST for one hour at room temperature.

After the blocking step, incubation with the primary antibodies was performed at 4 °C overnight (18-20 hours) on an end-over-end rocker. Washing was performed using TBST.

Incubation with secondary antibodies was performed for one hour at room temperature. After the final washing steps, the membranes were imaged using the LI-COR Odyssey Blot imager.

Cell Culture

HCT116 human colorectal carcinoma cells lines (a generous gift from Dr. Ian Macara, Vanderbilt University) were maintained in Dulbecco's Modified Eagle Medium (DMEM) (Corning Life Sciences, Manassas, VA) with 10% fetal bovine serum (FBS) (VWR, Radnor, PA) and 1% penicillin-streptomycin-glutamine (P/S/G) (Life Technologies) and were used at a passage number of less than 25. To generate KO+WT (WT), KO+N209I (N209I), and KO+P211S (P211S) cells (referred to collectively as rescue cells), NRMT1 KO cells were transduced with WT NRMT1, N209I, and P211S lentivirus (production detailed in Chapter II Materials and Methods) to a MOI of 1. Calculations performed to estimate MOI are based on the detection of GFP-positive cells by microscopy, and the dilution of virus necessary to achieve this. Virus-containing media was replaced with virus-free media three days later.

Cell Growth Assays and Drug Treatment

Seeding conditions were 5.0×10^4 cells per well in 12-well plates (only fig. 14 HCT116 toleration of doxorubicin treatment), 2.4×10^4 cells per well in 24-well plates, or 1000 cells per well in 96-well plates; figure legends indicate which condition was used. For viability (cell growth) assays (CellTiter 96® AQueous One Solution Cell Proliferation Assay), cells were plated in triplicate in 24-well (or 96-well) plates in 500 μ L (or 100 μ l) of media. For experiments examining DNA damage, cells were treated with doxorubicin (dox) (Sigma Aldrich) at 0, 0.1, or 1 μ M 24 hours following seeding. After the treatment time or day of measured growth (indicated by figure legend), or recovery time post-treatment (48 hours), 80 μ l (for 24-well plates) or 20 μ l (for 96-well plates) of Aqueous One Solution (Promega, Madison, WI) was added to all replicates, and the absorbance at 490 nm was read after two hours. Data was analyzed by two-way ANOVA and Tukey's post-hoc test.

For western blots, cells were seeded according to either seeding condition outlined above; figure legends indicate which condition was used. Cells were plated and treated as indicated above. Following the indicated

treatment (24 hours) or recovery time post-treatment (48 hours), cells were lysed in 2X Laemmli's SDS-Sample Buffer (4X, Boston Bioproducts, Ashland, MA) supplemented with β -mercaptoethanol (5% v/v).

Immunofluorescence Experiments

To assess the subcellular localization of the mutants, 3.0×10^5 HCT116 cont. cells were seeded on coverslips in 6-well plates. The jetPRIME® transfection reagent (Polyplus, New York, NY) was used to transiently transfect 0.5 μ g WT NRMT1, N209I, or P211S, which were all C-terminally GFP-tagged. For each transfection, 2 μ l of jetPRIME reagent was added to the DNA in 200 μ l of the provided buffer. After an incubation of 25 minutes, the transfection mixture was added directly to the cells. 18 hours post-transfection, media was removed, cells were washed with PBS and then fixed in 10% formalin for 10 minutes at room temperature. Coverslips were mounted with Vectashield containing DAPI (Vector Laboratories, Burlingame, CA). Cells were imaged using a confocal fluorescence microscope (Olympus IX SLA). Images were then imported into Photoshop (Adobe Systems, Inc.) for processing. Images are from one section and are not an overlay.

For studies with doxorubicin and γ -H2AX foci visualization, 5.0×10^5 HCT116 cont. and NRMT1 KO cells were seeded on coverslips in 6-well plates. One day after seeding, media was removed, and cells were treated with 0, 0.1, or 1 μ M doxorubicin for 24 hours. Cells were fixed in 10% formalin as above, followed by permeabilization in 0.5% Triton X-100 in PBS for 5 minutes at room temperature. Cells were then blocked for one hour in 2% BSA/1% goat serum in PBS. Stain and antibodies used are as follows: primary 1:500 rabbit γ -H2AX (Abcam, 20E3), prepared in 2% BSA/1% goat serum in PBS; 1:250 rhodamine phalloidin (Molecular Probes, R415, Eugene, OR), prepared in 2% BSA/1% goat serum in PBS; and secondary 1:1000 goat α -rabbit Alexa Fluor® 488 (Invitrogen, A11008, Carlsbad, CA), prepared in 2% BSA/1% goat serum in PBS. Primary antibody incubation was one hour at room temperature; rhodamine phalloidin and secondary antibody incubation was for 30 minutes at room temperature in the dark. Coverslips were mounted with Vectashield containing DAPI (Vector Laboratories). γ -H2AX, phalloidin, and DAPI were visualized by confocal microscopy as described above.

siRNA Knockdown Experiments

To assess the effects of transient knockdown of NRMT1 in HCT116 cells, cells were seeded at a density of 2.4×10^4 cells per well in a 24-well plate. Two days after seeding (when cells had reached approximately 70% confluency), transfection was performed using 10 pM siRNA. The target sequences for the siRNA oligos utilized are as follows:

NRMT1 a, 3'UTR: CTGGCAGGAGAACTGAGGAA

NRMT1 b, 3' UTR: GAGTGTCGAGGCACCACTAAA

NRMT1, ORF: GGCCCGAACAAGACAGGAAtt (sense);

UUCCUGUCUUGUUCGGGCtt (antisense)

21 hours post-transfection, media was replaced, and cells were treated with 1 μ M doxorubicin or 250 μ M etoposide for six hours. Cell lysates were then analyzed for NRMT1 knockdown by western blot analysis.

RESULTS

Mutant NRMT1 Methylation Pattern Is Not Unique to RCC1

From Chapter II, the methylation pattern for RCC1 displayed by the NRMT1 cancer mutants was established using *in vitro* methyltransferase assays. To determine the pattern in a cellular context, I independently re-established these cell lines by stably expressing these mutants in HCT116 cells lacking endogenous NRMT1. Specifically, I used lentivirus expressing WT, N209I, and P211S NRMT1. The cells were established, and the expression was confirmed by western blot (Fig. 11). As a CRISPR control, I used cells expressing pSpCas9 only (hereby referred to as cont. cells).

Western blots with the trimethylated SPK (me3RCC1) antibody shows that only WT NRMT1 was able to rescue the trimethylation pattern (Figs. 9, 11, 23). Thus, while the *in vitro* data suggested that the NRMT1 cancer mutants possessed an inefficient ability to trimethylate substrates, they could not do so in a cellular context.

NRMT1 recognizes over 300 putative targets (44) with many different consensus sequences; however, only a handful of those substrates possess the SPK consensus sequence.

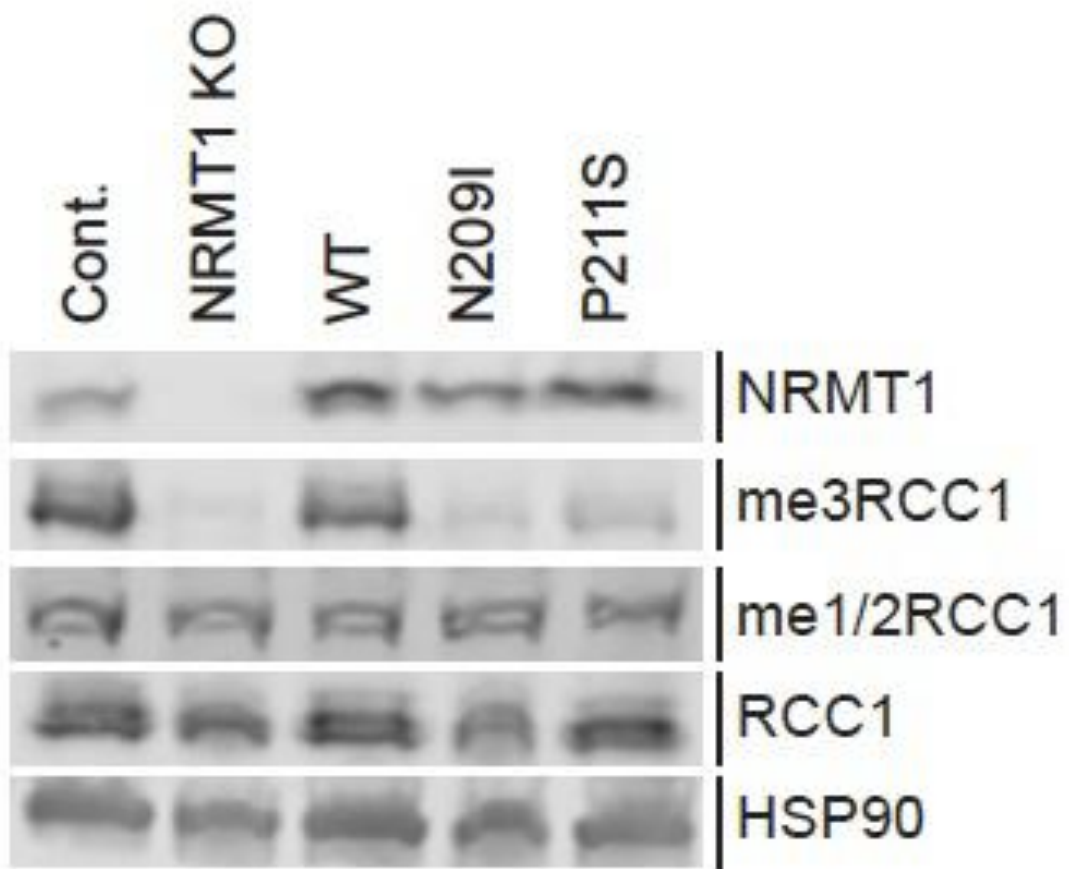


Figure 11. NRMT1 KO cells transduced with lentivirus.

NRMT1 KO cells were transduced with lentivirus expressing WT, N209I or P211S NRMT1 at a MOI of 1. After cells were established, protein lysates were obtained, and western blot performed with the indicated antibodies. NRMT1 expression and trimethylation of RCC1 in WT lane is comparable to that of cont., while this is barely detectable in the N209I and P211S lanes. Mono-/dimethylation of RCC1 is the same across all five cell lines. The levels of RCC1 are also the same in all lines. HSP90 was used as a loading control. Shown is a representative Western blot from three independent experiments.

From Figure 23, the band that migrates at 45 kD (indicated by the asterisk) is RCC1.

The other prominent band detected by the tri-SPK antibody migrates at approximately 20 kD. According to Petkowski et al. (44) (who expanded the originally defined NRMT1 consensus sequence, as well as performed additional in-depth work to pinpoint putative NRMT1 targets), a protein of this size possessing the SPK sequence could potentially be the VCX-A protein. However, VCX-A has only been detected in the testis and germ cells, linking it with potential roles in spermatogenesis (173). Thus, the exact identity of this band in HCT116 cells has yet to be elucidated. Nevertheless, the presence of this band was also rescued by wild-type NRMT1 in the KO cells.

N209I Subcellular Localization Differs from WT NRMT1

The subcellular localization of WT NRMT1 is predominantly nuclear (46,47). To determine if the NRMT1 mutants localize appropriately, I performed confocal microscopy. HCT116 cont. cells were transfected with C-terminally GFP-tagged WT, N209I, or P211S constructs, and processed for confocal microscopy. The nucleus was visualized by DAPI staining. From two independent

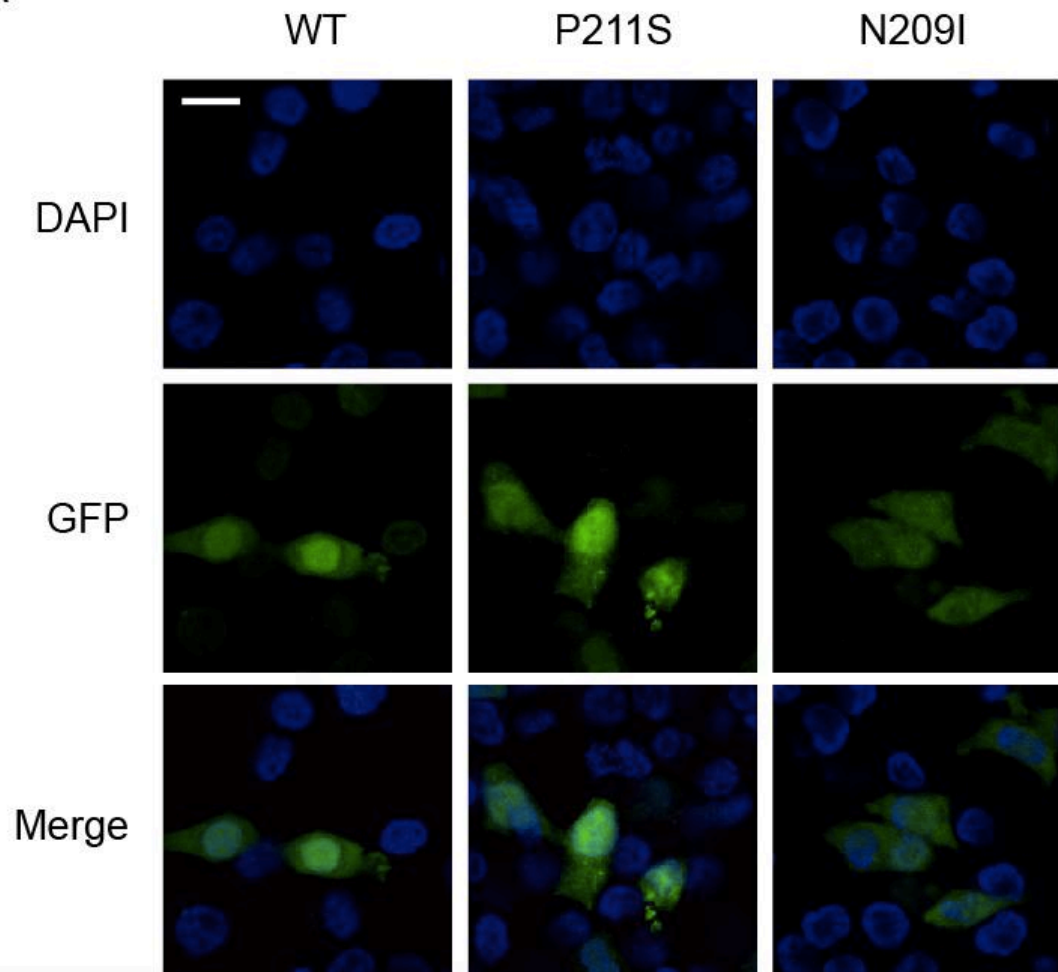
experiments, WT NRMT1 displayed the predominantly nuclear localization pattern, with minimal cytoplasmic localization, as expected (Fig. 12). Similarly, the subcellular localization of the P211S mutant was also predominantly nuclear (Fig. 12). In contrast, the N209I mutant exhibited noticeably more cytoplasmic localization (Fig. 12). Thus, in addition to loss of trimethylation activity, the N209I mutant may exhibit reduced nuclear localization in cells.

Viability Studies of HCT116 Cells

Prior to studying DNA damage in the HCT116 cells, I examined the proliferation levels of the cell lines that I re-established, to determine if the cancer mutants could rescue the proliferation defect in KO cells that was previously described (109). Using the CellTiter assay, I assessed the proliferation of the five cell lines on days 0, 1, 3, and 5 after seeding. A total of nine experiments were performed on separate days with a summary graph shown in Figure 13 (Fig. 24 in the Appendix).

The summary graph shown in Figure 13 exemplifies the type of data recorded. In eight out of the nine experiments, the KO cells proliferated more slowly than the

A



B

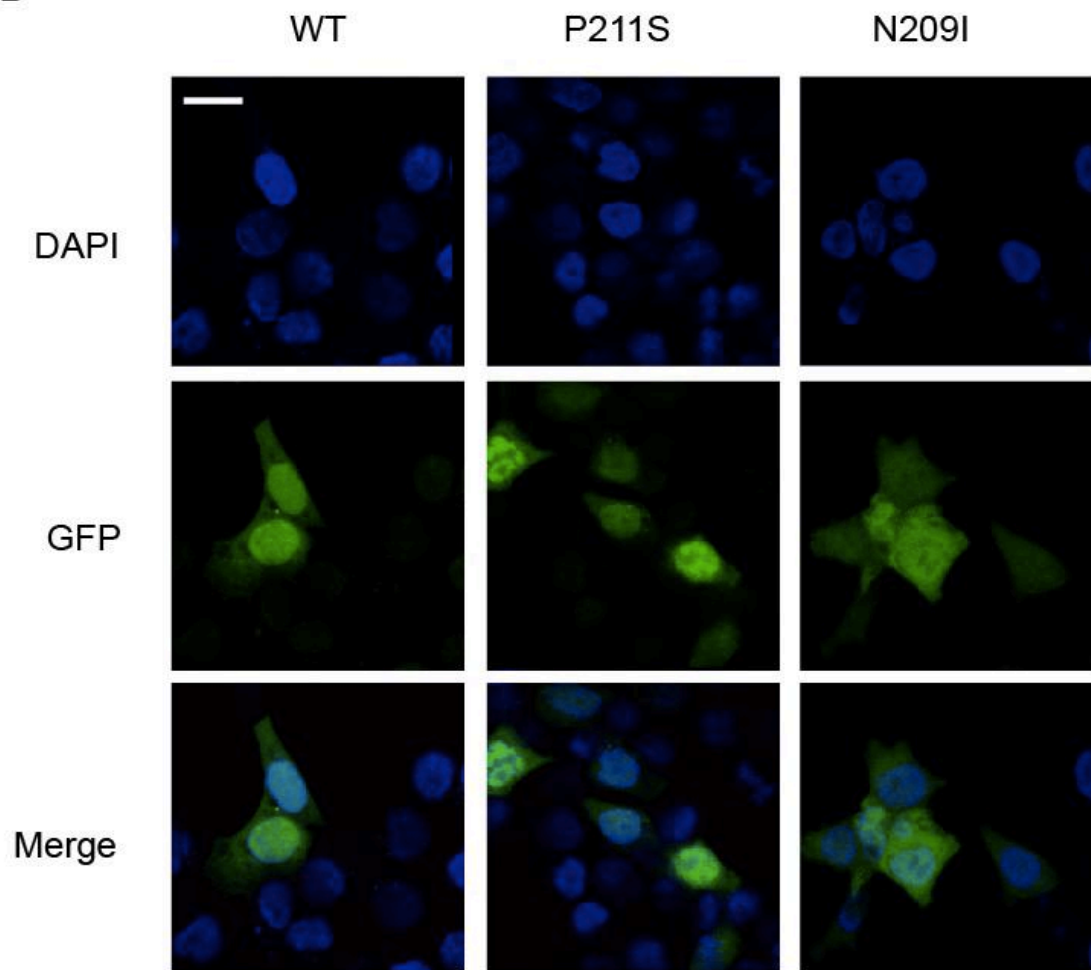


Figure 12. Subcellular localization of WT and mutant NRMT1.

(A-B) HCT116 cells were transiently transfected with C-terminally GFP-tagged WT, N209I or P211S NRMT1. After 24 hours, cells were processed for confocal microscopy using the Olympus IX SLA microscope. DAPI, GFP, and merge images are shown. Images were obtained using a 40X objective with 3.0X digital magnification. Bar, 20 μ m. Images are from one section and are not an overlay. WT and P211S NRMT1 show predominantly nuclear localization. N209I manifests greater cytoplasmic localization, compared to WT. Experiment was performed twice.

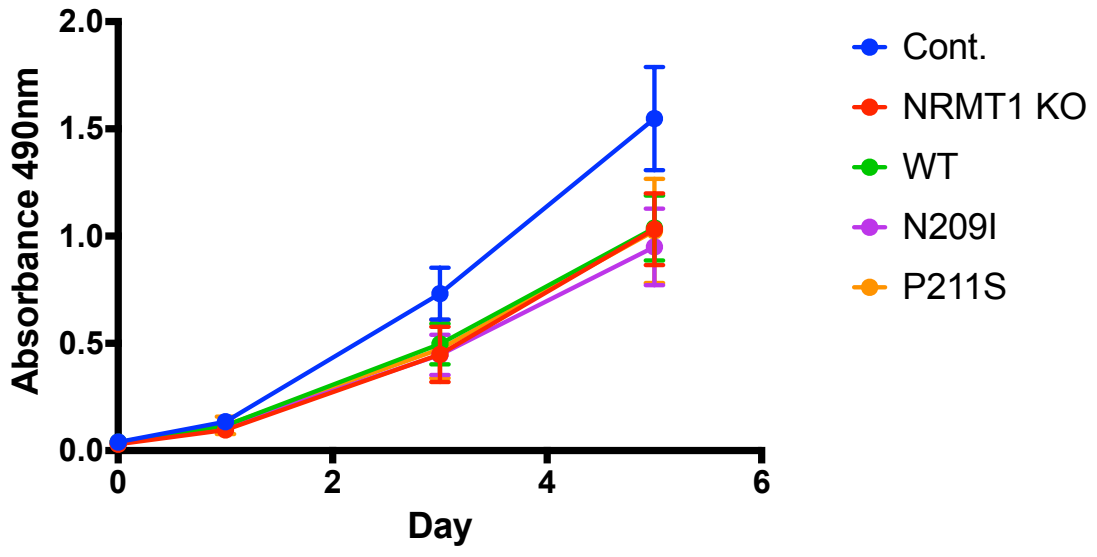


Figure 13. Viability studies of HCT116 cells.

Four sets of triplicates were made for each of the five HCT116 cell lines. Cells were seeded at a density of 1000 cells per well in 96-well plates on day 0. On the day of plating (day 0), 20 μ l of Aqueous One Solution (Promega, Madison, WI) was added to the first set of triplicates for each cell line, and the absorbance at 490 nm was read after two hours. Readings were also taken on days 1, 3, and 5. Raw absorbance values are shown on the Y-axis. Results shown are the mean \pm standard deviation of data from nine independent experiments and triplicate measurements per experiment. Individual experimental results are shown in Figure 24.

cont. cells (Figs. 13, 24), in agreement with what I previously reported (109). This is especially apparent on Day 5 of the assay (Figs. 13, 24). However, in my experiments, the expression of WT protein into the KO cells did not rescue the proliferation defect as was previously shown (109).

DNA Damage Studies of HCT116 Cells Towards Doxorubicin

I next assessed whether my cell lines would exhibit differences in response to DNA damage, given that previous work demonstrated that NRMT1-depleted cells have a heightened sensitivity to DNA damaging agents (50,51). For example, NRMT1 knockdown breast cancer cells treated with the DNA-damaging agent etoposide had slower rates of proliferation, as well as an increase in γ -H2AX foci, which is an early indicator of DNA damage (50,174,175). I decided to use doxorubicin as the DNA damaging agent, given that the effect of this drug has been well characterized (171).

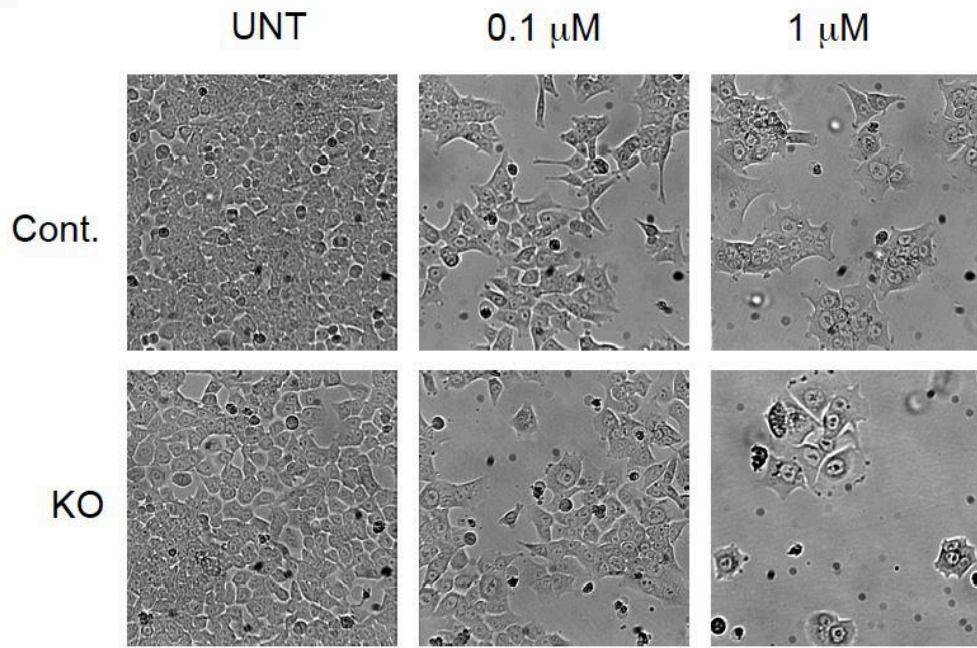
Typically, a dose of 0.1-1.0 μ M doxorubicin causes cell death in HCT116 cells after 24 hours (172). Prior to determining the effects of doxorubicin on DNA damage signaling, cells were first treated to confirm that

doxorubicin caused cell death in my HCT116 cell lines. HCT116 cont. and NRMT1 KO cells were treated with 0.1 or 1 μ M doxorubicin for 24 hours or left untreated as a control (Fig. 14). Cells were then allowed to recover for 48 hours following doxorubicin treatment. The micrographs from two independent experiments are shown in Figure 14. As expected, doxorubicin caused cell death at both concentrations, but especially at 1 μ M (Fig. 14).

To quantitatively measure the cell viability in response to doxorubicin, I performed CellTiter assays (the reduction of a metabolite is correlated to the number of viable cells). I first assessed this in the cont. and KO cells after treating with doxorubicin for 24 hours. A total of five experiments were performed with a summary graph depicted in Figure 15 (Fig. 25 in the appendix). There was a trend for KO cells to exhibit increased sensitivity toward doxorubicin at 1 μ M.

I then performed four additional series of experiments to include the rescue cell lines. This time, I only treated the cells at 1 μ M doxorubicin for 24 hours, along with untreated controls. The data are depicted in Figures 16 and 26. In this set of experiments, the KO cells were not consistently more sensitive to the doxorubicin treatment, indicating this trend was not

A



B

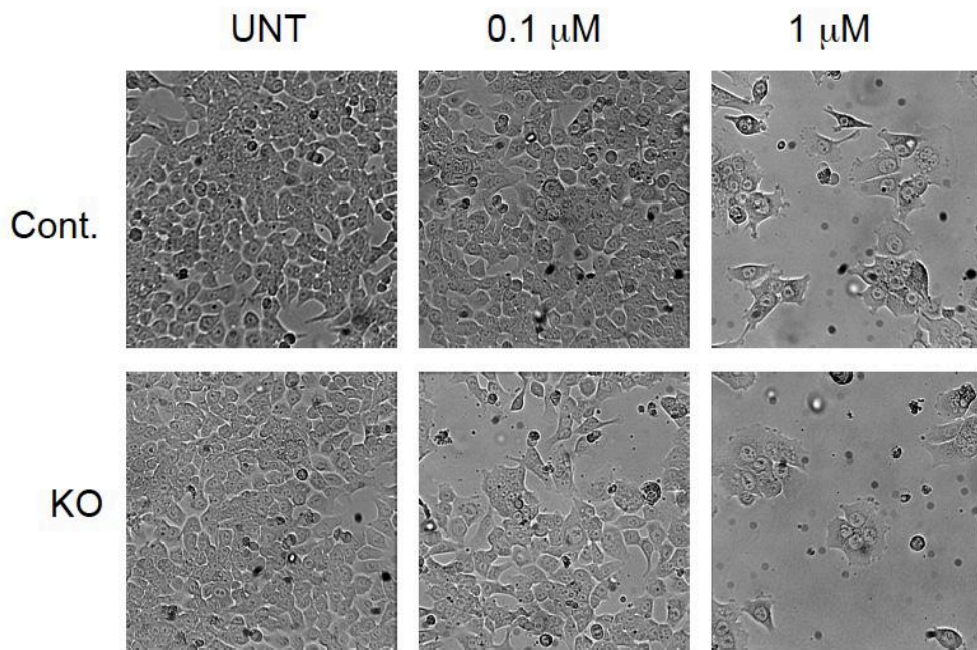


Figure 14. HCT116 toleration of doxorubicin treatment.

(A-B) 5.0×10^4 cells per well were seeded into 12-well plates. HCT116 cont. and NRMT1 KO cells were treated with 0, 0.1, or 1 μ M doxorubicin for 24 hours. Afterward, media was replaced, and cells were allowed to recover for 48 hours. Representative pictures were taken immediately following recovery period. Experiment was performed twice; total magnification was 10X.

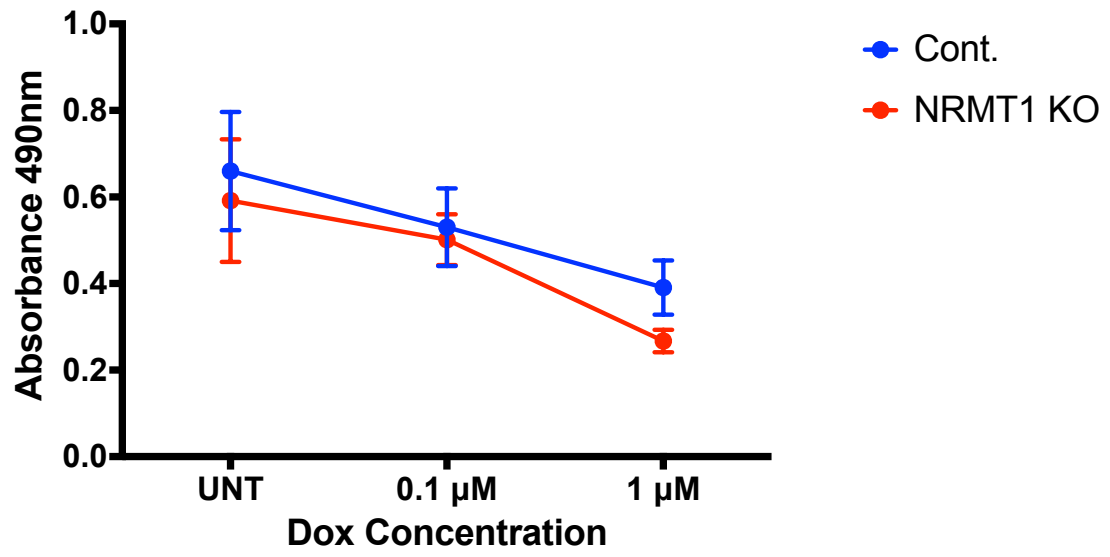


Figure 15. Viability assay of doxorubicin-treated cont. and NRMT1 KO cells.

2.4×10^4 cells per well were seeded into 24-well plates. Three sets of triplicates were made for cont. and NRMT1 KO cells. CellTiter was performed on cells that were treated with 0.1 or 1 μ M doxorubicin (or the untreated controls) for 24 hours. Following treatment, 80 μ l of Aqueous One Solution was added to each well, and the absorbance at 490 nm was read after two hours. Y-axis units are arbitrary units of absorbance at 490 nm. Results shown are the mean \pm standard deviation of data from five independent experiments and triplicate measurements per experiment. Individual experimental results are shown in Figure 25.

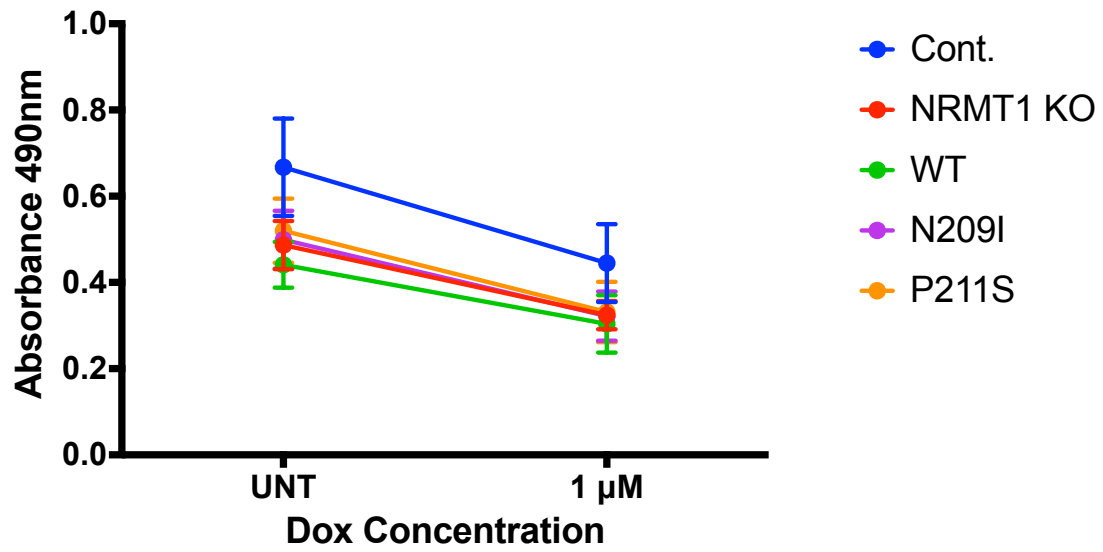


Figure 16. Viability assay of doxorubicin-treated cells.

2.4×10^4 cells per well were seeded into 24-well plates.

Two sets of triplicates were made for each cell line.

CellTiter was performed on cells that were treated with $1 \mu\text{M}$ doxorubicin (or the untreated controls) for 24 hours.

Following treatment, $80 \mu\text{l}$ of Aqueous One Solution was added to each well, and the absorbance at 490 nm was read after two hours. Y-axis units are arbitrary units of absorbance at 490 nm. Results shown are the mean \pm standard deviation of data from four independent experiments and triplicate measurements per experiment. Individual experimental results are shown in Figure 26.

reproducible. Also, similar to Figure 13, WT cells did not rescue proliferation levels, and neither mutant cell line grew significantly differently than the KO cells.

Since my data thus far suggested that NRMT1 did not have an effect on cell viability after 24-hour treatment, I performed another set of experiments to assess whether NRMT1 might have a role at later time points (i.e. during the recovery phase). Thus, I performed two additional series of experiments using 1 μ M doxorubicin and assessed cell viability after 48 hours. As can be seen from the data (Fig. 17), there was no consistent difference between the cell lines after treatment.

Assessment of γ -H2AX Foci After Treatment with Doxorubicin

My data, thus far, is different than what was reported for the role of NRMT1 in etoposide-treated or irradiated breast cancer cells (50). I therefore wanted to ensure that, in my experiments, I was indeed inducing DNA damage.

When cells are exposed to ionizing radiation or other DNA damaging agents, the histone H2A variant, H2AX, becomes phosphorylated at sites of DSBs on residue Ser 139 (referred to as γ -H2AX) (174,175). This is an early event in the DNA damage response (174,175), and is thus a

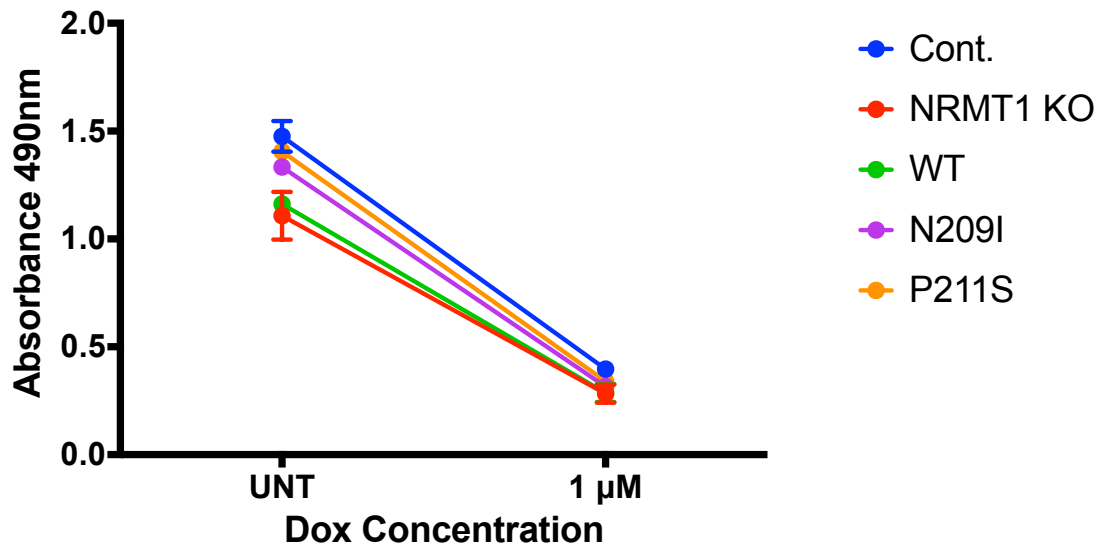


Figure 17. Viability assay of recovered doxorubicin-treated cells.

2.4×10^4 cells per well were seeded into 24-well plates. Two sets of triplicates were made for each cell line. CellTiter was performed on cells that were treated with $1 \mu\text{M}$ doxorubicin (or the untreated controls) for 24 hours followed by a 48-hour recovery period. After treatment and recovery, $80 \mu\text{l}$ of Aqueous One Solution was added to each well, and the absorbance at 490 nm was read after two hours. Y-axis units are arbitrary units of absorbance at 490 nm. Results shown are the mean \pm standard deviation of data from two independent experiments and triplicate measurements per experiment.

suitable marker for this process. Therefore, as a first step to assess the DNA damage in the treated cells, confocal microscopy was performed. In brief, treated cells were fixed and probed with an antibody against γ -H2AX, which has an epitope against the phosphorylated residue Ser 139.

In the absence of doxorubicin, γ -H2AX foci could not be observed in untreated cells, as expected (Fig. 18). However, after 24-hour doxorubicin treatment, γ -H2AX was readily detected. To confirm this, I also performed western blot analysis using the same antibody. In agreement with the confocal results, the western blots showed an increase in γ -H2AX signal after doxorubicin treatment, suggesting that indeed, doxorubicin was causing DNA damage. Additionally, the similar levels of γ -H2AX in all the cell lines is consistent with the proliferation results.

Western Blot Analysis of Doxorubicin Treatment

While previous data has shown that loss of NRMT1 leads to an increased sensitivity to etoposide in breast cancer cell lines, my data shows that NRMT1 has no effect in doxorubicin-treated HCT116 cells. One explanation for these differences could be attributed to the different

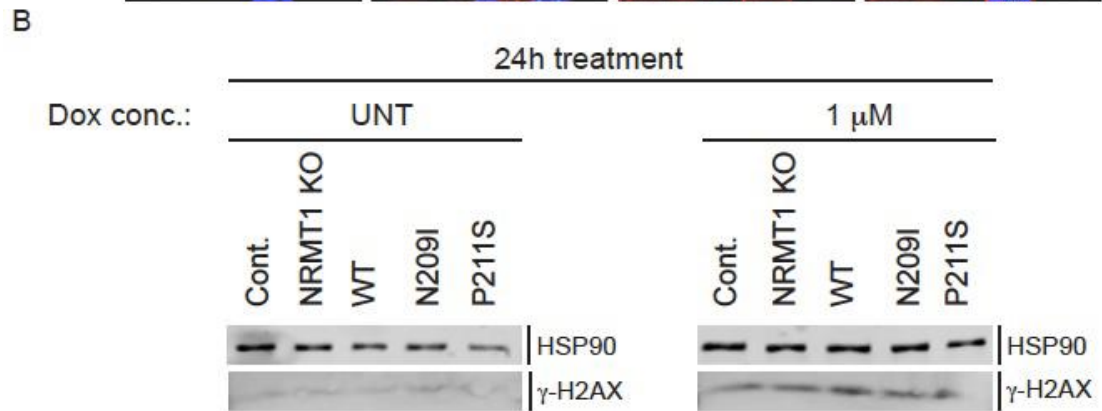
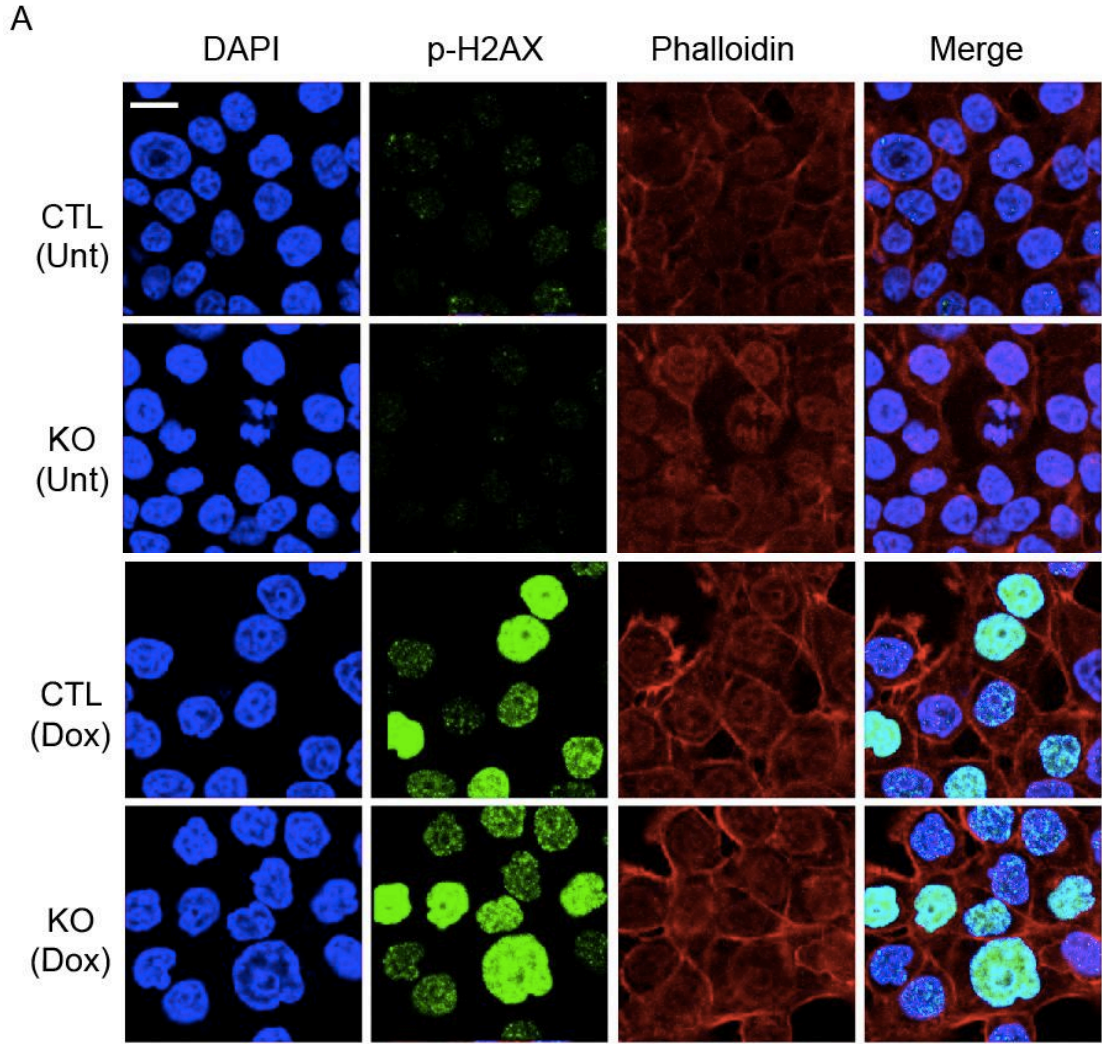


Figure 18. γ -H2AX foci following 24-hour doxorubicin treatment.

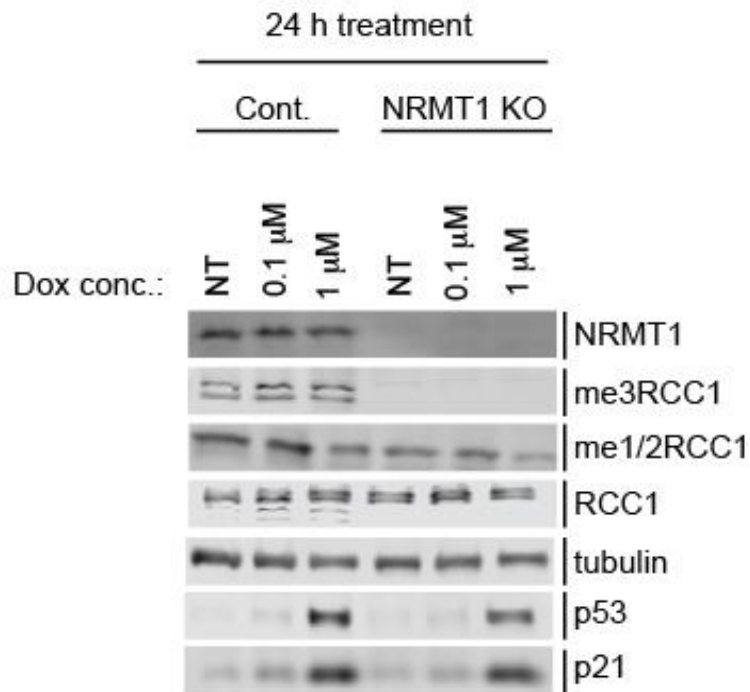
(A) Cells were seeded at a density of 5.0×10^5 cells onto coverslips in 6-well plates. Cells were then treated with 1 μ M doxorubicin for 24 hours before processing for confocal microscopy using the Olympus IX SLA microscope to visualize DAPI, γ -H2AX (p-H2AX), and phalloidin (actin). DAPI, GFP, and merge images are shown. Images were obtained using a 40X objective with 3.0X digital magnification. Bar, 20 μ m. Images are from one section and are not an overlay. Merge of each CTL (cont.) and KO condition shown on far right. Top two rows show untreated cells (Unt), and bottom two rows show cells treated with 1 μ M doxorubicin for 24 hours. Bar, 20 μ m. (B) For western blots, cells were seeded at a density of 2.4×10^4 cells per well in 24-well plates. Western blots show doxorubicin-treated cell lysates that were probed for HSP90, as a loading control, and γ -H2AX. This experiment was done once.

treatments and cell lines employed. However, it is also possible that compensatory changes in signaling pathways might be a factor. As such, I decided to perform western blots to look into a few key proteins involved in the DNA damage response.

For the first experiment, cont. and KO cells were treated with 1 μ M doxorubicin for 24 hours, followed by recovery for 48 hours. Untreated cells were used as a control. Lysates were obtained, and western blots were performed with the indicated antibodies (Figs. 19 and 21). Tubulin was used as a loading control, and the absence of NRMT1 and the me3RCC1 signal confirmed the identity of the KO cells. Next, I assessed the p53 and p21 levels, given their importance in the DNA damage response in HCT116 cells. After treatment with 1 μ M doxorubicin for 24 hours, both p53 and p21 exhibited increased levels in both cell lines. After an additional 48 hours (during recovery), p53 and p21 expression were still elevated in cont. cells, when compared to untreated cells. However, in the KO cells, the levels of these two proteins had returned to levels comparable to untreated cells.

Although this observation in the differences in p53 and p21 levels seemed promising, subsequent experiments indicated that it was not reproducible. For the next

A



B

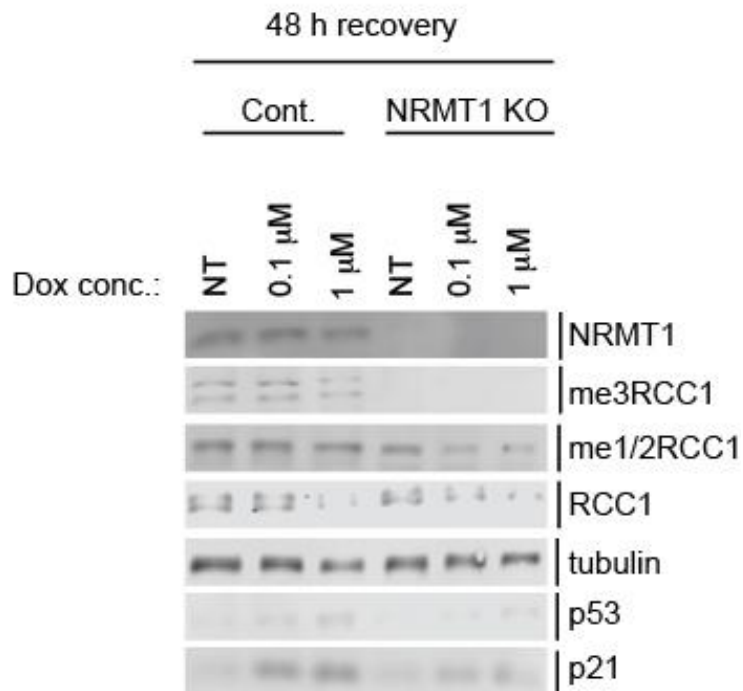


Figure 19. DNA damage signaling of cont. and NRMT1 KO cells.

5.0×10^4 cells per well were seeded into 12-well plates. Cells were then treated with doxorubicin at the indicated concentrations for 24 hours, and then immediately lysed (A), or the media was replaced, and cells were allowed to recover for 48 hours before lysis (B). Western blot analysis was conducted using the antibodies indicated in the figure. Blots are representative images of three independent experiments.

series of experiments, I performed western blot analysis as indicated above for all five lines. For example, in one set of data, after treatment with doxorubicin for 24 hours, p53 expression was elevated (Figs. 20A and 21). However, p21 expression was barely detectable.

In another set of experiments, I performed western blot analysis during the recovery period (Figs. 20B and 21). In this instance, p53 expression was elevated when compared to untreated cells; however, the levels of p53 were the same in each line. Thus, the difference in p53 levels observed in Figure 19 was not reproducible.

Finally, I also evaluated a couple of NRMT1 substrates to see if they exhibited expression differences. Specifically, I looked at Rb and DDB2, which are known to be involved in the DNA damage response (50). As shown in Figure 20B, there was no appreciable difference in the expression of these two proteins among the five cell lines.

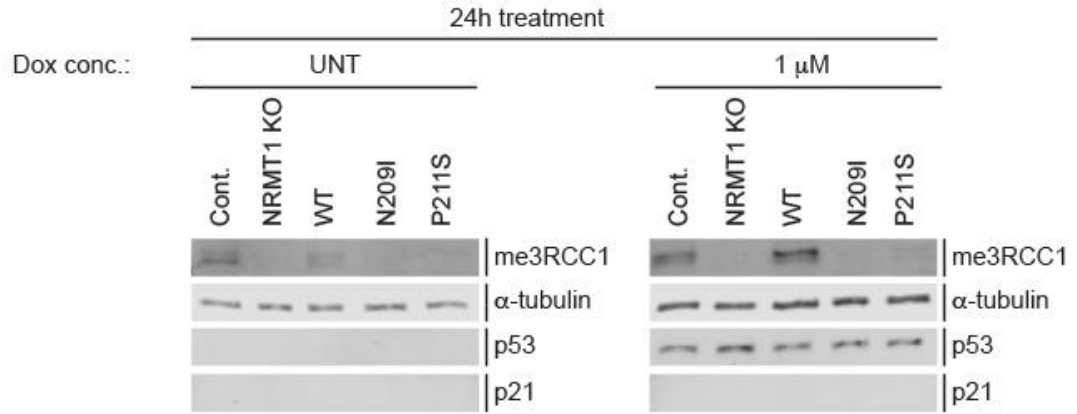
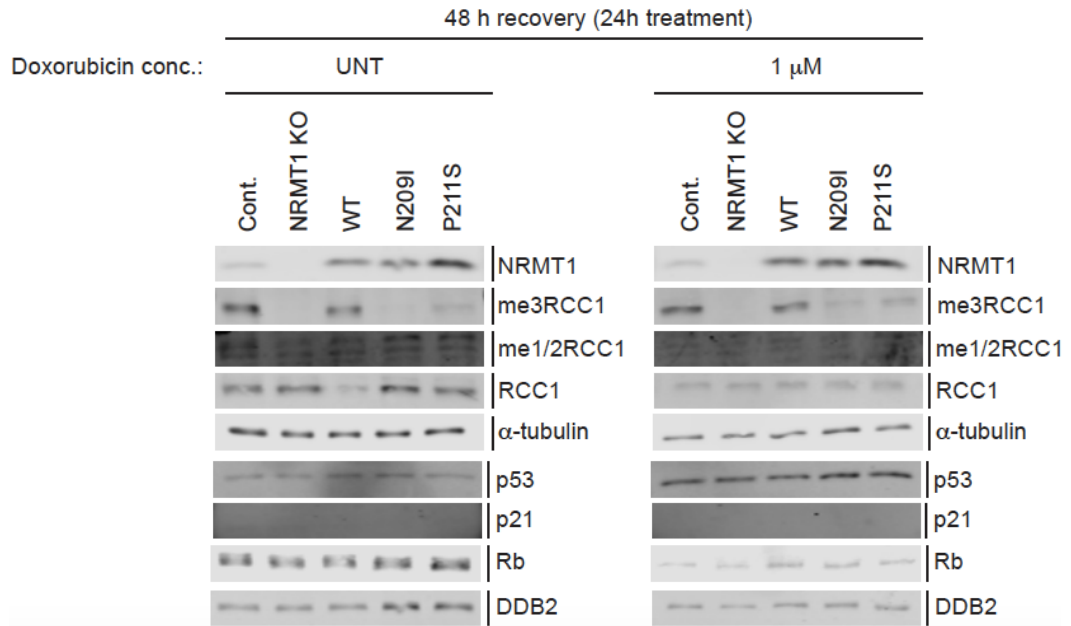
A**B**

Figure 20. DNA damage signaling of rescue cell lines.

The five HCT116 cell lines were seeded at 2.4×10^4 cells per well in 24-well plates. Cells were then treated with 0 or 1 μM doxorubicin for 24 hours, and then immediately lysed (A), or the media was replaced, and cells were allowed to recover for 48 hours before lysis (B). Western blot analysis was conducted using the antibodies indicated in the figure. Results are representative of two independent experiments.

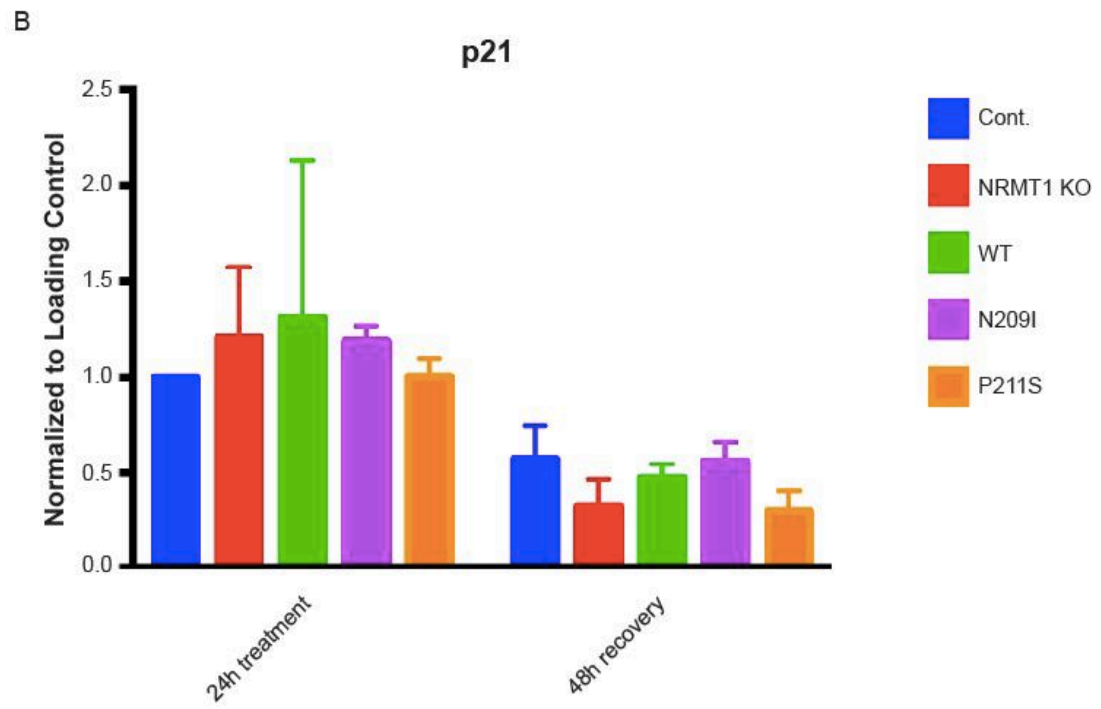
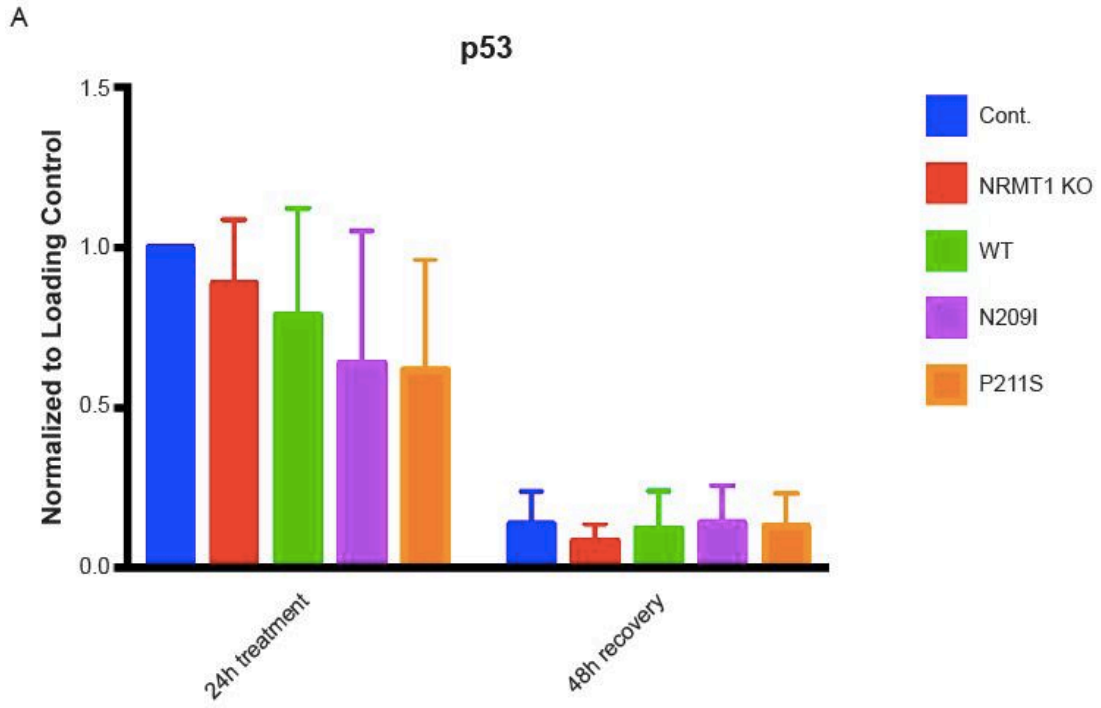


Figure 21. DNA damage signaling quantification.

Densitometry quantification of p53 (A) and p21 (B) bands for the 1 μ M doxorubicin treatment. The quantification pertains to western blots displayed in figures 19 and 20. For comparison purposes, cont. 24h treatment was set to 1.0. Quantification for p53 was performed from three independent experiments, while quantification for p21 was performed from two independent experiments (blank p21 blots in Figure 20 not included).

DISCUSSION

Recent work has experimentally verified a handful of predicted NRMT1 substrates and has determined that the N-terminal trimethylation by NRMT1 is necessary for their function (20,52,118,119). Studies have furthermore detailed the peptide-binding channel of NRMT1 (110), as well as resolved the enzymatic mechanism of NRMT1 (133). Despite this crucial work to uncover basic knowledge about NRMT1, little attention has been devoted to the impact of NRMT1 cancer mutants on basic cellular function and the response to DNA damage. Importantly, therefore, my work was the first attempt to address the role of the NRMT1 cancer mutants N209I (endometrial) and P211S (lung) in the DNA damage response.

I first examined the mutant NRMT1 methylation pattern in cells. Despite my *in vitro* data showing that the N209I and P211S mutants are catalytically inefficient and slower enzymes (Chapter II), they both lacked the ability to rescue trimethylation in HCT116 cells. The reason for the difference between the *in vitro* and cellular data is unknown but could potentially be due to regulation. In an *in vitro* methylation reaction, the only factors present are enzyme, substrate, and SAM methyl donor. In a cellular

environment, however, there are also, likely, factors present that contribute to the regulation of methylation reactions. Future studies to identify these factors should provide important insight into NRMT1 function.

I furthermore found that the N209I mutant exhibited a more pronounced cytoplasmic localization when compared to WT protein. Although the significance of this is not known, one could easily speculate that this would affect the access of NRMT1 to its substrates or binding partners.

Next, I examined the effect of the cancer mutants on cellular proliferation. We previously reported that loss of NRMT1 in HCT116 cells causes decreased proliferation (109), an observation that I reproduced. However, in these later studies, expression of WT NRMT1 failed to rescue the proliferation defect. Similarly, expression of the cancer mutants also had no effect when compared to KO cells. The data are not in agreement with what I have reported (109), which showed that both WT and N209I could rescue the proliferation defect of KO cells.

I offer the following possibility for the above discrepancy. RCC1 was one of the first NRMT1 substrates identified and characterized (47). Experiments in MDCK cells showed that a methylation-defective mutant of RCC1 bound to chromatin less than wild-type protein during

mitosis and caused spindle-pole defects (120,122). Thus, the loss of NRMT1 (and defective RCC1 methylation) could result in adaptive changes in cells to bypass this crisis. This could be one plausible explanation as to why re-expressing wild-type NRMT1 had no effect in KO cells that had been established. An alternative approach to circumvent this problem was to introduce transient NRMT1 deficiency by siRNA knockdown. Unfortunately, after trying three different siRNA oligos, I could not achieve successful knockdown in HCT116 cells (Fig. 27).

This was not a technical issue, as a control siRNA targeting an unrelated gene worked well (Fig. 27). Nevertheless, I evaluated whether expression of the NRMT1 cancer mutants or WT protein would have any effect during the DNA damage response. Although initial experiments suggested that KO cells were more sensitive to doxorubicin, those results were not reproducible. Furthermore, the response of the rescue cell lines towards doxorubicin was not significantly different compared to that of KO cells. As such, I conclude that NRMT1 likely has no effect on the DNA damage response in HCT116 cells in response to doxorubicin.

If adaptive changes have occurred in the KO cells, as I mentioned above, then obviously this could also be a

contributing factor to how the cells respond to doxorubicin. Besides the possibility of adaptive changes, there are some other possible technical explanations for the discrepancy observed.

First, cells could be positive for mycoplasma and affected by it. Second, my cell lines had not been authenticated since the time that they were originally obtained from ATCC. As these HCT116 cells were obtained several years ago, it is possible that cross-contamination or even mis-labelling had occurred. Third, high passage numbers of the cells could result in genetic drift and alter cell characteristics and phenotypes over time. Additionally, the ATCC media recommendation for HCT116 cells is McCoy's 5A. Despite this recommendation, I used DMEM media (as other studies have also done for HCT116 cells (176,177)), which could potentially contribute to changes in growth or other characteristics over time.

Lastly, an equally plausible scenario is that NRMT1 could be crucial for the DNA damage response in breast cancer cell lines, but not in HCT116 cells. In breast cancer cell lines, it has been shown that the depletion of NRMT1 and treatment with etoposide decreased cell viability. The treatment also produced more γ -H2AX foci in the NRMT1-depleted cells (50).

In my experiments with doxorubicin in HCT116 cells, 1 μ M treatment did not result in enhanced DNA damage sensitivity, unlike in the original experiments with breast cancer cell lines employing etoposide treatment (50). Thus, if the effect of the NRMT1 cancer mutants are to be further studied in the context of DNA damage, it would seem more sensible to do so in breast cancer cell lines.

CHAPTER IV: FUTURE DIRECTIONS

My dissertation research was born out of an interest sparked from a 2011 study. That work demonstrated that some B-cell lymphoma patients possess a Y641 aromatic cage active site mutation in the histone methyltransferase EZH2 (105,111,115). The mutation was found to change the catalytic specificity of EZH2 from a mono- to a trimethylase (105,111,115). This altered gene expression and increased oncogenicity (105,111,115). These findings, coupled with a similarity in the spatial alignment between EZH2 and NRMT1/2, lead me to pursue whether the catalytic specificities of NRMT1 or NRMT2 are altered by their harbored mutations found in some cancers, or in the aromatic cage itself.

My findings from Chapter II show that the aromatic cage mutations of both NRMT1 and NRMT2 yielded no significant alterations in activity when compared to the wild-type protein. In contrast, some cancer mutations of both NRMT1 (N209I and P211S) and NRMT2 (V224L) significantly altered the catalytic specificity.

Specifically, the N209I and P211S mutants were found to require increased time and substrate concentration to match the activity of wild type NRMT1. This led me to propose that they are slower, catalytically inefficient enzymes. Finally, the NRMT2 V224L breast cancer mutant had little detectable activity.

In Chapter III, I sought to characterize the significance of the N209I and P211S mutants in a cellular context. My approach was to express these mutants and WT NRMT1 in a knockout line that had been generated by CRISPR in HCT116 cells ("KO" cells). As a control, I utilized HCT116 cells that went through the same process as the KO cells, except no guide RNAs were used – empty vector (cont. cells).

Although the results in Chapter II demonstrate that the cancer mutants are inefficient *in vitro*, they seem to lack notable trimethylase activity in cells. I further discovered that N209I had increased cytoplasmic localization compared to the predominantly nuclear localization of wild type NRMT1 (46,47) and P211S proteins. Whether this contributes to an oncogenic phenotype is uncertain at this point.

Having established my rescue cell lines, I then attempted to assess the importance of the NRMT1 cancer

mutants in a cellular context. Based on my data, I concluded that the expression of the cancer mutants or WT NRMT1 protein had no effect on KO cells with respect to proliferation. Thus, part of my data is in contrast to what we previously published (109).

Concurrently, I explored the potential effects of the NRMT1 mutants in the context of DNA damage, given that it was previously shown that shRNA knockdown of NRMT1 in breast cancer cells caused an increased sensitivity to DNA damage (50). Using the cont., KO, and rescue cell lines, I induced DNA damage with the chemotherapeutic drug doxorubicin. My initial observations indicated that KO cells may be more sensitive to doxorubicin (either by cell viability assay or p53/p21 induction). However, the data was not consistently repeatable. In conclusion, neither the KO nor rescue cell lines showed a significant difference in doxorubicin sensitivity compared to cont. cells.

Future Biochemical Studies for NRMT1

In Chapter II, I demonstrated that N209I (endometrial cancer) and P211S (lung cancer) NRMT1 mutants have decreased trimethylation and increased mono-/dimethylation

activity toward substrates. This suggests that the mutants could have impaired kinetic parameters, and assays should be performed to determine any alterations to K_m and V_{max} values. Given the increased need of the mutants for time and substrate levels, alterations to K_m , or perhaps V_{max} , seem plausible. An increase in K_m would demonstrate that the mutants require a higher substrate concentration to reach half maximal velocity, compared to WT NRMT1. Furthermore, a decrease in V_{max} would demonstrate that the mutants catalyze methylation reactions at a lower rate compared to WT NRMT1.

I investigated these questions using several different methyltransferase assay kits, which measure levels of SAH (a by-product of methylation reactions). However, using full-length recombinant protein, I was unable to detect much signal over background. Since I can detect methylation of substrate by western blot, it is possible that these assay kits are not sensitive enough to detect the levels of SAH normally generated by reaction with NRMT1. Given this difficulty I encountered using full-length recombinant protein with multiple assay kits, this would need to be conducted using peptide substrate. However, as this would utilize only a small portion of the N-terminus of the substrate protein, this would be less

biologically relevant. An alternative would be to use full-length protein substrate and measure the kinetics by radioactive means or metabolite labeling.

In addition to discovering the kinetics of N209I and P211S, the binding affinity or folding of the mutant proteins could also be investigated. Besides the possibility of N209I and P211S possessing altered kinetic parameters, contributing to the observed shift in catalytic specificity, the mutants could also exhibit a decreased binding affinity for their substrates. In order to determine differences in binding affinity between WT NRMT1 and the mutants, isothermal titration calorimetry could be employed. It is plausible that the mutants have decreased substrate binding affinity, which could additionally contribute to the observed change in catalytic specificity.

Lastly, the folding of the mutants could be studied. It is possible that the location of the mutants in the peptide-binding channel of NRMT1, and their hypothesized effects on the global structure (based on molecular modeling), could impact the folding of the proteins. In order to determine if folding of the proteins are affected by the mutations, circular dichroism could be utilized. A defect in protein folding could impact the overall

activity, giving the altered catalytic specificity seen with the mutants.

Studying the kinetics, binding affinity, and folding of N209I and P211S may contribute to general biochemical knowledge of the mutations. This may be informative for the cancers that harbor these mutations (N209I, endometrial cancer; P211S, lung cancer).

Future Studies for NRMT1 and the DNA Damage Response

While my studies suggest that NRMT1 did not play a role in the DNA damage response in HCT116 cells, it was shown to do so in breast cancer cell lines (50). Thus, the study of DNA damage in breast cancer seems to be a more appropriate avenue to explore with respect to the NRMT1 cancer mutants that I characterized in Chapter II.

Within the list of potential NRMT1 substrates, only a handful are involved in the DNA damage response, including Rb, DDB2, PARP3, and BAP1 (50). At present, it is unknown whether or how methylation by NRMT1 facilitates the function of these targets. Methylation could affect the localization of these targets to sites of DNA damage through direct DNA binding; or, it could regulate protein-protein interactions crucial for downstream functions. For

example, while methylation of DDB2 is necessary for its recruitment to sites of DNA damage (52), the methylation of PARP3 is not (118).

Thus, a preliminary working model for how NRMT1 might function during DNA damage in breast cancer cells is depicted in Figure 22. DNA damaging agents, such as etoposide, cause DSBs, resulting in p53 activation and transcriptional upregulation of DNA repair proteins, which can lead to cell survival (178). One potential role for NRMT1 could involve the maintenance of p53 expression. Additionally, NRMT1 may be exerting influence over the DNA damage response through trimethylation of an unknown protein. This methylation could facilitate either the localization of DNA repair proteins to sites of DNA damage, or regulate protein-protein interactions, which would result in downstream localization to the DSBs. Since the N209I and P211S mutants do not result in rescue of N-terminal trimethylation in cells, I hypothesize that these mutants will be incapable of rescuing the sensitivity towards DNA damage in breast cancer cells deficient in NRMT1.

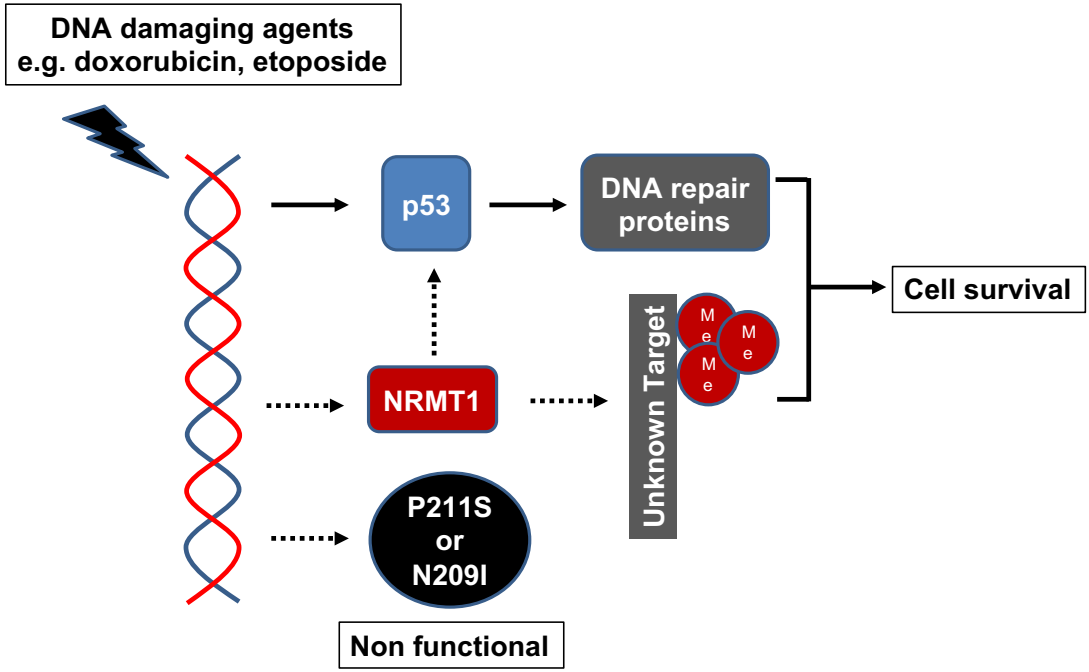


Figure 22. Model of NRMT1 in the DNA damage response.

The role of NRMT1 in the DNA damage response remains unclear, with the following model proposed. Upon doxorubicin treatment, p53 becomes activated and upregulates the expression of DNA repair proteins, leading to cell survival. In response to doxorubicin, NRMT1 is proposed to influence the expression of p53, which would further increase DNA repair protein (some of which are verified NRMT1 substrates) expression and cell survival. NRMT1 may be exerting additional clout over this response through trimethylation of an unknown protein, which could be one of its repair protein substrates, leading to further cell survival. As the NRMT1 mutants N209I and P211S do not rescue N-terminal trimethylation in cells, they are hypothesized to be incapable of rescuing the effects of the DNA damage and are therefore proposed to be nonfunctional in this context.

Developing More Tools to Study NRMT1 Substrates

There are many putative targets of NRMT1, and one challenge is to identify specific targets in different pathways. One area that needs attention is the lack of antibodies against other NRMT1 substrate consensus sequences, besides the existing SPK antibodies. An example would include antibodies that recognize the trimethylated PPK consensus (for targets such as Rb). A more tedious, but unbiased, approach would be to employ mass spectrometry to determine the substrate(s) differentially methylated by NRMT1 during various cellular processes, such as the DNA damage response.

Once these differentially methylated substrates are identified, they can then be tested for their importance in the pathway. As an example, suppose there was a substrate of NRMT1 named "SubX," for simplicity. CRISPR/Cas9 methodology could then be utilized to create a knockout cell line lacking SubX. Preliminary studies could then quickly assess the importance of SubX in a pathway.

Subsequently, the knockout cell line would then be rescued with either wild type SubX or a non-methylatable mutant. This would further allow me to determine the importance of methylation of the protein in the pathway.

Finally, generation of knockin mice for this mutant will allow the determination of its physiological importance.

Future Studies for NRMT1 and Oxidative Stress

One important observation gained from the studies of NRMT1 KO mice and MEFs is their increased sensitivity towards oxidative stress (51). Thus, NRMT1 could also act through this pathway to influence cell survival in response to certain chemotherapeutic drugs which cause oxidative stress (179,180).

As an initial study, I would use the H₂DCF-DA reagent (Invitrogen) to detect total cellular ROS levels in NRMT1-deficient cells in response to drugs, or other insults (181). Using the MitoSOX™ Red reagent (Thermo Fisher Scientific), which is oxidized by superoxide, would further allow me to examine mitochondrial ROS generation (182). If these preliminary experiments proved fruitful, one could then utilize state-of-the-art techniques, such as electron spin resonance (183,184).

REFERENCES

1. Clamp, M., Fry, B., Kamal, M., Xie, X., Cuff, J., Lin, M. F., Kellis, M., Lindblad-Toh, K., and Lander, E. S. (2007) Distinguishing protein-coding and noncoding genes in the human genome. *Proceedings of the National Academy of Sciences* **104**, 19428–19433.
2. Ezkurdia, L., Juan, D., Rodriguez, J. M., Frankish, A., Diekhans, M., Harrow, J., Vazquez, J., Valencia, A., and Tress, M. L. (2014) Multiple evidence strands suggest that there may be as few as 19 000 human protein-coding genes. *Human Molecular Genetics* **23**, 5866–5878.
3. Human Genome Sequencing, C. (2004) Finishing the euchromatic sequence of the human genome. *Nature* **431**, 931–945.
4. Doll, S. B., Alma L. (2015) Mass spectrometry-based detection and assignment of protein posttranslational modifications. *ACS Chemical Biology* **10**, 63–71.
5. Duan, G., and Walther, D. (2015) The Roles of Post-translational Modifications in the Context of Protein

- Interaction Networks. *PLoS Computational Biology* **11**, e1004049
6. Tooley, J. G., and Schaner Tooley, C. E. (2014) New roles for old modifications: Emerging roles of N-terminal post-translational modifications in development and disease. *Protein Science* **23**, 1641-1649.
 7. Varland, S., Osberg, C., and Arnesen, T. (2015) N-terminal modifications of cellular proteins: The enzymes involved, their substrate specificities and biological effects. *Proteomics* **15**, 2385-2401.
 8. Wang, Y.-C., Peterson, S. E., and Loring, J. F. (2013) Protein Post-Translational Modifications and Regulation of Pluripotency in Human Stem Cells. *Cell Research* **24**, 143-160.
 9. Brown, J. S., and Jackson, S. P. (2015) Ubiquitylation, neddylation and the DNA damage response. *Open Biology* **5**, 150018.
 10. Erin, E. W., Paul, R. T., and Lorne, J. H. (2015) Protein Arginine Deiminases and Associated Citrullination: Physiological Functions and Diseases Associated with Dysregulation. *Current Drug Targets* **16**, 700-710.

11. Markolovic, S., Wilkins, S. E., and Schofield, C. J. (2015) Protein Hydroxylation Catalyzed by 2-Oxoglutarate-dependent Oxygenases. *Journal of Biological Chemistry* **290**, 20712–20722.
12. Spiro, R. G. (2002) Protein glycosylation: nature, distribution, enzymatic formation, and disease implications of glycopeptide bonds. *Glycobiology* **12**, 43R–56R.
13. Rossetto, D., Avvakumov, N., and Côté, J. (2012) Histone phosphorylation: A chromatin modification involved in diverse nuclear events. *Epigenetics* **7**, 1098–1108.
14. Swatek, K. N., and Komander, D. (2016) Ubiquitin modifications. *Cell Res* **26**, 399–422.
15. Verdin, E., and Ott, M. (2015) 50 years of protein acetylation: from gene regulation to epigenetics, metabolism and beyond. *Nat Rev Mol Cell Biol* **16**, 258–264.
16. Zhang, X., Wen, H., and Shi, X. (2012) Lysine methylation: beyond histones. *Acta Biochimica et Biophysica Sinica* **44**, 14–27.
17. Bowman, G. D., and Poirier, M. G. (2015) Post-Translational Modifications of Histones That Influence Nucleosome Dynamics. *Chemical Reviews* **115**, 2274–2295.

18. Cox, M. M. D., Jennifer A.; Michael O'Donnell. (2012) *Molecular Biology: Principles and Practice*, W. H. Freeman and Company, 41 Madison Ave., New York, NY 10010, USA, and Houndmills, Basingstoke RG21 6XS, England.
19. Cao, J., and Yan, Q. (2012) Histone Ubiquitination and Deubiquitination in Transcription, DNA Damage Response, and Cancer. *Frontiers in Oncology* **2**
20. Bailey, A. O., Panchenko, T., Sathyan, K. M., Petkowski, J. J., Pai, P.-J., Bai, D. L., Russell, D. H., Macara, I. G., Shabanowitz, J., Hunt, D. F., Black, B. E., and Foltz, D. R. (2013) Posttranslational modification of CENP-A influences the conformation of centromeric chromatin. *Proceedings of the National Academy of Sciences of the United States of America* **110**, 11827-11832.
21. Biggar, K. K., and Li, S. S. C. (2015) Non-histone protein methylation as a regulator of cellular signalling and function. *Nat Rev Mol Cell Biol* **16**, 5-17.
22. Kapoor-Vazirani, P., and Vertino, P. M. (2014) A Dual Role for the Histone Methyltransferase PR-SET7/SETD8 and Histone H4 Lysine 20 Monomethylation in the Local

- Regulation of RNA Polymerase II Pausing. *Journal of Biological Chemistry* **289**, 7425-7437.
23. Martin, C., and Zhang, Y. (2005) The diverse functions of histone lysine methylation. *Nat Rev Mol Cell Biol* **6**, 838-849.
24. Schotta, G., Sengupta, R., Kubicek, S., Malin, S., Kauer, M., Callén, E., Celeste, A., Pagani, M., Opravil, S., De La Rosa-Velazquez, I. A., Espejo, A., Bedford, M. T., Nussenzweig, A., Busslinger, M., and Jenuwein, T. (2008) A chromatin-wide transition to H4K20 monomethylation impairs genome integrity and programmed DNA rearrangements in the mouse. *Genes & Development* **22**, 2048-2061.
25. Zhang, X., Bernatavichute, Y. V., Cokus, S., Pellegrini, M., and Jacobsen, S. E. (2009) Genome-wide analysis of mono-, di- and trimethylation of histone H3 lysine 4 in *Arabidopsis thaliana*. *Genome Biology* **10**, R62.
26. Zhang, Y., and Reinberg, D. (2001) Transcription regulation by histone methylation: interplay between different covalent modifications of the core histone tails. *Genes & Development* **15**, 2343-2360.

27. Arnesen, T. (2011) Towards a Functional Understanding of Protein N-Terminal Acetylation. *PLOS Biology* **9**, e1001074
28. Avrahami, D., and Shai, Y. (2004) A New Group of Antifungal and Antibacterial Lipopeptides Derived from Non-membrane Active Peptides Conjugated to Palmitic Acid. *Journal of Biological Chemistry* **279**, 12277-12285.
29. Góngora-Benítez, M., Tulla-Puche, J., and Albericio, F. (2014) Multifaceted Roles of Disulfide Bonds. Peptides as Therapeutics. *Chemical Reviews* **114**, 901-926.
30. Hunter, T. (2000) Signaling—2000 and Beyond. *Cell* **100**, 113-127.
31. Kim, K.-H., and Seong, B. L. (2001) Peptide amidation: Production of peptide hormones in vivo and in vitro. *Biotechnology and Bioprocess Engineering* **6**, 244-251.
32. Clarke, S. G. (2013) Protein methylation at the surface and buried deep: thinking outside the histone box. *Trends in Biochemical Sciences* **38**, 243-252.
33. Fukata, Y., and Fukata, M. (2010) Protein palmitoylation in neuronal development and synaptic plasticity. *Nat Rev Neurosci* **11**, 161-175.

34. Hamamoto, R., Saloura, V., and Nakamura, Y. (2015) Critical roles of non-histone protein lysine methylation in human tumorigenesis. *Nat Rev Cancer* **15**, 110-124.
35. Humphrey, S. J., James, D. E., and Mann, M. (2015) Protein Phosphorylation: A Major Switch Mechanism for Metabolic Regulation. *Trends in Endocrinology & Metabolism* **26**, 676-687.
36. Murn, J., and Shi, Y. (2017) The winding path of protein methylation research: milestones and new frontiers. *Nature Reviews Molecular Cell Biology* **18**, 517-527.
37. Nakamura, T., Tu, S., Akhtar, Mohd W., Sunico, Carmen R., Okamoto, S.-i., and Lipton, Stuart A. (2013) Aberrant Protein S-Nitrosylation in Neurodegenerative Diseases. *Neuron* **78**, 596-614.
38. Ploumakis, A., and Coleman, M. L. (2015) OH, the Places You'll Go! Hydroxylation, Gene Expression, and Cancer. *Molecular Cell* **58**, 729-741.
39. Xu, C., and Ng, D. T. W. (2015) Glycosylation-directed quality control of protein folding. *Nat Rev Mol Cell Biol* **16**, 742-752.
40. Yang, Y.-S., Wang, C.-C., Chen, B.-H., Hou, Y.-H., Hung, K.-S., and Mao, Y.-C. (2015) Tyrosine Sulfation

as a Protein Post-Translational Modification.

Molecules **20**, 2138–2164.

41. Bonissone, S., Gupta, N., Romine, M., Bradshaw, R. A., and Pevzner, P. A. (2013) N-terminal Protein Processing: A Comparative Proteogenomic Analysis. *Molecular & Cellular Proteomics : MCP* **12**, 14–28.
42. Helbig, A. O., Gauci, S., Raijmakers, R., van Breukelen, B., Slijper, M., Mohammed, S., and Heck, A. J. R. (2010) Profiling of N-Acetylated Protein Termini Provides In-depth Insights into the N-terminal Nature of the Proteome. *Molecular & Cellular Proteomics : MCP* **9**, 928–939.
43. Scott, D. C., Monda, J. K., Bennett, E. J., Harper, J. W., and Schulman, B. A. (2011) N-Terminal Acetylation Acts as an Avidity Enhancer Within an Interconnected Multiprotein Complex. *Science (New York, N.Y.)* **334**, 674–678.
44. Petkowski, J. J., Schaner Tooley, C. E., Anderson, L. C., Shumilin, I. A., Balsbaugh, J. L., Shabanowitz, J., Hunt, D. F., Minor, W., and Macara, I. G. (2012) Substrate Specificity of Mammalian N-Terminal α -Amino Methyltransferase NRMT. *Biochemistry* **51**, 5942–5950.
45. Polevoda, B., and Sherman, F. (2003) N-terminal Acetyltransferases and Sequence Requirements for N-

- terminal Acetylation of Eukaryotic Proteins. *Journal of Molecular Biology* **325**, 595-622.
46. Petkowski, Janusz J., Bonsignore, Lindsay A., Tooley, John G., Wilkey, Daniel W., Merchant, Michael L., Macara, Ian G., and Schaner Tooley, Christine E. (2013) NRMT2 is an N-terminal monomethylase that primes for its homologue NRMT1. *Biochemical Journal* **456**, 453-462.
47. Schaner Tooley, C. E., Petkowski, J. J., Muratore-Schroeder, T. L., Balsbaugh, J. L., Shabanowitz, J., Sabat, M., Minor, W., Hunt, D. F., and Macara, I. G. (2010) NRMT is an α -N-methyltransferase that methylates RCC1 and retinoblastoma protein. *Nature* **466**, 1125-1128.
48. Kouzarides, T. (2007) Chromatin Modifications and Their Function. *Cell* **128**, 693-705.
49. Strahl, B. D., and Allis, C. D. (2000) The language of covalent histone modifications. *Nature* **403**, 41-45.
50. Bonsignore, L. A., Butler, J. S., Klinge, C. M., and Schaner Tooley, C. E. (2015) Loss of the N-terminal methyltransferase NRMT1 increases sensitivity to DNA damage and promotes mammary oncogenesis. *Oncotarget* **6**, 12248-12263.

51. Bonsignore, L. A., Tooley, J. G., Van Hoose, P. M., Wang, E., Cheng, A., Cole, M. P., and Schaner Tooley, C. E. (2015) NRMT1 knockout mice exhibit phenotypes associated with impaired DNA repair and premature aging. *Mechanisms of Ageing and Development* **146–148.**, 42–52.
52. Cai, Q., Fu, L., Wang, Z., Gan, N., Dai, X., and Wang, Y. (2014) α -N-Methylation of Damaged DNA-binding Protein 2 (DDB2) and Its Function in Nucleotide Excision Repair. *The Journal of Biological Chemistry* **289**, 16046–16056.
53. Greeson, N. T., Sengupta, R., Arida, A. R., Jenuwein, T., and Sanders, S. L. (2008) Di-methyl H4 Lysine 20 Targets the Checkpoint Protein Crb2 to Sites of DNA Damage. *The Journal of Biological Chemistry* **283**, 33168–33174.
54. Richards, E. J., and Elgin, S. C. R. (2002) Epigenetic Codes for Heterochromatin Formation and Silencing. *Cell* **108**, 489–500.
55. Santos-Rosa, H., Schneider, R., Bannister, A. J., Sherriff, J., Bernstein, B. E., Emre, N. C. T., Schreiber, S. L., Mellor, J., and Kouzarides, T. (2002) Active genes are tri-methylated at K4 of histone H3. *Nature* **419**, 407–411.

56. Smith, B. C., and Denu, J. M. (2009) Chemical mechanisms of histone lysine and arginine modifications. *Biochimica et biophysica acta* **1789**, 45-57.
57. Moore, K. E., and Gozani, O. (2014) An Unexpected Journey: Lysine Methylation Across the Proteome. *Biochimica et biophysica acta* **1839**, 1395-1403.
58. Bedford, M. T., and Clarke, S. G. (2009) Protein Arginine Methylation in Mammals: Who, What, and Why. *Molecular Cell* **33**, 1-13.
59. Cloutier, P., Lavallée-Adam, M., Faubert, D., Blanchette, M., and Coulombe, B. (2013) A Newly Uncovered Group of Distantly Related Lysine Methyltransferases Preferentially Interact with Molecular Chaperones to Regulate Their Activity. *PLoS Genetics* **9**, e1003210
60. Rhein, V. F., Carroll, J., Ding, S., Fearnley, I. M., and Walker, J. E. (2017) Human METTL12 is a mitochondrial methyltransferase that modifies citrate synthase. *Febs Letters* **591**, 1641-1652.
61. Sakaguchi, A., Joyce, E., Aoki, T., Schedl, P., and Steward, R. (2012) The Histone H4 Lysine 20 Monomethyl Mark, Set by PR-Set7 and Stabilized by L(3)mbt, Is

Necessary for Proper Interphase Chromatin Organization. *PLOS ONE* **7**, e45321

62. Wu, H., Min, J., Lunin, V. V., Antoshenko, T., Dombrowski, L., Zeng, H., Allali-Hassani, A., Campagna-Slater, V., Vedadi, M., Arrowsmith, C. H., Plotnikov, A. N., and Schapira, M. (2010) Structural Biology of Human H3K9 Methyltransferases. *PLOS ONE* **5**, e8570
63. Bernt, K. M., Zhu, N., Sinha, A. U., Vempati, S., Faber, J., Krivtsov, A. V., Feng, Z., Punt, N., Daigle, A., Bullinger, L., Pollock, R. M., Richon, V. M., Kung, A. L., and Armstrong, S. A. (2011) MLL-rearranged Leukemia is Dependent on Aberrant H3K79 Methylation by DOT1L. *Cancer Cell* **20**, 66–78.
64. Garske, A. L., Craciun, G., and Denu, J. M. (2008) A Combinatorial H4 Tail Library to Explore the Histone Code. *Biochemistry* **47**, 8094–8102.
65. Boriack-Sjodin, P. A., and Swinger, K. K. (2016) Protein Methyltransferases: A Distinct, Diverse, and Dynamic Family of Enzymes. *Biochemistry* **55**, 1557–1569.
66. Cheng, X., and Zhang, X. (2007) Structural dynamics of protein lysine methylation and demethylation. *Mutation Research/Fundamental and Molecular Mechanisms of Mutagenesis* **618**, 102–115.

67. Han, H.-S., Choi, D., Choi, S., and Koo, S.-H. (2014) Roles of Protein Arginine Methyltransferases in the Control of Glucose Metabolism. *Endocrinol Metab* **29**, 435-440.
68. Black, J. C., Van Rechem, C., and Whetstine, J. R. (2012) Histone Lysine Methylation Dynamics: Establishment, Regulation, and Biological Impact. *Molecular cell* **48**, 10.1016/j.molcel.2012.1011.1006
69. Chaturvedi, C.-P., Somasundaram, B., Singh, K., Carpenedo, R. L., Stanford, W. L., Dilworth, F. J., and Brand, M. (2012) Maintenance of gene silencing by the coordinate action of the H3K9 methyltransferase G9a/KMT1C and the H3K4 demethylase Jarid1a/KDM5A. *Proceedings of the National Academy of Sciences of the United States of America* **109**, 18845-18850.
70. Temimi, A. H. K. A., Reddy, Y. V., White, P. B., Guo, H., Qian, P., and Mecinović, J. (2017) Lysine Possesses the Optimal Chain Length for Histone Lysine Methyltransferase Catalysis. *Scientific Reports* **7**, 16148
71. Tian, X., Zhang, S., Liu, H.-M., Zhang, Y.-B., Blair, C. A., Mercola, D., Sassone-Corsi, P., and Zi, X. (2013) Histone Lysine-Specific Methyltransferases and Demethylases in Carcinogenesis: New Targets for Cancer

- Therapy and Prevention. *Current cancer drug targets* **13**, 558–579.
72. Yang, Y., and Bedford, M. T. (2013) Protein arginine methyltransferases and cancer. *Nat Rev Cancer* **13**, 37–50.
73. Kong, X., Ouyang, S., Liang, Z., Lu, J., Chen, L., Shen, B., Li, D., Zheng, M., Li, K. K., Luo, C., and Jiang, H. (2011) Catalytic Mechanism Investigation of Lysine-Specific Demethylase 1 (LSD1): A Computational Study. *PLOS ONE* **6**, e25444
74. Yang, Y., Yin, X., Yang, H., and Xu, Y. (2015) Histone Demethylase LSD2 Acts as an E3 Ubiquitin Ligase and Inhibits Cancer Cell Growth through Promoting Proteasomal Degradation of OGT. *Molecular Cell* **58**, 47–59.
75. Labbé, R. M., Holowatyj, A., and Yang, Z.-Q. (2014) Histone lysine demethylase (KDM) subfamily 4: structures, functions and therapeutic potential. *American Journal of Translational Research* **6**, 1–15.
76. Gao, C., Herold, J. M., Kireev, D., Wigle, T., Norris, J. L., and Frye, S. (2011) Biophysical Probes Reveal a “Compromise” Nature of the Methyl-lysine Binding Pocket in L3MBTL1. *Journal of the American Chemical Society* **133**, 5357–5362.

77. Moore, S. A., Ferhatoglu, Y., Jia, Y., Al-Jiab, R. A., and Scott, M. J. (2010) Structural and Biochemical Studies on the Chromo-barrel Domain of Male Specific Lethal 3 (MSL3) Reveal a Binding Preference for Mono- or Dimethyllysine 20 on Histone H4. *Journal of Biological Chemistry* **285**, 40879-40890.
78. Baubec, T., Colombo, D. F., Wirbelauer, C., Schmidt, J., Burger, L., Krebs, A. R., Akalin, A., and Schubeler, D. (2015) Genomic profiling of DNA methyltransferases reveals a role for DNMT3B in genic methylation. *Nature* **520**, 243-247.
79. Lu, R., and Wang, G. G. (2013) Tudor: a versatile family of histone methylation 'readers'. *Trends in Biochemical Sciences* **38**, 546-555.
80. Sanchez, R., and Zhou, M.-M. (2011) The PHD finger: a versatile epigenome reader. *Trends in Biochemical Sciences* **36**, 364-372.
81. Yap, K. L. Z., Ming-Ming. (2011) Structure and mechanisms of lysine methylation recognition by the chromodomain in gene transcription. *Biochemistry* **50**, 1966-1980.
82. Lee, J., Thompson, J. R., Botuyan, M. V., and Mer, G. (2008) Distinct binding modes specify the recognition

- of methylated histones H3K4 and H4K20 by JMJD2A-tudor. *Nature structural & molecular biology* **15**, 109–111.
83. Phillips, T. S., K. (2008) Chromatin remodeling in eukaryotes. *Nature Education* **1**, 209.
84. Denslow, S. A., and Wade, P. A. (2007) The human Mi-2//NuRD complex and gene regulation. *Oncogene* **26**, 5433–5438.
85. Ramírez, J., Dege, C., Kutateladze, T. G., and Hagman, J. (2012) MBD2 and Multiple Domains of CHD4 Are Required for Transcriptional Repression by Mi-2/NuRD Complexes. *Molecular and Cellular Biology* **32**, 5078–5088.
86. Deshpande, A. J., Deshpande, A., Sinha, A. U., Chen, L., Chang, J., Cihan, A., Fazio, M., Chen, C.-w., Zhu, N., Koche, R., Dzhekieva, L., Ibáñez, G., Dias, S., Banka, D., Krivtsov, A., Luo, M., Roeder, R. G., Bradner, J. E., Bernt, K. M., and Armstrong, S. A. (2014) AF10 Regulates Progressive H3K79 Methylation and HOX Gene Expression in Diverse AML Subtypes. *Cancer cell* **26**, 896–908.
87. Greer, E. L., and Shi, Y. (2012) Histone methylation: a dynamic mark in health, disease and inheritance. *Nature reviews. Genetics* **13**, 343–357.

88. Krivtsov, A. V., Feng, Z., Lemieux, M. E., Faber, J., Vempati, S., Sinha, A. U., Xia, X., Jesneck, J., Bracken, A. P., Silverman, L. B., Kutok, J. L., Kung, A. L., and Armstrong, S. A. (2008) H3K79 methylation profiles define murine and human MLL-AF4 leukemias. *Cancer cell* **14**, 355–368.
89. Okada, Y., Feng, Q., Lin, Y., Jiang, Q., Li, Y., Coffield, V. M., Su, L., Xu, G., and Zhang, Y. (2005) hDOT1L Links Histone Methylation to Leukemogenesis. *Cell* **121**, 167–178.
90. Landau, Dan A., Clement, K., Ziller, Michael J., Boyle, P., Fan, J., Gu, H., Stevenson, K., Sougnez, C., Wang, L., Li, S., Kotliar, D., Zhang, W., Ghandi, M., Garraway, L., Fernandes, Stacey M., Livak, Kenneth J., Gabriel, S., Gnirke, A., Lander, Eric S., Brown, Jennifer R., Neuberg, D., Kharchenko, Peter V., Hacohen, N., Getz, G., Meissner, A., and Wu, Catherine J. (2014) Locally Disordered Methylation Forms the Basis of Intratumor Methylome Variation in Chronic Lymphocytic Leukemia. *Cancer Cell* **26**, 813–825.
91. Bach, C., and Slany, Robert K. (2014) DOTting the Path to Doom: How Acceleration of Histone Methylation Leads to Leukemia. *Cancer Cell* **26**, 781–782.

92. Voet, D., Voet, Judith G., Pratt, Charlotte W. (2008) *Fundamentals of Biochemistry*, 3 ed., John Wiley & Sons, Inc., United States of America
93. Khare, V., and Eckert, K. A. (2002) The proofreading 3' → 5' exonuclease activity of DNA polymerases: a kinetic barrier to translesion DNA synthesis. *Mutation Research/Fundamental and Molecular Mechanisms of Mutagenesis* **510**, 45-54.
94. Jeggo, P. A., Pearl, L. H., and Carr, A. M. (2016) DNA repair, genome stability and cancer: a historical perspective. *Nat Rev Cancer* **16**, 35-42.
95. Ciccia, A., and Elledge, S. J. (2010) The DNA Damage Response: Making It Safe to Play with Knives. *Molecular Cell* **40**, 179-204.
96. Weber, S. (2005) Light-driven enzymatic catalysis of DNA repair: a review of recent biophysical studies on photolyase. *Biochimica et Biophysica Acta (BBA) - Bioenergetics* **1707**, 1-23.
97. Kim, Y.-J., and Wilson, D. M. (2012) Overview of Base Excision Repair Biochemistry. *Current molecular pharmacology* **5**, 3-13.
98. Krokan, H. E., and Bjørås, M. (2013) Base Excision Repair. *Cold Spring Harbor Perspectives in Biology*

99. Lehmann, A. R. (2001) The xeroderma pigmentosum group D (XPD) gene: one gene, two functions, three diseases. *Genes & Development* **15**, 15-23.
100. Ray Chaudhuri, A., and Nussenzweig, A. (2017) The multifaceted roles of PARP1 in DNA repair and chromatin remodelling. *Nat Rev Mol Cell Biol* **18**, 610-621.
101. Leung, K. K. K., and Shilton, B. H. (2015) Binding of DNA-Intercalating Agents to Oxidized and Reduced Quinone Reductase 2. *Biochemistry* **54**, 7438-7448.
102. Fell, V. L., and Schild-Poulter, C. (2012) Ku Regulates Signaling to DNA Damage Response Pathways through the Ku70 von Willebrand A Domain. *Molecular and Cellular Biology* **32**, 76-87.
103. Alberts, B., Johnson, Alexander, Lewis, Julian, Raff, Martin, Roberts, Keith, Walter, Peter. (2008) *Molecular Biology of the Cell*, 5 ed., Garland Science, Taylor & Francis Group, LLC, 270 Madison Ave., New York NY 10016, USA, and 2 Park Square, Milton Park, Abingdon, OX14 4RN, UK.
104. Ciferri, C., Lander, G. C., Maiolica, A., Herzog, F., Aebbersold, R., and Nogales, E. (2012) Molecular architecture of human polycomb repressive complex 2. *eLife* **1**, e00005

105. Yap, D. B., Chu, J., Berg, T., Schapira, M., Cheng, S. W. G., Moradian, A., Morin, R. D., Mungall, A. J., Meissner, B., Boyle, M., Marquez, V. E., Marra, M. A., Gascoyne, R. D., Humphries, R. K., Arrowsmith, C. H., Morin, G. B., and Aparicio, S. A. J. R. (2011) Somatic mutations at EZH2 Y641 act dominantly through a mechanism of selectively altered PRC2 catalytic activity, to increase H3K27 trimethylation. *Blood* **117**, 2451-2459.
106. Xiao, B., Wilson, J. R., and Gamblin, S. J. (2003) SET domains and histone methylation. *Current Opinion in Structural Biology* **13**, 699-705.
107. Xiao, B., Jing, C., Wilson, J. R., Walker, P. A., Vasisht, N., Kelly, G., Howell, S., Taylor, I. A., Blackburn, G. M., and Gamblin, S. J. (2003) Structure and catalytic mechanism of the human histone methyltransferase SET7/9. *Nature* **421**, 652-656.
108. Dong, C., Mao, Y., Tempel, W., Qin, S., Li, L., Loppnau, P., Huang, R., and Min, J. (2015) Structural basis for substrate recognition by the human N-terminal methyltransferase 1. *Genes & Development* **29**, 2343-2348.
109. Shields, K. M., Tooley, J. G., Petkowski, J. J., Wilkey, D. W., Garbett, N. C., Merchant, M. L., Cheng,

- A., and Schaner Tooley, C. E. (2017) Select human cancer mutants of NRMT1 alter its catalytic activity and decrease N-terminal trimethylation. *Protein Science* **26**, 1639-1652.
110. Wu, R., Yue, Y., Zheng, X., and Li, H. (2015) Molecular basis for histone N-terminal methylation by NRMT1. *Genes & Development* **29**, 1-6.
111. Béguelin, W., Popovic, R., Teater, M., Jiang, Y., Bunting, Karen L., Rosen, M., Shen, H., Yang, Shao N., Wang, L., Ezponda, T., Martinez-Garcia, E., Zhang, H., Zheng, Y., Verma, Sharad K., McCabe, Michael T., Ott, Heidi M., Van Aller, Glenn S., Kruger, Ryan G., Liu, Y., McHugh, Charles F., Scott, David W., Chung, Young R., Kelleher, N., Shaknovich, R., Creasy, Caretha L., Gascoyne, Randy D., Wong, K.-K., Cerchietti, L., Levine, Ross L., Abdel-Wahab, O., Licht, Jonathan D., Elemento, O., and Melnick, Ari M. (2013) EZH2 Is Required for Germinal Center Formation and Somatic EZH2 Mutations Promote Lymphoid Transformation. *Cancer Cell* **23**, 677-692.
112. Bracken, A. P., Pasini, D., Capra, M., Prosperini, E., Colli, E., and Helin, K. (2003) EZH2 is downstream of the pRB-E2F pathway, essential for proliferation and amplified in cancer. *The EMBO Journal* **22**, 5323-5335.

113. Heyn, H., and Esteller, M. (2013) EZH2: An Epigenetic Gatekeeper Promoting Lymphomagenesis. *Cancer Cell* **23**, 563-565.
114. Tan, J.-z., Yan, Y., Wang, X.-x., Jiang, Y., and Xu, H. E. (2014) EZH2: biology, disease, and structure-based drug discovery. *Acta Pharmacol Sin* **35**, 161-174.
115. Wigle, T. J., Knutson, S. K., Jin, L., Kuntz, K. W., Pollock, R. M., Richon, V. M., Copeland, R. A., and Scott, M. P. (2011) The Y641C mutation of EZH2 alters substrate specificity for histone H3 lysine 27 methylation states. *FEBS Letters* **585**, 3011-3014.
116. Kamakaka, R. T., and Biggins, S. (2005) Histone variants: deviants? *Genes & Development* **19**, 295-316.
117. Dai, X., Otake, K., You, C., Cai, Q., Wang, Z., Masumoto, H., and Wang, Y. (2013) Identification of Novel α -N-Methylation of CENP-B That Regulates Its Binding to the Centromeric DNA. *Journal of Proteome Research* **12**, 4167-4175.
118. Dai, X., Rulten, S. L., You, C., Caldecott, K. W., and Wang, Y. (2015) Identification and Functional Characterizations of N-Terminal α -N-Methylation and Phosphorylation of Serine 461 in Human Poly(ADP-ribose) Polymerase 3. *Journal of Proteome Research* **14**, 2575-2582.

119. Sathyan, K. M., Fachinetti, D., and Foltz, D. R. (2017) α -amino trimethylation of CENP-A by NRMT is required for full recruitment of the centromere. *Nature Communications* **8**
120. Chen, T., Muratore, T. L., Schaner-Tooley, C. E., Shabanowitz, J., Hunt, D. F., and Macara, I. G. (2007) N-terminal [alpha]-methylation of RCC1 is necessary for stable chromatin association and normal mitosis. *Nat Cell Biol* **9**, 596-603.
121. Furuta, M., Hori, T., and Fukagawa, T. (2016) Chromatin binding of RCC1 during mitosis is important for its nuclear localization in interphase. *Molecular Biology of the Cell* **27**, 371-381.
122. Hao, Y., and Macara, I. G. (2008) Regulation of chromatin binding by a conformational switch in the tail of the Ran exchange factor RCC1. *The Journal of Cell Biology* **182**, 827-836.
123. Hasegawa, K., Ryu, S. J., and Kaláb, P. (2013) Chromosomal gain promotes formation of a steep RanGTP gradient that drives mitosis in aneuploid cells. *The Journal of Cell Biology* **200**, 151-161.
124. Li, H. Y., Wirtz, D., and Zheng, Y. (2003) A mechanism of coupling RCC1 mobility to RanGTP production on the

- chromatin in vivo. *The Journal of Cell Biology* **160**, 635-644.
125. Nemergut, M. E., Mizzen, C. A., Stukenberg, T., Allis, C. D., and Macara, I. G. (2001) Chromatin Docking and Exchange Activity Enhancement of RCC1 by Histones H2A and H2B. *Science* **292**, 1540-1543.
126. Blus, B. J., Wiggins, K., and Khorasanizadeh, S. (2011) Epigenetic virtues of chromodomains. *Critical Reviews in Biochemistry and Molecular Biology* **46**, 507-526.
127. Vermeulen, M., Eberl, H. C., Matarese, F., Marks, H., Denissov, S., Butter, F., Lee, K. K., Olsen, J. V., Hyman, A. A., Stunnenberg, H. G., and Mann, M. (2010) Quantitative Interaction Proteomics and Genome-wide Profiling of Epigenetic Histone Marks and Their Readers. *Cell* **142**, 967-980.
128. Tooley, C. E., Petkowski, J. J., Muratore-Schroeder, T. L., Balsbaugh, J. L., Shabanowitz, J., Sabat, M., Minor, W., Hunt, D. F., and Macara, I. G. (2010) NRMT is an alpha-N-methyltransferase that methylates RCC1 and retinoblastoma protein. *Nature* **466**, 1125-1128
129. Chen, T., Brownawell, A. M., and Macara, I. G. (2004) Nucleocytoplasmic Shuttling of JAZ, a New Cargo

- Protein for Exportin-5. *Molecular and Cellular Biology* **24**, 6608-6619.
130. Ran, F. A., Hsu, P. D., Wright, J., Agarwala, V., Scott, D. A., and Zhang, F. (2013) Genome engineering using the CRISPR-Cas9 system. *Nature protocols* **8**, 2281-2308.
131. Wu, R., Yue, Y., Zheng, X., and Li, H. (2015) Molecular basis for histone N-terminal methylation by NRMT1. *Genes Dev* **29**, 2337-2342
132. Dong, C., Mao, Y., Tempel, W., Qin, S., Li, L., Loppnau, P., Huang, R., and Min, J. (2015) Structural basis for substrate recognition by the human N-terminal methyltransferase 1. *Genes Dev* **29**, 2343-2348
133. Richardson, S. L., Mao, Y., Zhang, G., Hanjra, P., Peterson, D. L., and Huang, R. (2015) Kinetic Mechanism of Protein N-terminal Methyltransferase 1. *Journal of Biological Chemistry* **290**, 11601-11610.
134. Kim, D. E., Chivian, D., and Baker, D. (2004) Protein structure prediction and analysis using the Robetta server. *Nucleic Acids Res* **32**, W526-531
135. Das, G., Hickey, D. R., McLendon, D., McLendon, G., and Sherman, F. (1989) Dramatic thermostabilization of yeast iso-1-cytochrome c by an asparagine----isoleucine replacement at position 57. *Proceedings of*

the National Academy of Sciences of the United States of America **86**, 496-499.

136. Kim, D. E., Chivian, D., and Baker, D. (2004) Protein structure prediction and analysis using the Robetta server. *Nucleic Acids Research* **32**, W526-W531.
137. Liu, J., Lee, W., Jiang, Z., Chen, Z., Jhunjunwala, S., Haverty, P. M., Gnad, F., Guan, Y., Gilbert, H. N., Stinson, J., Klijn, C., Guillory, J., Bhatt, D., Vartanian, S., Walter, K., Chan, J., Holcomb, T., Dijkgraaf, P., Johnson, S., Koeman, J., Minna, J. D., Gazdar, A. F., Stern, H. M., Hoeflich, K. P., Wu, T. D., Settleman, J., de Sauvage, F. J., Gentleman, R. C., Neve, R. M., Stokoe, D., Modrusan, Z., Seshagiri, S., Shames, D. S., and Zhang, Z. (2012) Genome and transcriptome sequencing of lung cancers reveal diverse mutational and splicing events. *Genome Res* **22**, 2315-2327
138. Lee, E.-S., Son, D.-S., Kim, S.-H., Lee, J., Jo, J., Han, J., Kim, H., Lee, H. J., Choi, H. Y., Jung, Y., Park, M., Lim, Y. S., Kim, K., Shim, Y. M., Kim, B. C., Lee, K., Huh, N., Ko, C., Park, K., Lee, J. W., Choi, Y. S., and Kim, J. (2008) Prediction of Recurrence-Free Survival in Postoperative Non-Small Cell Lung Cancer Patients by Using an Integrated Model

- of Clinical Information and Gene Expression. *Clinical Cancer Research* **14**, 7397-7404.
139. Finak, G., Bertos, N., Pepin, F., Sadekova, S., Souleimanova, M., Zhao, H., Chen, H., Omeroglu, G., Meterissian, S., Omeroglu, A., Hallett, M., and Park, M. (2008) Stromal gene expression predicts clinical outcome in breast cancer. *Nat Med* **14**, 518-527.
140. Lee, S., Chen, J., Zhou, G., Shi, R. Z., Bouffard, G. G., Kocherginsky, M., Ge, X., Sun, M., Jayathilaka, N., Kim, Y. C., Emmanuel, N., Bohlander, S. K., Minden, M., Kline, J., Ozer, O., Larson, R. A., LeBeau, M. M., Green, E. D., Trent, J., Karrison, T., Liu, P. P., Wang, S. M., and Rowley, J. D. (2006) Gene expression profiles in acute myeloid leukemia with common translocations using SAGE. *Proceedings of the National Academy of Sciences of the United States of America* **103**, 1030-1035.
141. Neale, G., Su, X., Morton, C. L., Phelps, D., Gorlick, R., Lock, R. B., Reynolds, C. P., Maris, J. M., Friedman, H. S., Dome, J., Khoury, J., Triche, T. J., Seeger, R. C., Gilbertson, R., Khan, J., Smith, M. A., and Houghton, P. J. (2008) Molecular Characterization of the Pediatric Preclinical Testing Panel. *Clinical*

cancer research : an official journal of the American Association for Cancer Research **14**, 4572-4583.

142. Nikolsky, Y., Sviridov, E., Yao, J., Dosymbekov, D., Ustyansky, V., Kaznacheev, V., Dezso, Z., Mulvey, L., Macconail, L. E., Winckler, W., Serebryiskaya, T., Nikolskaya, T., and Polyak, K. (2008) Genome-Wide Functional Synergy between Amplified and Mutated Genes in Human Breast Cancer. *Cancer Research* **68**, 9532-9540.
143. Hong, Y., Downey, T., Eu, K. W., Koh, P. K., and Cheah, P. Y. (2010) A 'metastasis-prone' signature for early-stage mismatch-repair proficient sporadic colorectal cancer patients and its implications for possible therapeutics. *Clinical & Experimental Metastasis* **27**, 83-90.
144. Kaiser, S., Park, Y.-K., Franklin, J. L., Halberg, R. B., Yu, M., Jessen, W. J., Freudenberg, J., Chen, X., Haigis, K., Jegga, A. G., Kong, S., Sakthivel, B., Xu, H., Reichling, T., Azhar, M., Boivin, G. P., Roberts, R. B., Bissahoyo, A. C., Gonzales, F., Bloom, G. C., Eschrich, S., Carter, S. L., Aronow, J. E., Kleimeyer, J., Kleimeyer, M., Ramaswamy, V., Settle, S. H., Boone, B., Levy, S., Graff, J. M., Doetschman, T., Groden, J., Dove, W. F., Threadgill, D. W., Yeatman, T. J., Coffey, R. J., and Aronow, B. J. (2007)

- Transcriptional recapitulation and subversion of embryonic colon development by mouse colon tumor models and human colon cancer. *Genome Biology* **8**, R131.
145. Sabates-Bellver, J., Van der Flier, L. G., de Palo, M., Cattaneo, E., Maake, C., Rehrauer, H., Laczko, E., Kurowski, M. A., Bujnicki, J. M., Menigatti, M., Luz, J., Ranalli, T. V., Gomes, V., Pastorelli, A., Faggiani, R., Anti, M., Jiricny, J., Clevers, H., and Marra, G. (2007) Transcriptome Profile of Human Colorectal Adenomas. *Molecular Cancer Research* **5**, 1263-1275.
146. Goulet, I., Gauvin, G., Boisvenue, S., and Côté, J. (2007) Alternative Splicing Yields Protein Arginine Methyltransferase 1 Isoforms with Distinct Activity, Substrate Specificity, and Subcellular Localization. *Journal of Biological Chemistry* **282**, 33009-33021.
147. Ertel, A., Dean, J. L., Rui, H., Liu, C., Witkiewicz, A. K., Knudsen, K. E., and Knudsen, E. S. (2010) RB-pathway disruption in breast cancer: Differential association with disease subtypes, disease-specific prognosis and therapeutic response. *Cell cycle (Georgetown, Tex.)* **9**, 4153-4163.
148. Collard, T. J., Urban, B. C., Patsos, H. A., Hague, A., Townsend, P. A., Paraskeva, C., and Williams, A.

- C. (2012) The retinoblastoma protein (Rb) as an anti-apoptotic factor: expression of Rb is required for the anti-apoptotic function of BAG-1 protein in colorectal tumour cells. *Cell Death & Disease* **3**, e408
149. Williams, J. P., Stewart, T., Li, B., Mulloy, R., Dimova, D., and Classon, M. (2006) The Retinoblastoma Protein Is Required for Ras-Induced Oncogenic Transformation. *Molecular and Cellular Biology* **26**, 1170-1182.
150. Kim, N. S., Mee; Kim, Somin; Seo, Yujeong; Kim, Yonghwan; Yoon, Sukjoon. (2016) Differential regulation and synthetic lethality of exclusive RB1 and CDKN2A mutations in lung cancer. *International Journal of Oncology* **48**, 367-375.
151. Christofori, G., and Semb, H. (1999) The role of the cell-adhesion molecule E-cadherin as a tumour-suppressor gene. *Trends in Biochemical Sciences* **24**, 73-76.
152. Pećina-Šlaus, N. (2003) Tumor suppressor gene E-cadherin and its role in normal and malignant cells. *Cancer Cell International* **3**, 17
153. Lewis-Tuffin, L. J., Rodriguez, F., Giannini, C., Scheithauer, B., Necela, B. M., Sarkaria, J. N., and Anastasiadis, P. Z. (2010) Misregulated E-Cadherin

Expression Associated with an Aggressive Brain Tumor Phenotype. *PLOS ONE* **5**, e13665

154. Lieberman, H. B., Bernstock, J. D., Broustas, C. G., Hopkins, K. M., Leloup, C., and Zhu, A. (2011) The role of RAD9 in tumorigenesis. *Journal of Molecular Cell Biology* **3**, 39-43.
155. Pelosi, G., Fumagalli, C., Trubia, M., Sonzogni, A., Rekhtman, N., Maisonneuve, P., Galetta, D., Spaggiari, L., Veronesi, G., Scarpa, A., Malpeli, G., and Viale, G. (2010) Dual Role of RASSF1 as a Tumor Suppressor and an Oncogene in Neuroendocrine Tumors of the Lung. *Anticancer Research* **30**, 4269-4281.
156. Knutson, S. K., Kawano, S., Minoshima, Y., Warholic, N. M., Huang, K.-C., Xiao, Y., Kadowaki, T., Uesugi, M., Kuznetsov, G., Kumar, N., Wigle, T. J., Klaus, C. R., Allain, C. J., Raimondi, A., Waters, N. J., Smith, J. J., Porter-Scott, M., Chesworth, R., Moyer, M. P., Copeland, R. A., Richon, V. M., Uenaka, T., Pollock, R. M., Kuntz, K. W., Yokoi, A., and Keilhack, H. (2014) Selective Inhibition of EZH2 by EPZ-6438 Leads to Potent Antitumor Activity in EZH2-Mutant Non-Hodgkin Lymphoma. *Molecular Cancer Therapeutics* **13**, 842-854.

157. Knutson, S. K., Warholic, N. M., Johnston, L. D., Klaus, C. R., Wigle, T. J., Iwanowicz, D., Littlefield, B. A., Porter-Scott, M., Smith, J. J., Moyer, M. P., Copeland, R. A., Pollock, R. M., Kuntz, K. W., Raimondi, A., and Keilhack, H. (2014) Synergistic Anti-Tumor Activity of EZH2 Inhibitors and Glucocorticoid Receptor Agonists in Models of Germinal Center Non-Hodgkin Lymphomas. *PLoS ONE* **9**, e111840
158. McCabe, M. T., Ott, H. M., Ganji, G., Korenchuk, S., Thompson, C., Van Aller, G. S., Liu, Y., Graves, A. P., Iii, A. D. P., Diaz, E., LaFrance, L. V., Mellinger, M., Duquenne, C., Tian, X., Kruger, R. G., McHugh, C. F., Brandt, M., Miller, W. H., Dhanak, D., Verma, S. K., Tummino, P. J., and Creasy, C. L. (2012) EZH2 inhibition as a therapeutic strategy for lymphoma with EZH2-activating mutations. *Nature* **492**, 108-112.
159. Zhang, G., Richardson, S. L., Mao, Y., and Huang, R. (2015) Design, synthesis, and kinetic analysis of potent protein N-terminal methyltransferase 1 inhibitors(). *Organic & biomolecular chemistry* **13**, 4149-4154.
160. Zhang, G., and Huang, R. (2016) Facile synthesis of SAM-peptide conjugates through alkyl linkers targeting

- protein N-terminal methyltransferase 1. *RSC Adv* **6**, 6768–6771
161. Aruoma, O. I. H., Barry. (2008) *DNA & Free Radicals: Techniques, Mechanisms & Applications*, OICA International, Bodmin, Cornwall, Great Britain
162. Montecuccio, A., Zanetta, F., and Biamonti, G. (2015) Molecular mechanisms of etoposide. *EXCLI Journal* **14**, 95–108.
163. Wang, P., Song, J. H., Song, D. K., Zhang, J., and Hao, C. (2006) Role of death receptor and mitochondrial pathways in conventional chemotherapy drug induction of apoptosis. *Cellular Signalling* **18**, 1528–1535.
164. Jung, K., and Reszka, R. (2001) Mitochondria as subcellular targets for clinically useful anthracyclines. *Advanced Drug Delivery Reviews* **49**, 87–105.
165. Wu, G. S., and Ding, Z. (2002) Caspase 9 is required for p53-dependent apoptosis and chemosensitivity in a human ovarian cancer cell line. *Oncogene* **21**
166. Yang, F., Teves, S. S., Kemp, C. J., and Henikoff, S. (2014) Doxorubicin, DNA torsion, and chromatin dynamics. *Biochimica et Biophysica Acta (BBA) - Reviews on Cancer* **1845**, 84–89.

167. De Iuliis, F., Salerno, G., Corvino, R., D'Aniello, D., Cefalì, K., Taglieri, L., Lanza, R., and Scarpa, S. (2017) Anthracycline-Free Neoadjuvant Chemotherapy Ensures Higher Rates of Pathologic Complete Response in Breast Cancer. *Clinical Breast Cancer* **17**, 34-40.
168. Karch, A., Koch, A., and Grünwald, V. (2016) A phase II trial comparing pazopanib with doxorubicin as first-line treatment in elderly patients with metastatic or advanced soft tissue sarcoma (EPAZ): study protocol for a randomized controlled trial. *Trials* **17**, 312.
169. Khaliq, N. U., Sandra, F. C., Park, D. Y., Lee, J. Y., Oh, K. S., Kim, D., Byun, Y., Kim, I.-S., Kwon, I. C., Kim, S. Y., and Yuk, S. H. (2016) Doxorubicin/heparin composite nanoparticles for caspase-activated prodrug chemotherapy. *Biomaterials* **101**, 131-142.
170. Leroy, B., Girard, L., Hollestelle, A., Minna, J. D., Gazdar, A. F., and Soussi, T. (2014) Analysis of TP53 Mutation Status in Human Cancer Cell Lines: A Reassessment. *Human mutation* **35**, 756-765.
171. Bunz, F., Hwang, P. M., Torrance, C., Waldman, T., Zhang, Y., Dillehay, L., Williams, J., Lengauer, C., Kinzler, K. W., and Vogelstein, B. (1999) Disruption

- of p53 in human cancer cells alters the responses to therapeutic agents. *J Clin Invest* **104**, 263-269.
172. Zhang, Y., Gao, Y., Zhang, G., Huang, S., Dong, Z., Kong, C., Su, D., Du, J., Zhu, S., Liang, Q., Zhang, J., Lu, J., and Huang, B. (2011) DNMT3a plays a role in switches between doxorubicin-induced senescence and apoptosis of colorectal cancer cells. *International Journal of Cancer* **128**, 551-561.
173. Zou, S. W., Zhang, J. C., Zhang, X. D., Miao, S. Y., Zong, S. D., Sheng, Q., and Wang, L. F. (2003) Expression and localization of VCX/Y proteins and their possible involvement in regulation of ribosome assembly during spermatogenesis. *Cell Research* **13**, 171-177.
174. Ivashkevich, A., Redon, C. E., Nakamura, A. J., Martin, R. F., and Martin, O. A. (2012) USE OF THE γ -H2AX ASSAY TO MONITOR DNA DAMAGE AND REPAIR IN TRANSLATIONAL CANCER RESEARCH. *Cancer letters* **327**, 123-133.
175. Sharma, P. M., Ponnaiya, B., Taveras, M., Shuryak, I., Turner, H., and Brenner, D. J. (2015) High Throughput Measurement of γ H2AX DSB Repair Kinetics in a Healthy Human Population. *PLoS ONE* **10**, e0121083

176. Ravi, R., Mookerjee, B., Bhujwala, Z. M., Sutter, C. H., Artemov, D., Zeng, Q., Dillehay, L. E., Madan, A., Semenza, G. L., and Bedi, A. (2000) Regulation of Tumor Angiogenesis by p53-Induced Degradation of Hypoxia-Inducible Factor 1 α . *Genes & Development* **14**, 34-44.
177. Yeung, T. M., Gandhi, S. C., Wilding, J. L., Muschel, R., and Bodmer, W. F. (2010) Cancer Stem Cells from Colorectal Cancer-Derived Cell Lines. *Proceedings of the National Academy of Sciences* **107**, 3722-3727.
178. Nowsheen, S., and Yang, E. S. (2012) THE INTERSECTION BETWEEN DNA DAMAGE RESPONSE AND CELL DEATH PATHWAYS. *Experimental Oncology* **34**, 243-254.
179. Conklin, K. A. (2004) Chemotherapy-Associated Oxidative Stress: Impact on Chemotherapeutic Effectiveness. *Integrative Cancer Therapies* **3**, 294-300.
180. Yokoyama, C., Sueyoshi, Y., Ema, M., Mori, Y., Takaishi, K., and Hisatomi, H. (2017) Induction of oxidative stress by anticancer drugs in the presence and absence of cells. *Oncology Letters* **14**, 6066-6070.
181. Lüpertz, R., Wätjen, W., Kahl, R., and Chovolou, Y. (2010) Dose- and time-dependent effects of doxorubicin

- on cytotoxicity, cell cycle and apoptotic cell death in human colon cancer cells. *Toxicology* **271**, 115-121.
182. Mukhopadhyay, P., Rajesh, M., Yoshihiro, K., Haskó, G., and Pacher, P. (2007) Simple quantitative detection of mitochondrial superoxide production in live cells. *Biochemical and biophysical research communications* **358**, 203-208.
183. Kohno, M. (2010) Applications of Electron Spin Resonance Spectrometry for Reactive Oxygen Species and Reactive Nitrogen Species Research. *Journal of Clinical Biochemistry and Nutrition* **47**, 1-11.
184. Kopáni, M., Celec, P., Danišovič, L., Michalka, P., and Biró, C. (2006) Oxidative stress and electron spin resonance. *Clinica Chimica Acta* **364**, 61-66.

APPENDICES: SUPPLEMENTAL DATA

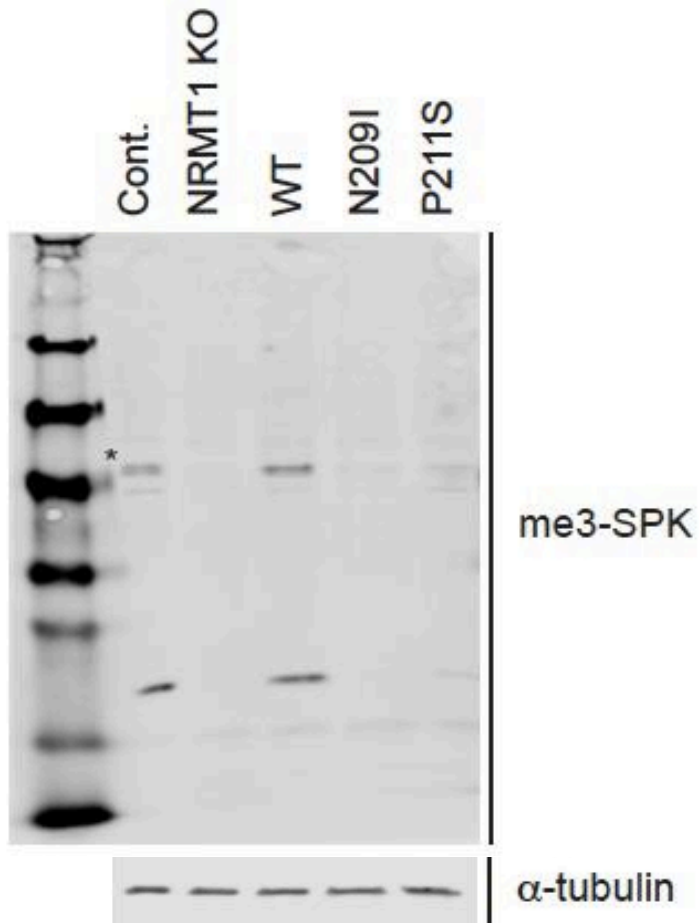
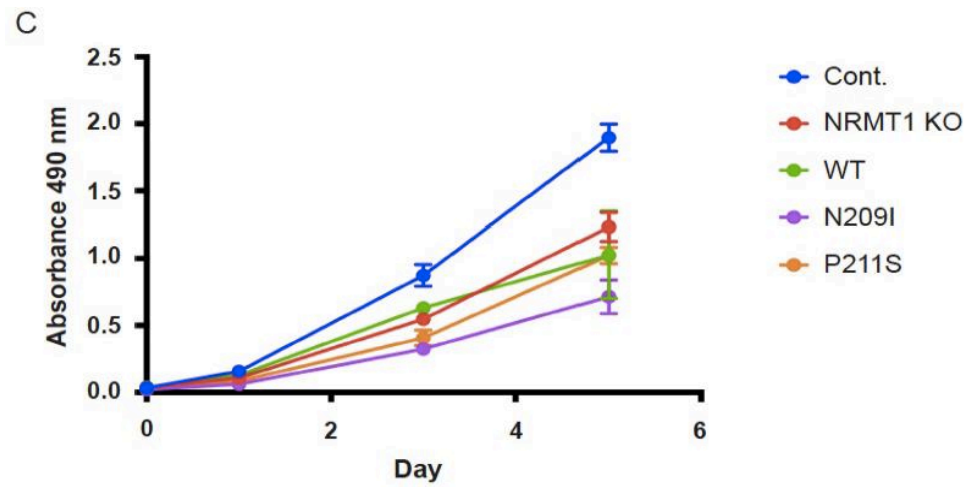
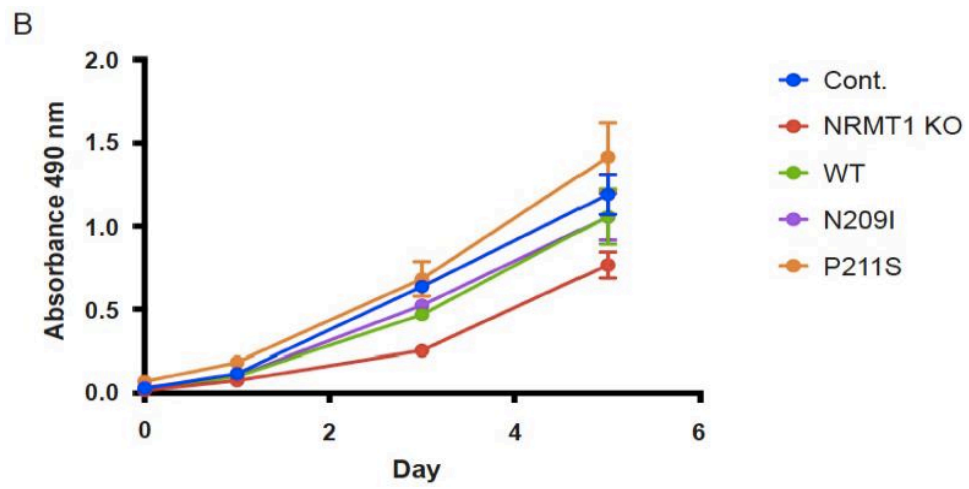
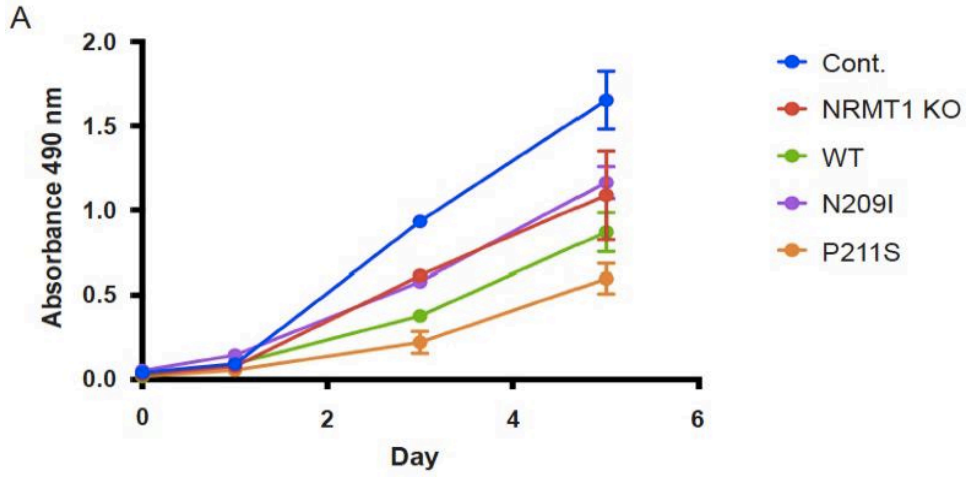
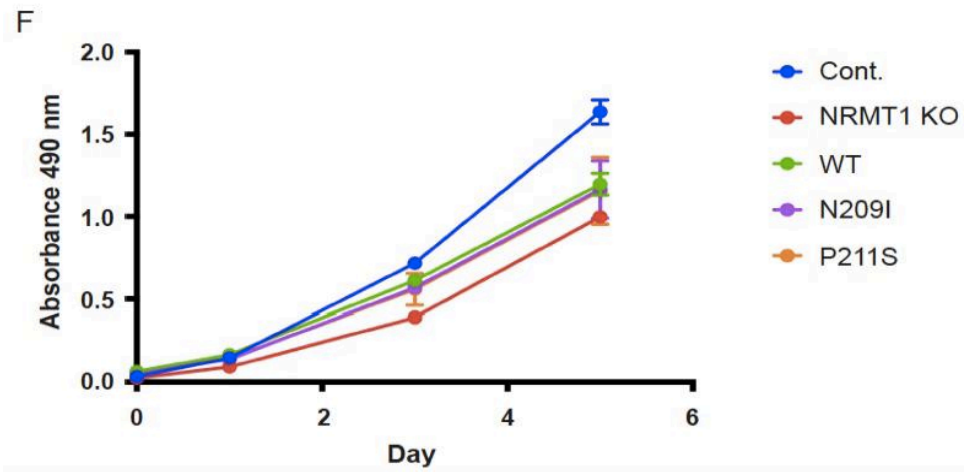
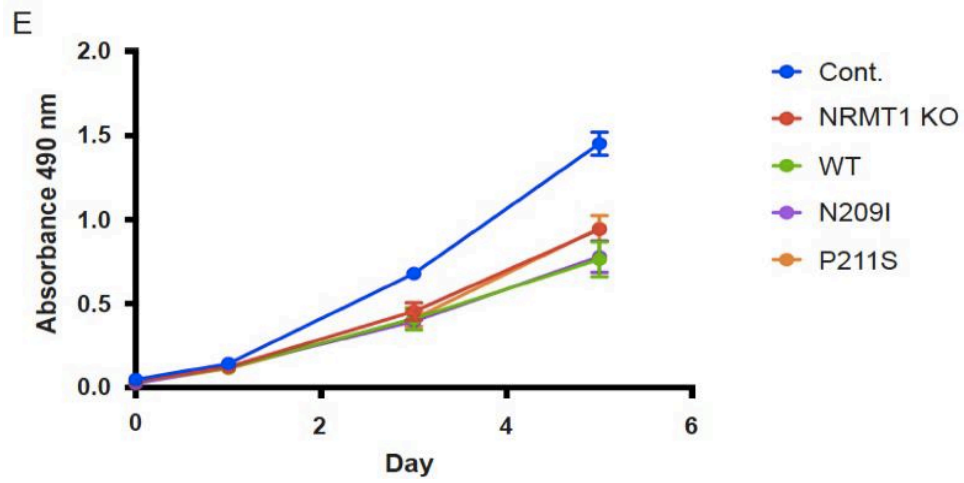
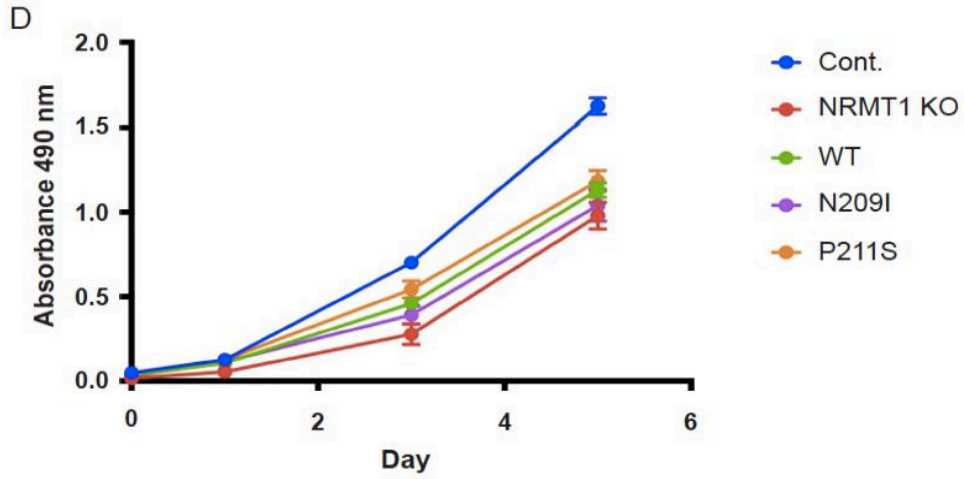


Figure 23. Mutant NRMT1 SPK methylation pattern.

Whole cell lysates from the five featured cell lines were probed with the tri-SPK (me3RCC1) antibody. Band indicated by asterisk is RCC1. NRMT1 recognizes many substrates with a variety of consensus sequences; only a handful of those have the SPK consensus sequence. α -tubulin included as a loading control. Blots are representative images of three independent experiments.





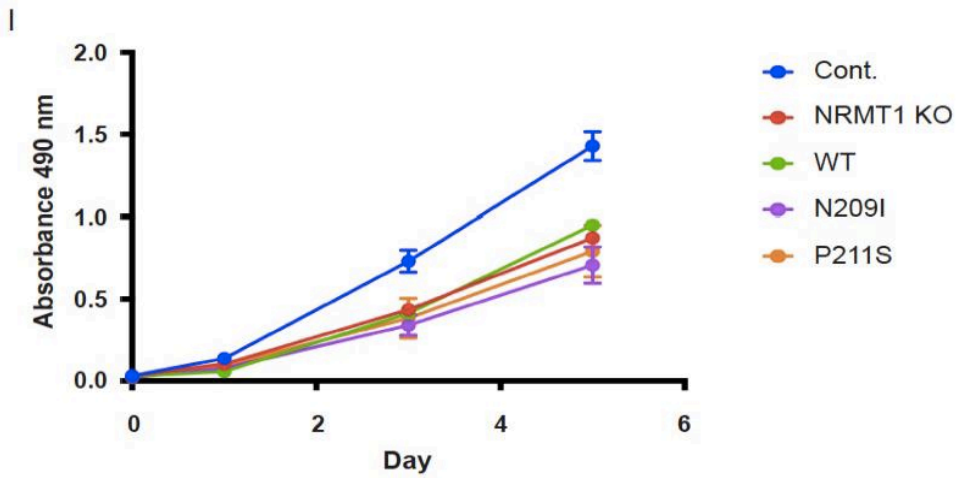
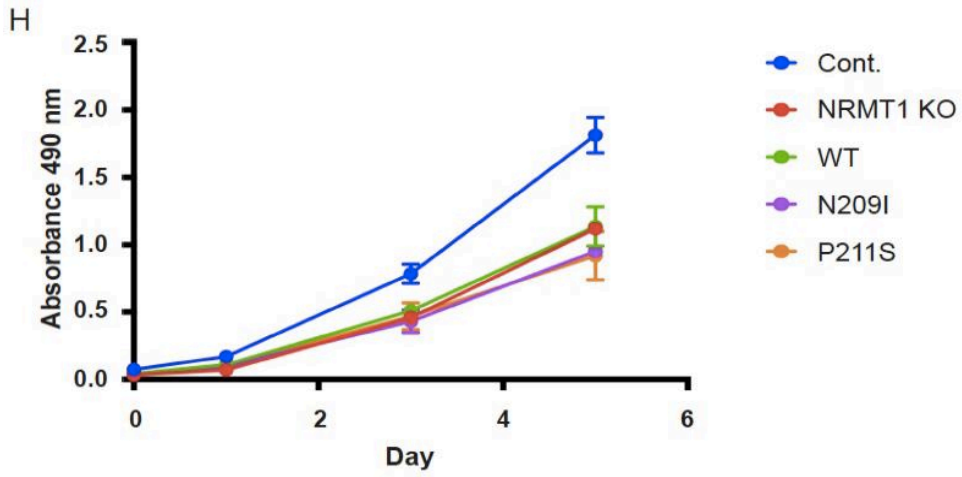
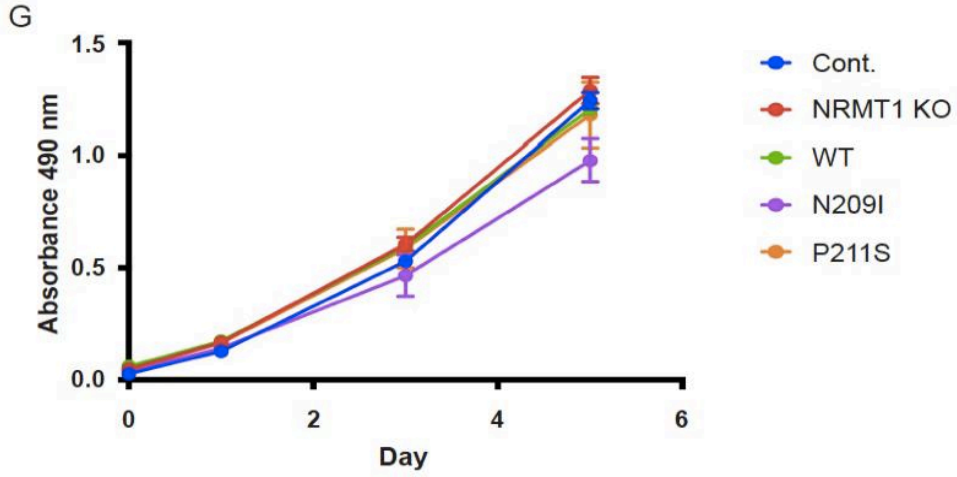
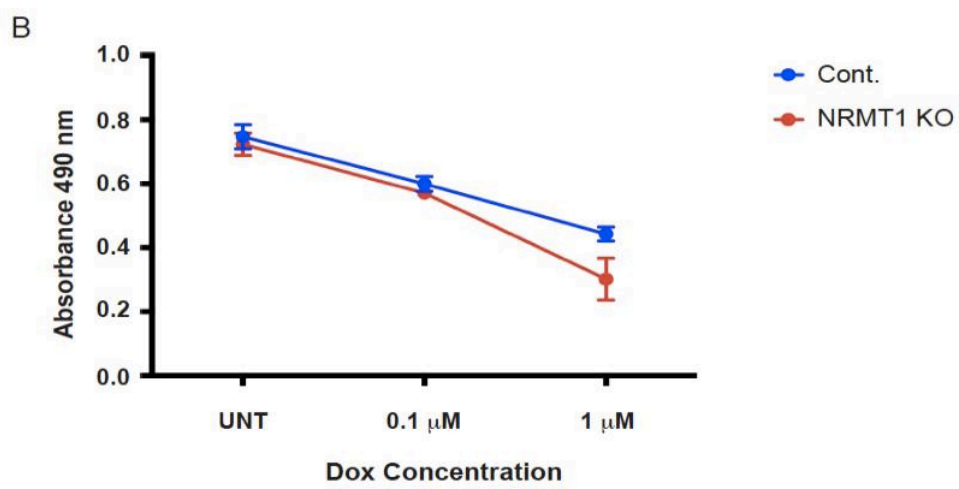
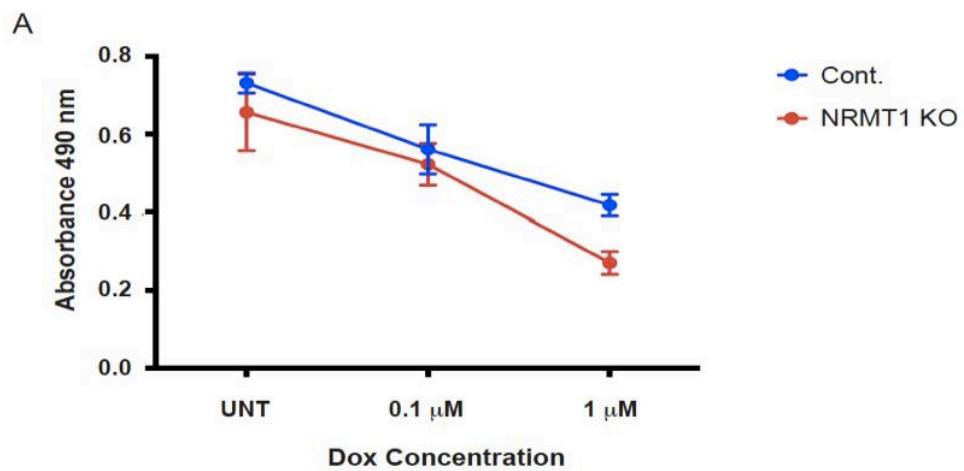


Figure 24. Viability studies of HCT116 cells.

Four sets of triplicates were made for each of the five HCT116 cell lines. Cells were seeded at a density of 1000 cells per well in 96-well plates. On the day of plating (day 0), 20 μ l of Aqueous One Solution (Promega, Madison, WI) was added to the first set of triplicates for each cell line, and the absorbance at 490 nm was read after two hours. Readings were also taken on days 1, 3, and 5. (A-I) Raw absorbance values are shown on the Y-axis. Each panel represents triplicate data.



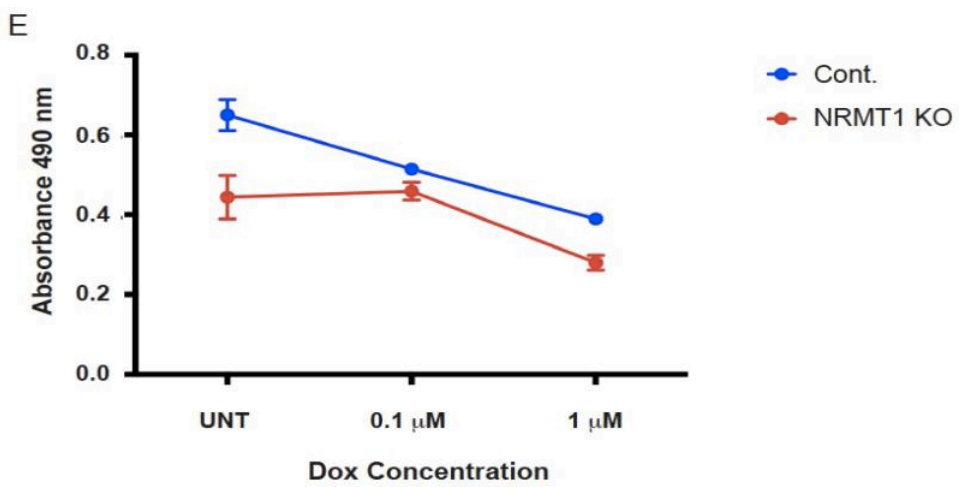
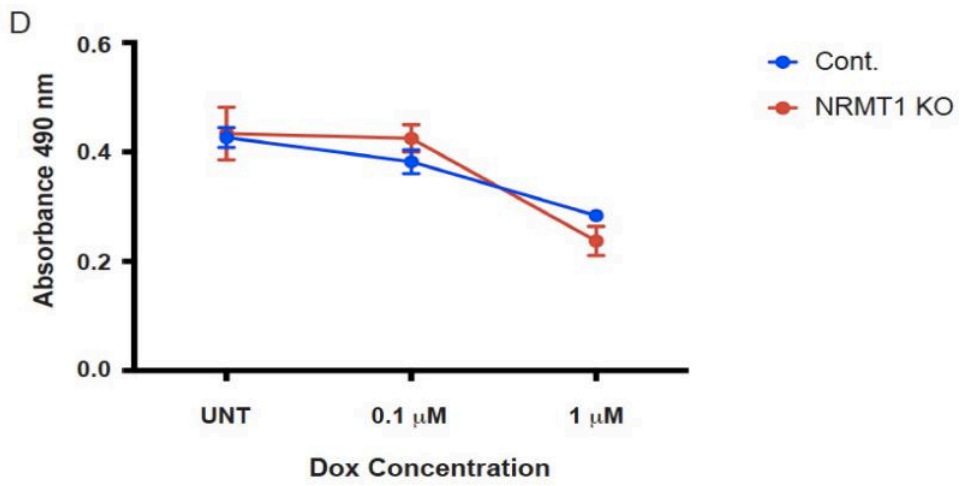
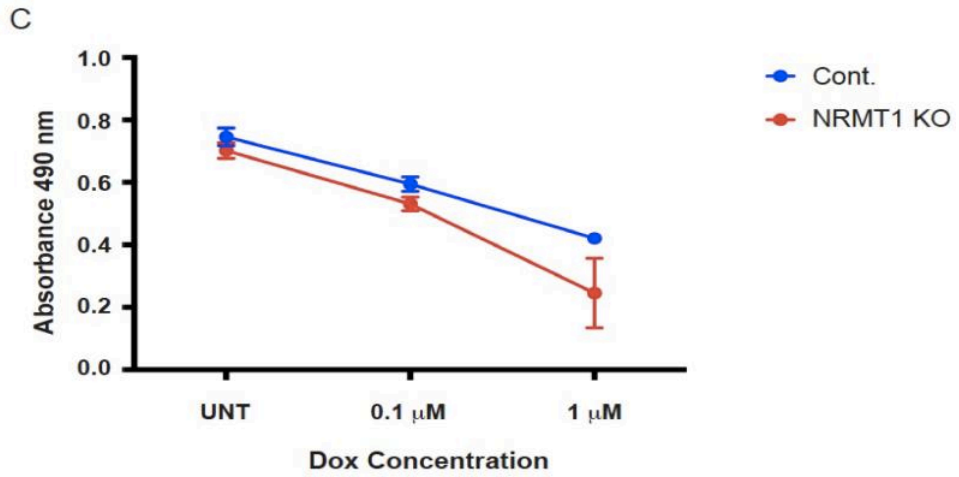
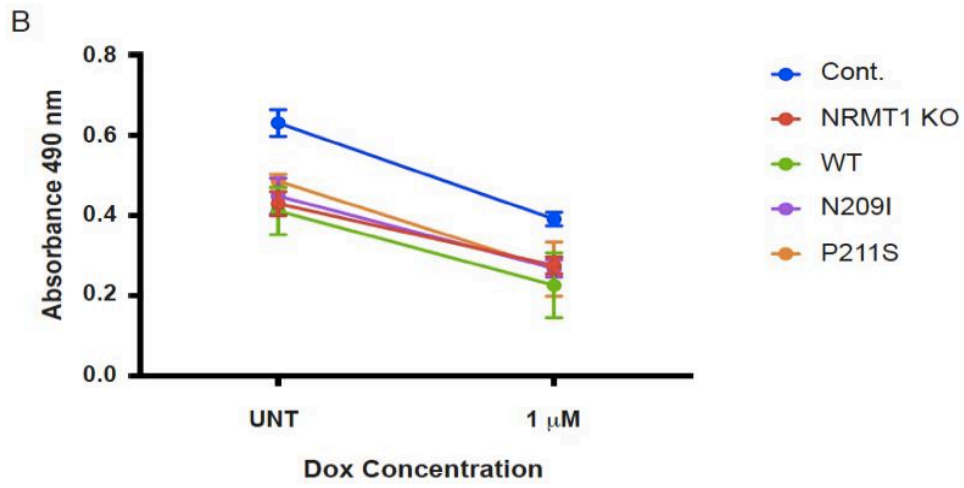
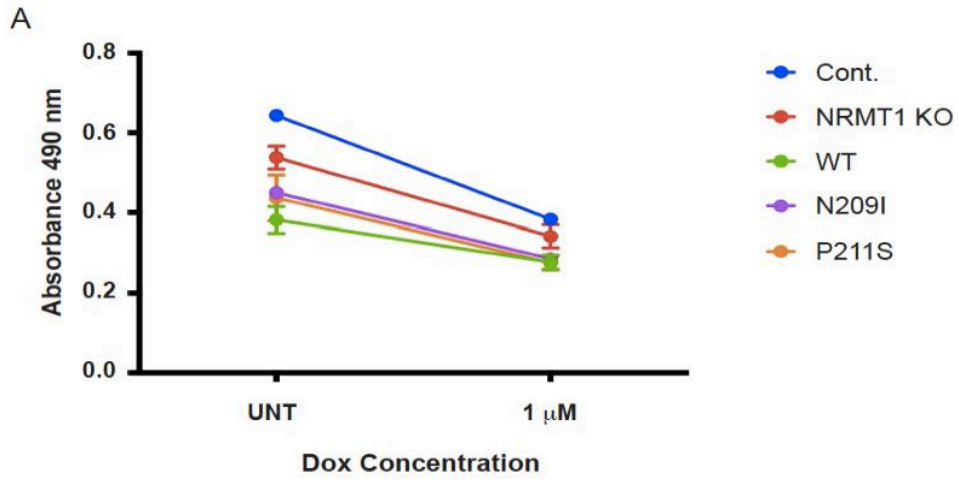


Figure 25. Viability assay of doxorubicin-treated cont. and NRMT1 KO cells.

2.4×10^4 cells per well were seeded into 24-well plates. Three sets of triplicates were made for cont. and NRMT1 KO cells. CellTiter was performed on cells that were treated with 0.1 or 1 μM doxorubicin (or the untreated controls) for 24 hours. Following treatment, 80 μl of Aqueous One Solution was added to each well, and the absorbance at 490 nm was read after two hours. Y-axis units are arbitrary units of absorbance at 490 nm. Data points represent triplicate data.



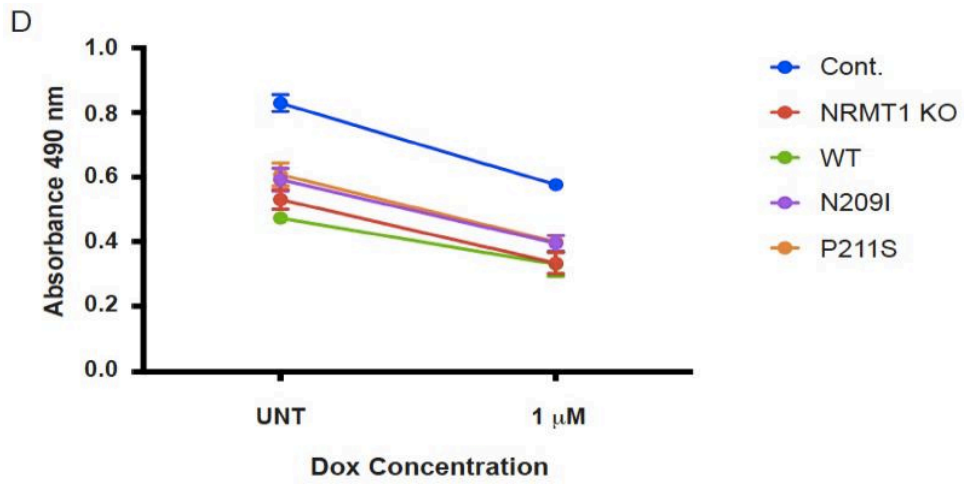
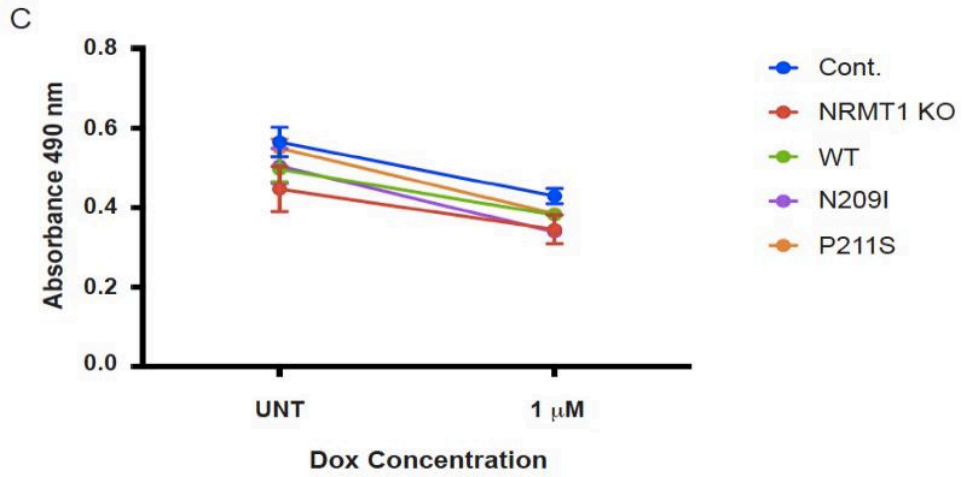


Figure 26. Viability assay of doxorubicin-treated cells.

2.4×10^4 cells per well were seeded into 24-well plates.

Two sets of triplicates were made for each cell line.

CellTiter was performed on cells that were treated with $1 \mu\text{M}$ doxorubicin (or the untreated controls) for 24 hours.

Following treatment, $80 \mu\text{l}$ of Aqueous One Solution was added to each well, and the absorbance at 490 nm was read after two hours. Y-axis units are arbitrary units of absorbance at 490 nm. Data points represent triplicate data.

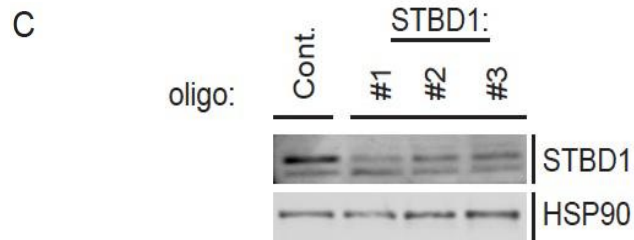
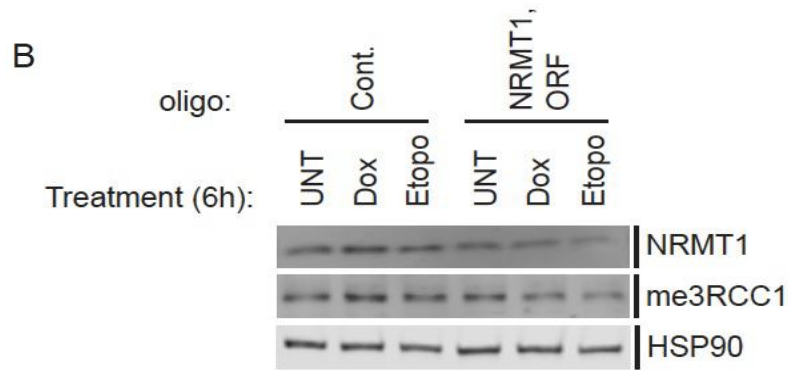
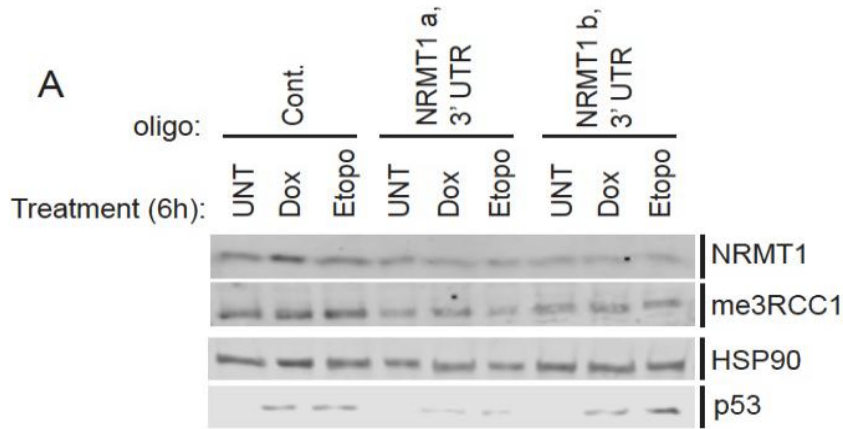


Figure 27. siRNA Studies in HCT116 cells.

2.4 X 10⁴ cells per well were seeded into 24-well plates. Cells were grown until they reached 70% confluency (two days after seeding). Cells were transfected with 10 pM siRNA. Media was changed 21 hours after transfections. Two days later, cells were treated with either 1 μM doxorubicin or 250 μM etoposide (untreated controls were included, as indicated in the figure) for six hours. Cell lysates were collected immediately following treatment. Lysates were subjected to western blot analysis, probing with the indicated antibodies. Experiment was done once.

APPENDICES: WORK DISCLAIMER

The data appearing in this dissertation are my own and were performed by me. Exceptions to this are Figures 4-6 and 8-10. Figures 4, 9, and 10 were performed by John Tooley, State University of New York at Buffalo. The molecular modeling exhibited in Figure 8 was performed by Janusz Petkowski, Massachusetts Institute of Technology. The graph in Figure 5 was created by me but is based upon the raw mass spectrometry data produced by the University of Louisville Mass Spectrometry Core Laboratory, which is displayed in Figure 6.

APPENDICES: COPYRIGHT PERMISSION

3/9/2018

RightsLink Printable License

JOHN WILEY AND SONS LICENSE TERMS AND CONDITIONS

Mar 09, 2018

This Agreement between Ms. Kaitlyn Shields ("You") and John Wiley and Sons ("John Wiley and Sons") consists of your license details and the terms and conditions provided by John Wiley and Sons and Copyright Clearance Center.

| | |
|-------------------------------------|---|
| License Number | 4304941445378 |
| License date | Mar 09, 2018 |
| Licensed Content Publisher | John Wiley and Sons |
| Licensed Content Publication | Protein Science |
| Licensed Content Title | Select human cancer mutants of NRMT1 alter its catalytic activity and decrease N-terminal trimethylation |
| Licensed Content Author | Kaitlyn M. Shields, John G. Tooley, Janusz J. Petkowski, Daniel W. Wilkey, Nichola C. Garbett, Michael L. Merchant, Alan Cheng, Christine E. Schaner Tooley |
| Licensed Content Date | Jun 11, 2017 |
| Licensed Content Pages | 14 |
| Type of use | Dissertation/Thesis |
| Requestor type | Author of this Wiley article |
| Format | Print and electronic |
| Portion | Full article |
| Will you be translating? | No |
| Title of your thesis / dissertation | INVESTIGATING THE IMPACT OF NRMT1 CANCER MUTANTS ON CATALYTIC SPECIFICITY AND THE DNA DAMAGE RESPONSE |
| Expected completion date | May 2018 |
| Expected size (number of pages) | 195 |
| Requestor Location | Ms. Kaitlyn Shields 900 Breckenridge Ln. Apt. D Louisville BEECHWOOD VILLAGE, KY 40207 United States Attn: Ms. Kaitlyn Shields |
| Publisher Tax ID | EU826007151 |
| Total | 0.00 USD |
| Terms and Conditions | |

TERMS AND CONDITIONS

This copyrighted material is owned by or exclusively licensed to John Wiley & Sons, Inc. or one of its group companies (each a "Wiley Company") or handled on behalf of a society with which a Wiley Company has exclusive publishing rights in relation to a particular work (collectively "WILEY"). By clicking "accept" in connection with completing this licensing transaction, you agree that the following terms and conditions apply to this transaction (along with the billing and payment terms and conditions established by the Copyright Clearance Center Inc., ("CCC's Billing and Payment terms and conditions"), at the time that

<https://s100.copyright.com/AppDispatchServlet>

1/5

you opened your RightsLink account (these are available at any time at <http://myaccount.copyright.com>).

Terms and Conditions

- The materials you have requested permission to reproduce or reuse (the "Wiley Materials") are protected by copyright.
- You are hereby granted a personal, non-exclusive, non-sub licensable (on a stand-alone basis), non-transferable, worldwide, limited license to reproduce the Wiley Materials for the purpose specified in the licensing process. This license, **and any CONTENT (PDF or image file) purchased as part of your order**, is for a one-time use only and limited to any maximum distribution number specified in the license. The first instance of republication or reuse granted by this license must be completed within two years of the date of the grant of this license (although copies prepared before the end date may be distributed thereafter). The Wiley Materials shall not be used in any other manner or for any other purpose, beyond what is granted in the license. Permission is granted subject to an appropriate acknowledgement given to the author, title of the material/book/journal and the publisher. You shall also duplicate the copyright notice that appears in the Wiley publication in your use of the Wiley Material. Permission is also granted on the understanding that nowhere in the text is a previously published source acknowledged for all or part of this Wiley Material. Any third party content is expressly excluded from this permission.
- With respect to the Wiley Materials, all rights are reserved. Except as expressly granted by the terms of the license, no part of the Wiley Materials may be copied, modified, adapted (except for minor reformatting required by the new Publication), translated, reproduced, transferred or distributed, in any form or by any means, and no derivative works may be made based on the Wiley Materials without the prior permission of the respective copyright owner. **For STM Signatory Publishers clearing permission under the terms of the [STM Permissions Guidelines](#) only, the terms of the license are extended to include subsequent editions and for editions in other languages, provided such editions are for the work as a whole in situ and does not involve the separate exploitation of the permitted figures or extracts**, You may not alter, remove or suppress in any manner any copyright, trademark or other notices displayed by the Wiley Materials. You may not license, rent, sell, loan, lease, pledge, offer as security, transfer or assign the Wiley Materials on a stand-alone basis, or any of the rights granted to you hereunder to any other person.
- The Wiley Materials and all of the intellectual property rights therein shall at all times remain the exclusive property of John Wiley & Sons Inc, the Wiley Companies, or their respective licensors, and your interest therein is only that of having possession of and the right to reproduce the Wiley Materials pursuant to Section 2 herein during the continuance of this Agreement. You agree that you own no right, title or interest in or to the Wiley Materials or any of the intellectual property rights therein. You shall have no rights hereunder other than the license as provided for above in Section 2. No right, license or interest to any trademark, trade name, service mark or other branding ("Marks") of WILEY or its licensors is granted hereunder, and you agree that you shall not assert any such right, license or interest with respect thereto
- NEITHER WILEY NOR ITS LICENSORS MAKES ANY WARRANTY OR REPRESENTATION OF ANY KIND TO YOU OR ANY THIRD PARTY, EXPRESS, IMPLIED OR STATUTORY, WITH RESPECT TO THE MATERIALS OR THE ACCURACY OF ANY INFORMATION CONTAINED IN THE

MATERIALS, INCLUDING, WITHOUT LIMITATION, ANY IMPLIED WARRANTY OF MERCHANTABILITY, ACCURACY, SATISFACTORY QUALITY, FITNESS FOR A PARTICULAR PURPOSE, USABILITY, INTEGRATION OR NON-INFRINGEMENT AND ALL SUCH WARRANTIES ARE HEREBY EXCLUDED BY WILEY AND ITS LICENSORS AND WAIVED BY YOU.

- WILEY shall have the right to terminate this Agreement immediately upon breach of this Agreement by you.
- You shall indemnify, defend and hold harmless WILEY, its Licensors and their respective directors, officers, agents and employees, from and against any actual or threatened claims, demands, causes of action or proceedings arising from any breach of this Agreement by you.
- IN NO EVENT SHALL WILEY OR ITS LICENSORS BE LIABLE TO YOU OR ANY OTHER PARTY OR ANY OTHER PERSON OR ENTITY FOR ANY SPECIAL, CONSEQUENTIAL, INCIDENTAL, INDIRECT, EXEMPLARY OR PUNITIVE DAMAGES, HOWEVER CAUSED, ARISING OUT OF OR IN CONNECTION WITH THE DOWNLOADING, PROVISIONING, VIEWING OR USE OF THE MATERIALS REGARDLESS OF THE FORM OF ACTION, WHETHER FOR BREACH OF CONTRACT, BREACH OF WARRANTY, TORT, NEGLIGENCE, INFRINGEMENT OR OTHERWISE (INCLUDING, WITHOUT LIMITATION, DAMAGES BASED ON LOSS OF PROFITS, DATA, FILES, USE, BUSINESS OPPORTUNITY OR CLAIMS OF THIRD PARTIES), AND WHETHER OR NOT THE PARTY HAS BEEN ADVISED OF THE POSSIBILITY OF SUCH DAMAGES. THIS LIMITATION SHALL APPLY NOTWITHSTANDING ANY FAILURE OF ESSENTIAL PURPOSE OF ANY LIMITED REMEDY PROVIDED HEREIN.
- Should any provision of this Agreement be held by a court of competent jurisdiction to be illegal, invalid, or unenforceable, that provision shall be deemed amended to achieve as nearly as possible the same economic effect as the original provision, and the legality, validity and enforceability of the remaining provisions of this Agreement shall not be affected or impaired thereby.
- The failure of either party to enforce any term or condition of this Agreement shall not constitute a waiver of either party's right to enforce each and every term and condition of this Agreement. No breach under this agreement shall be deemed waived or excused by either party unless such waiver or consent is in writing signed by the party granting such waiver or consent. The waiver by or consent of a party to a breach of any provision of this Agreement shall not operate or be construed as a waiver of or consent to any other or subsequent breach by such other party.
- This Agreement may not be assigned (including by operation of law or otherwise) by you without WILEY's prior written consent.
- Any fee required for this permission shall be non-refundable after thirty (30) days from receipt by the CCC.
- These terms and conditions together with CCC's Billing and Payment terms and conditions (which are incorporated herein) form the entire agreement between you and WILEY concerning this licensing transaction and (in the absence of fraud) supersedes all prior agreements and representations of the parties, oral or written. This Agreement

may not be amended except in writing signed by both parties. This Agreement shall be binding upon and inure to the benefit of the parties' successors, legal representatives, and authorized assigns.

- In the event of any conflict between your obligations established by these terms and conditions and those established by CCC's Billing and Payment terms and conditions, these terms and conditions shall prevail.
- WILEY expressly reserves all rights not specifically granted in the combination of (i) the license details provided by you and accepted in the course of this licensing transaction, (ii) these terms and conditions and (iii) CCC's Billing and Payment terms and conditions.
- This Agreement will be void if the Type of Use, Format, Circulation, or Requestor Type was misrepresented during the licensing process.
- This Agreement shall be governed by and construed in accordance with the laws of the State of New York, USA, without regards to such state's conflict of law rules. Any legal action, suit or proceeding arising out of or relating to these Terms and Conditions or the breach thereof shall be instituted in a court of competent jurisdiction in New York County in the State of New York in the United States of America and each party hereby consents and submits to the personal jurisdiction of such court, waives any objection to venue in such court and consents to service of process by registered or certified mail, return receipt requested, at the last known address of such party.

WILEY OPEN ACCESS TERMS AND CONDITIONS

Wiley Publishes Open Access Articles in fully Open Access Journals and in Subscription journals offering Online Open. Although most of the fully Open Access journals publish open access articles under the terms of the Creative Commons Attribution (CC BY) License only, the subscription journals and a few of the Open Access Journals offer a choice of Creative Commons Licenses. The license type is clearly identified on the article.

The Creative Commons Attribution License

The [Creative Commons Attribution License \(CC-BY\)](#) allows users to copy, distribute and transmit an article, adapt the article and make commercial use of the article. The CC-BY license permits commercial and non-

Creative Commons Attribution Non-Commercial License

The [Creative Commons Attribution Non-Commercial \(CC-BY-NC\) License](#) permits use, distribution and reproduction in any medium, provided the original work is properly cited and is not used for commercial purposes.(see below)

Creative Commons Attribution-Non-Commercial-NoDerivs License

The [Creative Commons Attribution Non-Commercial-NoDerivs License \(CC-BY-NC-ND\)](#) permits use, distribution and reproduction in any medium, provided the original work is properly cited, is not used for commercial purposes and no modifications or adaptations are made. (see below)

Use by commercial "for-profit" organizations

Use of Wiley Open Access articles for commercial, promotional, or marketing purposes requires further explicit permission from Wiley and will be subject to a fee.

Further details can be found on Wiley Online Library

<http://olabout.wiley.com/WileyCDA/Section/id-410895.html>

Other Terms and Conditions:

v1.10 Last updated September 2015

Questions? customer@copyright.com or +1-855-239-3415 (toll free in the US) or +1-978-646-2777.



CURRICULUM VITAE

Kaitlyn M. Shields

University of Louisville • Louisville, KY 40202 •

(502) 852-3572 • kmwend01@louisville.edu

Bellarmino University • Louisville, KY 40205 •

(502) 272-8053 • kshields2@bellarmine.edu

900 Breckenridge Ln., Apt. D • Louisville, KY 40207 •

(816) 824-4488 • kaitlyn.shields2014@gmail.com (preferred)

EDUCATION

MISSOURI SOUTHERN STATE UNIVERSITY—School of Arts and
Sciences, Joplin, MO, 2009–13

B.S., Biology

UNIVERSITY OF LOUISVILLE—School of Medicine, Louisville, KY,
2013–16

M.S., Biochemistry and Molecular Biology

UNIVERSITY OF LOUISVILLE—School of Medicine, Louisville, KY,
2013–18

Ph.D., Biochemistry and Molecular Biology

RESEARCH AND WORK EXPERIENCE

2014–18: **Graduate Research Assistant**, Dept. of
Biochemistry and Molecular Genetics,
University of Louisville/Dr. Alan Cheng, Dr.
Christine Schaner Tooley: Investigating the
Impact of NRMT1 Cancer Mutants on NRMT1
Catalytic Specificity and the DNA Damage
Response

2013: **Independent Study**, Dept. of Biology, Dept.
of Chemical and Physical Sciences, MSSU/Dr.
Bradley Creamer, Dr. Elliot Ennis: Natural
product isolation of mangiferin from mango,
and its DNA protective effects against
chemical mutagens

2009–13: **High school tutor**, Upward Bound,
MSSU/Megan Manley, Randy Hopper:
Assisted high school students with
basic and social sciences homework

TEACHING EXPERIENCE AND TRAINING

2018-present: **Adjunct Faculty**, Dept. of Biology,
Bellarmine University/Dr. Steven Wilt:

2016-present: **Adjunct Faculty**, Dept. of Chemistry and
Physics, Bellarmine University/Dr.
Patrick Holt:

Credit Load

Fall 2018

BIOL 130: Principles of Biology 4.00

Laboratory (two sections)

CHEM 103: General Chemistry I 2.67

Laboratory

CHEM 109: Liberal Arts Chemistry 1.33

Laboratory

Spring 2018

CHEM 109: Liberal Arts Chemistry 1.33

Laboratory

Fall 2017

CHEM 103: General Chemistry I 2.67

Laboratory

CHEM 109: Liberal Arts Chemistry 1.33

Laboratory

Guest Lecturer

Spring 2017

CHEM 103: General Chemistry I 2.67

Laboratory

CHEM 109: Liberal Arts Chemistry 1.33

Laboratory

Fall 2016

CHEM 109: Liberal Arts Chemistry 1.33

Laboratory

2015: **STEM Graduate Teaching Assistant Mini-Academy**, PLAN, University of Louisville:
Learned basic teaching techniques, including formative assessment, and engaged in micro-teaching

2015: **Teaching Assistant**, Dept. of Biochemistry and Molecular Genetics, University of Louisville/Dr. William Dean: Assisted with grading and writing homework for the graduate Advanced Biochemistry II course

2013: **Laboratory Teaching Assistant**, Dept. of Chemical and Physical Sciences, MSSU/Dr. Elliot Ennis: Oversaw a laboratory section of a general, organic and biochemistry class for nursing and allied health students; assisted with the laboratory, grading laboratory reports, and proctoring tests

MENTORING AND TRAINING

2018: **Austin Clark**, University of Louisville, School of Medicine medical student: Taught collection and processing of cellular lysate, RNA processing for qPCR, gel electrophoresis, western blotting, and imaging techniques

2017: **Abbey Bell**, University of Louisville, Dept. of Biochemistry and Molecular Genetics Master's degree student: Taught cell culture and cell imaging, gel electrophoresis, western blotting, and imaging techniques

2017: **Lane Peikert**, University of Louisville, Dept.
of Biochemistry and Molecular Genetics
Master's degree student: Taught gel
electrophoresis, western blotting, and
imaging techniques

2015-16: **Lilly Jensen**, University of Louisville,
duPont Manual High School student: Taught
common laboratory techniques including gel
electrophoresis, western blotting, DNA
purification techniques, and general
laboratory maintenance

FELLOWSHIPS, AWARDS AND HONORS

2013-15: Integrated Programs in Biomedical Sciences
Fellowship

2013: MSSU Student Research Grant Awardee

2013: Glenn Dolence Leadership Awardee

2012-13: Dr. E. Samuel Gibson Memorial Scholarship

2010-13: Phi Eta Sigma

2009-13: Excellence Scholarship

PUBLICATIONS

Kaitlyn M. Shields, John G. Tooley, Janusz J. Petkowski, Daniel W. Wilkey, Nichola C. Garbett, Michael L. Merchant, Alan Cheng, and Christine E. Schaner Tooley. (2017) Select human cancer mutants of NRMT1 alter its catalytic activity and decrease N- terminal trimethylation. *Protein Science* 26(8): 1639-1652.

PRESENTATIONS

SEMINARS

"Investigating the impact of NRMT1 cancer mutants on catalytic specificity and the DNA damage response." (2018) University of Louisville, Department of Biochemistry and Molecular Genetics Dissertation Defense.

"Investigating the impact of NRMT1 cancer mutants on catalytic specificity and the DNA damage response." (2017) University of Louisville, Department of Biochemistry and Molecular Genetics Research Conference.

"The role of altered N-terminal methylation in the DNA damage response." (2016) University of Louisville, Department of Biochemistry and Molecular Genetics Research Conference.

"Characterizing N-terminal methyltransferase mutations found in human cancers." (2015) University of Louisville, Department of Biochemistry and Molecular Genetics Seminar Series.

"Histone methylation: what is it good for?" (2015) University of Louisville, Department of Biochemistry and Molecular Genetics Seminar Series.

"ADAM10 α -secretase mutations: roles in the progression of Alzheimer's Disease." (2014) University of Louisville, Department of Biochemistry and Molecular Genetics Seminar Series.

POSTERS

Shields, K.M., Tooley, J.G., Petkowski, J.J., Wilkey, D.W., Garbett, N.C., Merchant, M.L., Cheng, A., and Schaner Tooley, C.E. (2017) Investigating the impact of NRMT1 cancer mutants on catalytic specificity and the DNA damage response. 7th Biennial Biochemistry and Molecular Genetics Colloquium. Louisville, Kentucky.

Shields, K.M., Wilkey, D.W., Merchant, M.L., and Schaner Tooley, C.E. (2015) Characterizing N-terminal methyltransferase mutations found in human cancers. Research!Louisville. Louisville, Kentucky.

Shields, K.M., Wilkey, D.W., Merchant, M.L., and Schaner Tooley, C.E. (2015) Characterizing N-terminal methyltransferase mutations found in human cancers. 6th Biennial Biochemistry and Molecular Genetics Colloquium. Louisville, Kentucky.

Shields, K.M. and Schaner Tooley, C.E. (2014) Characterizing N-terminal methyltransferase mutants found in human cancers. Research!Louisville. Louisville, Kentucky.

CONFERENCES

2nd Annual Adjunct Faculty Scholars Conference. (2017)
Indiana University Southeast. New Albany, Indiana.

PROFESSIONAL ASSOCIATIONS

American Chemical Society

American Society for Biochemistry and Molecular Biology

Kentucky Academy of Science

National Science Teachers Association

Society for College Science Teachers

SERVICE AND EXTRACURRICULAR ACTIVITIES

2016-present: Science fair judge for the Louisville
Regional Science & Engineering Fair

2015-present: Science fair judge for the DuPont
Manual Regional Science Fair

2015-16: Graduate Student Council departmental
representative

2012-13: Science community outreach with MSSU
Chemistry Club

2011-13: Vice President of MSSU Biology Club

2011-13: Science fair judge for the Missouri Southern
Regional Science Fair

2011: Volunteer for Joplin tornado disaster relief
efforts

2010-12: Deer aging for the Missouri Department of
Conservation